The present status of our knowledge about the highest-energy particles in Nature

Antonio Condorelli

LLR Colloquium, 17/10/2022

Outline

- ✳Introduction: UHECRs
- ✳The Pierre Auger Observatory & Telescope Array
- ✳UHECRs spectrum, mass composition and arrival direction
- ✳Astrophysical interpretation of UHECR data
- ✳Including source model
- ✳Conclusions and future perspectives

IJCLab Irène Joliot-Curie Laboratoire de Physique des 2 Infinis

Cosmic Ray Spectrum

- It spans over several order of magnitude in energy and flux;
- Several detection techniques are needed;
- Power law: it reflects acceleration mechanism;
- Features can be addressed to propagation and/or acceleration processes.

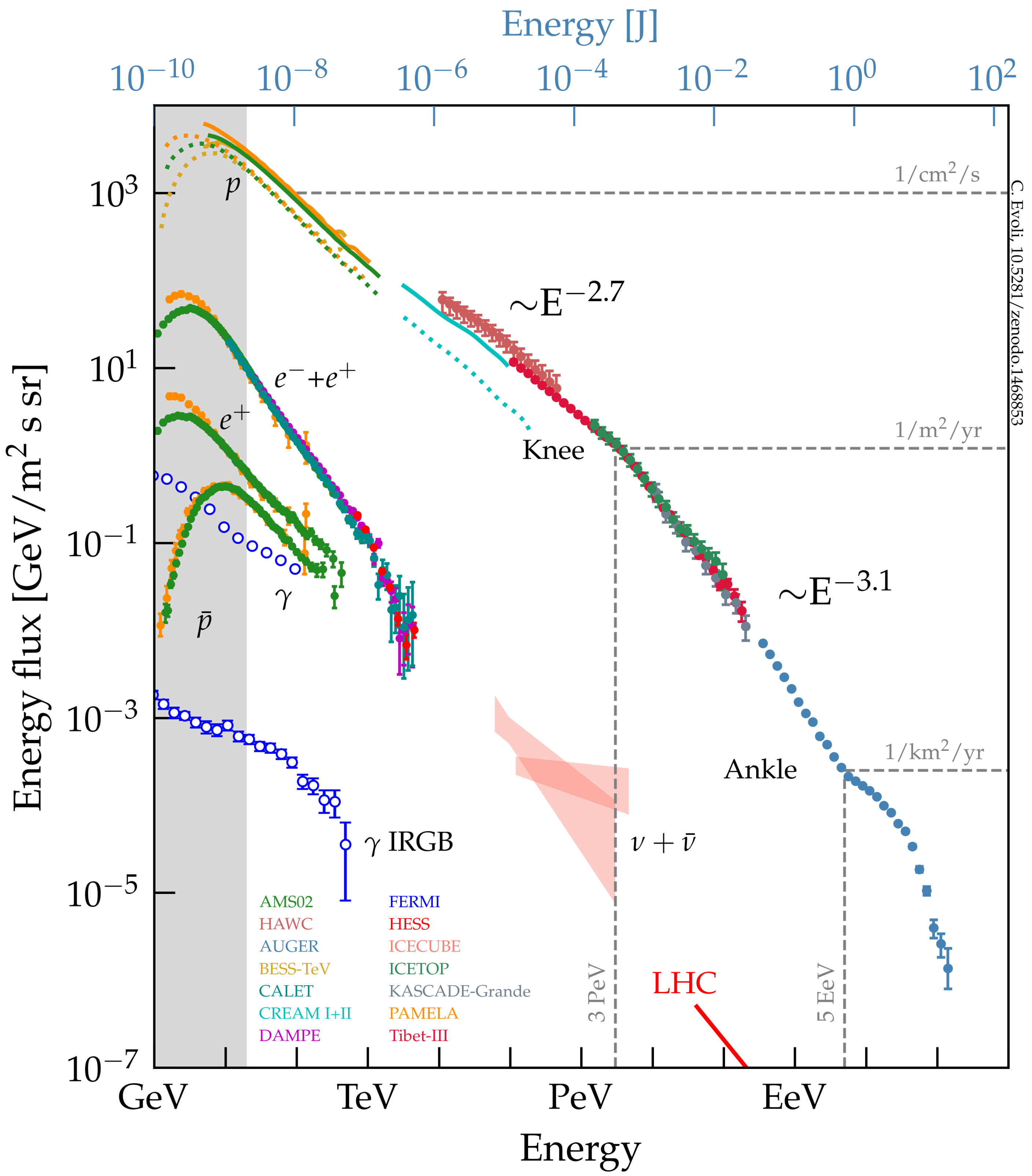

Where do the UHECRs come from?

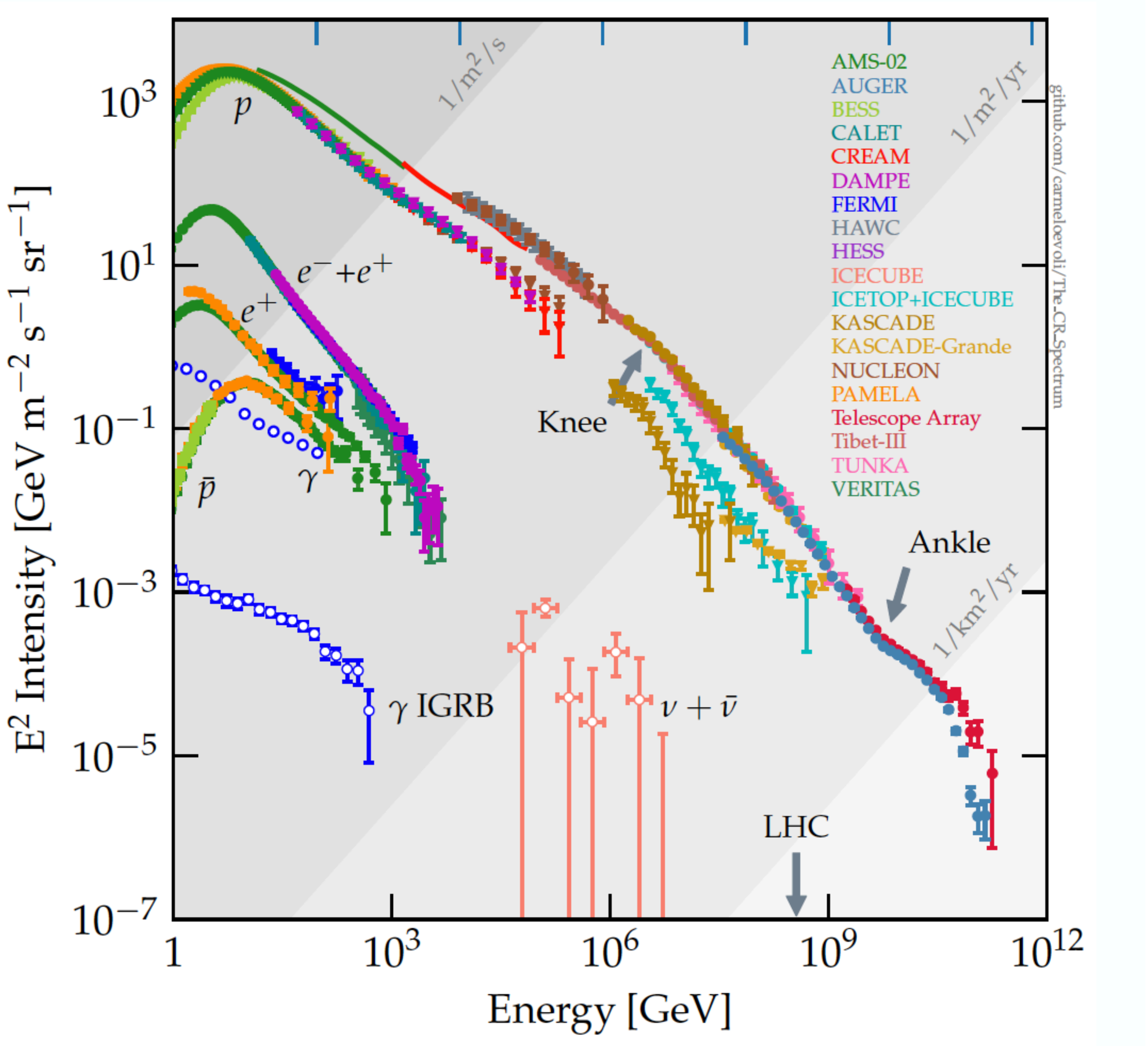

Where do the UHECRs come from?

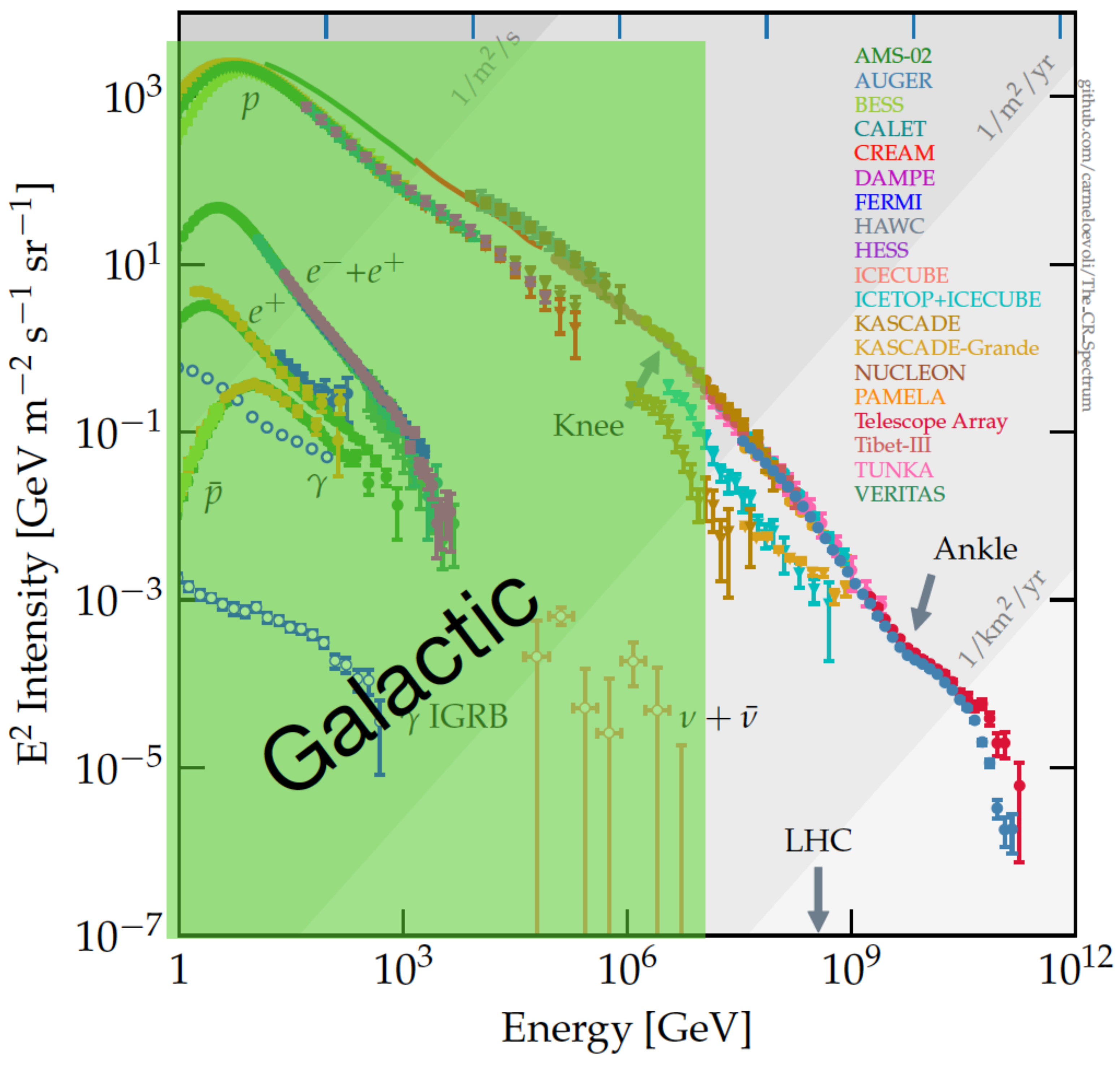

Where do the UHECRs come from?

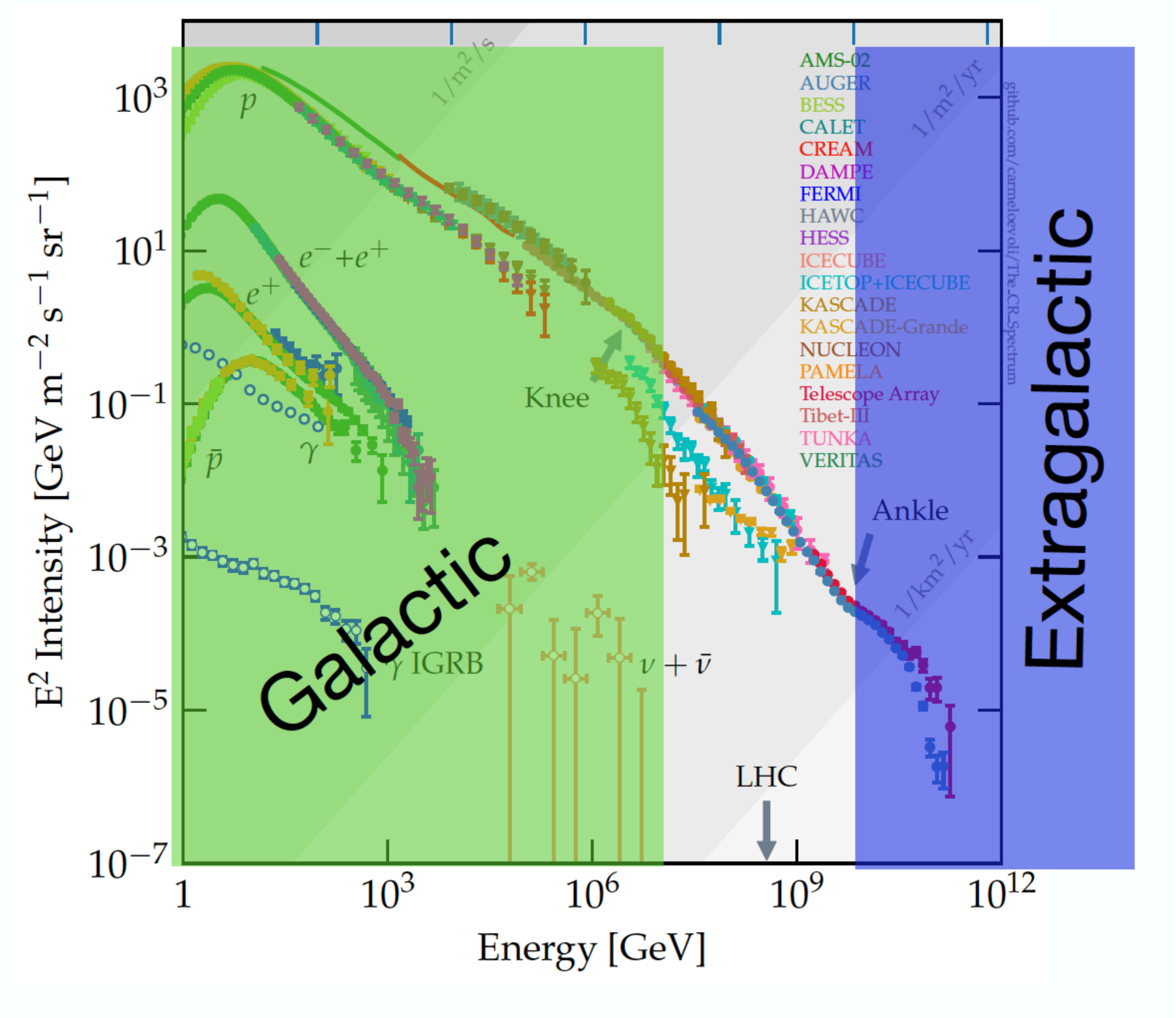

Where do the UHECRs come from?

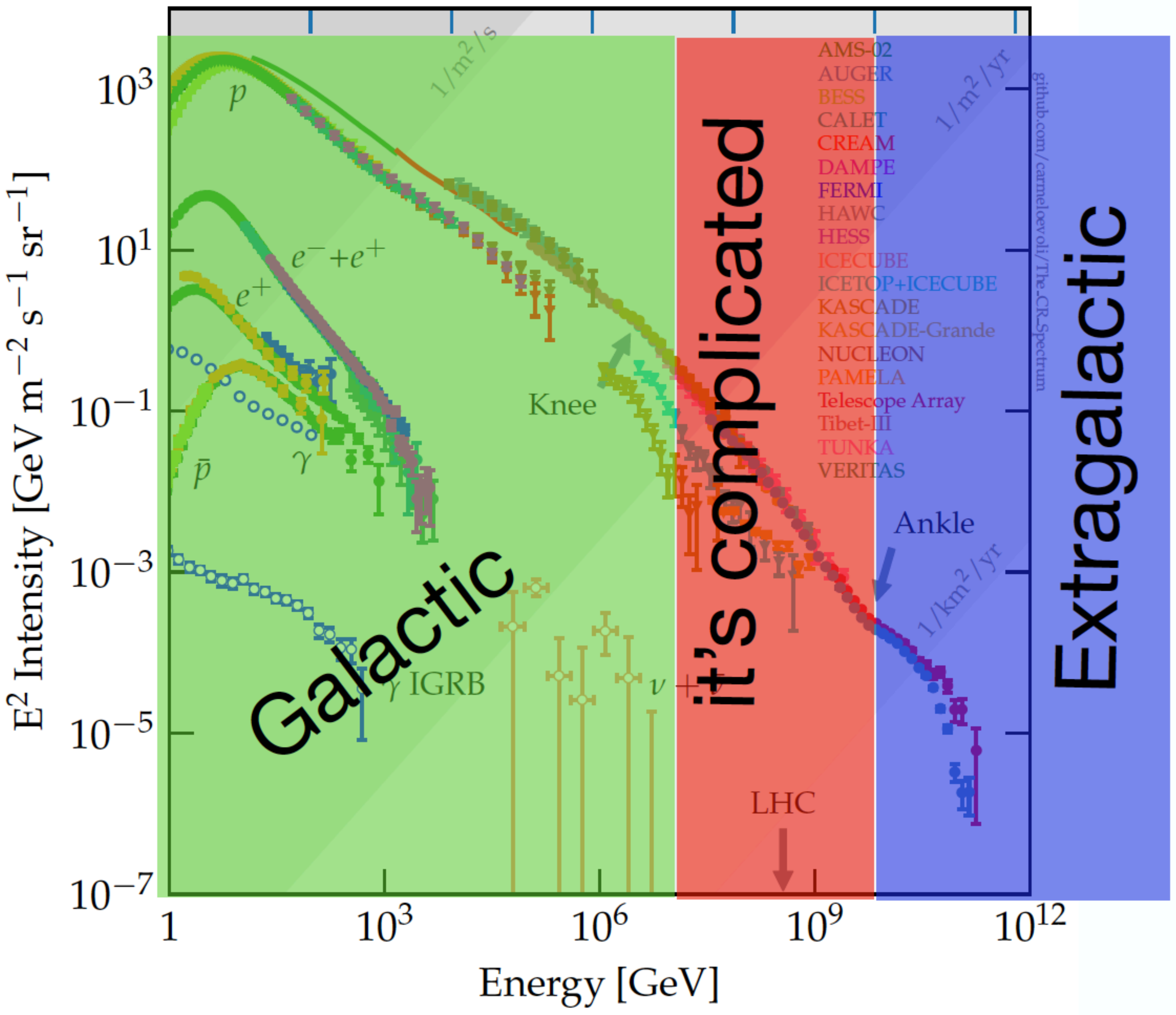

Propagation of UHECRs

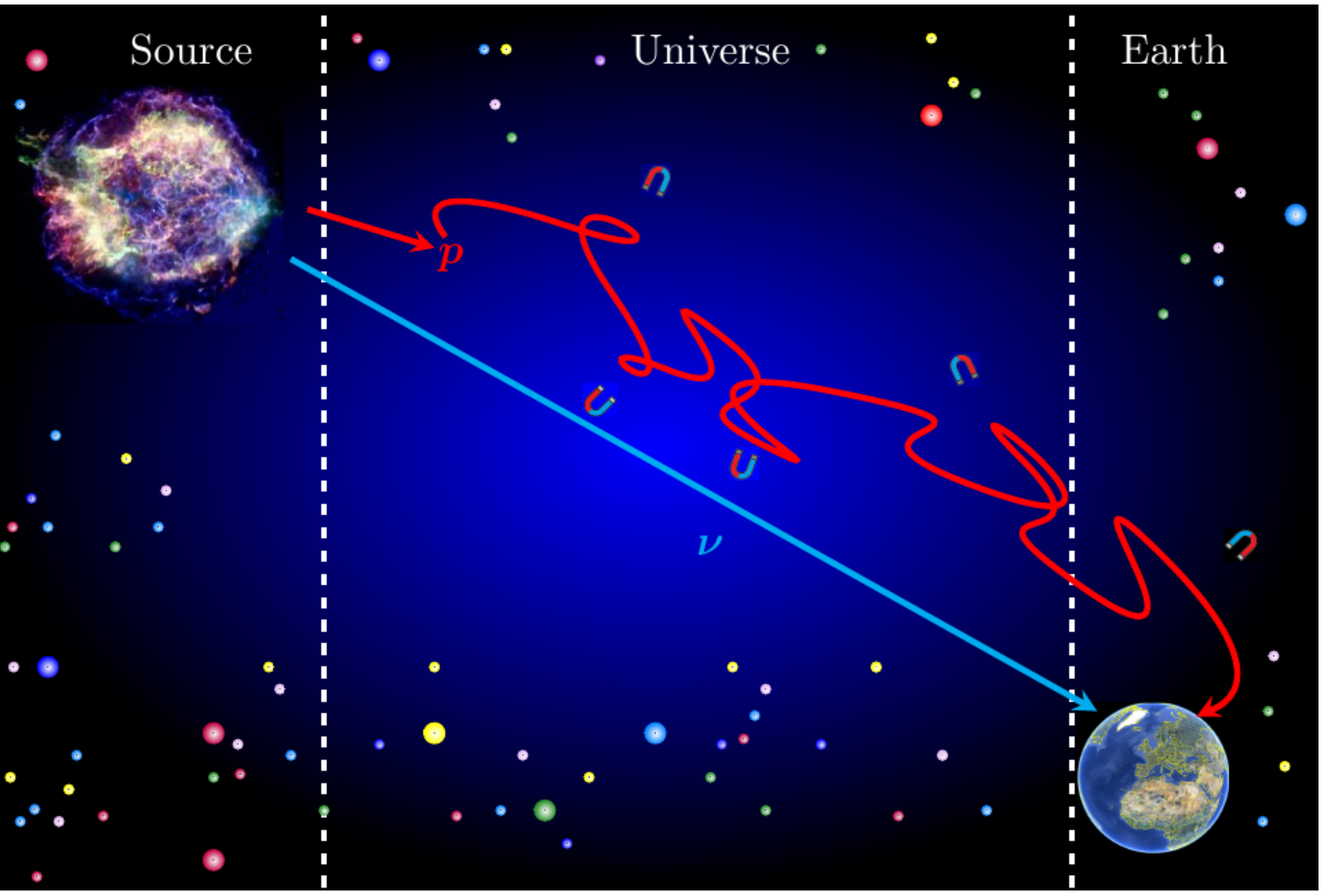

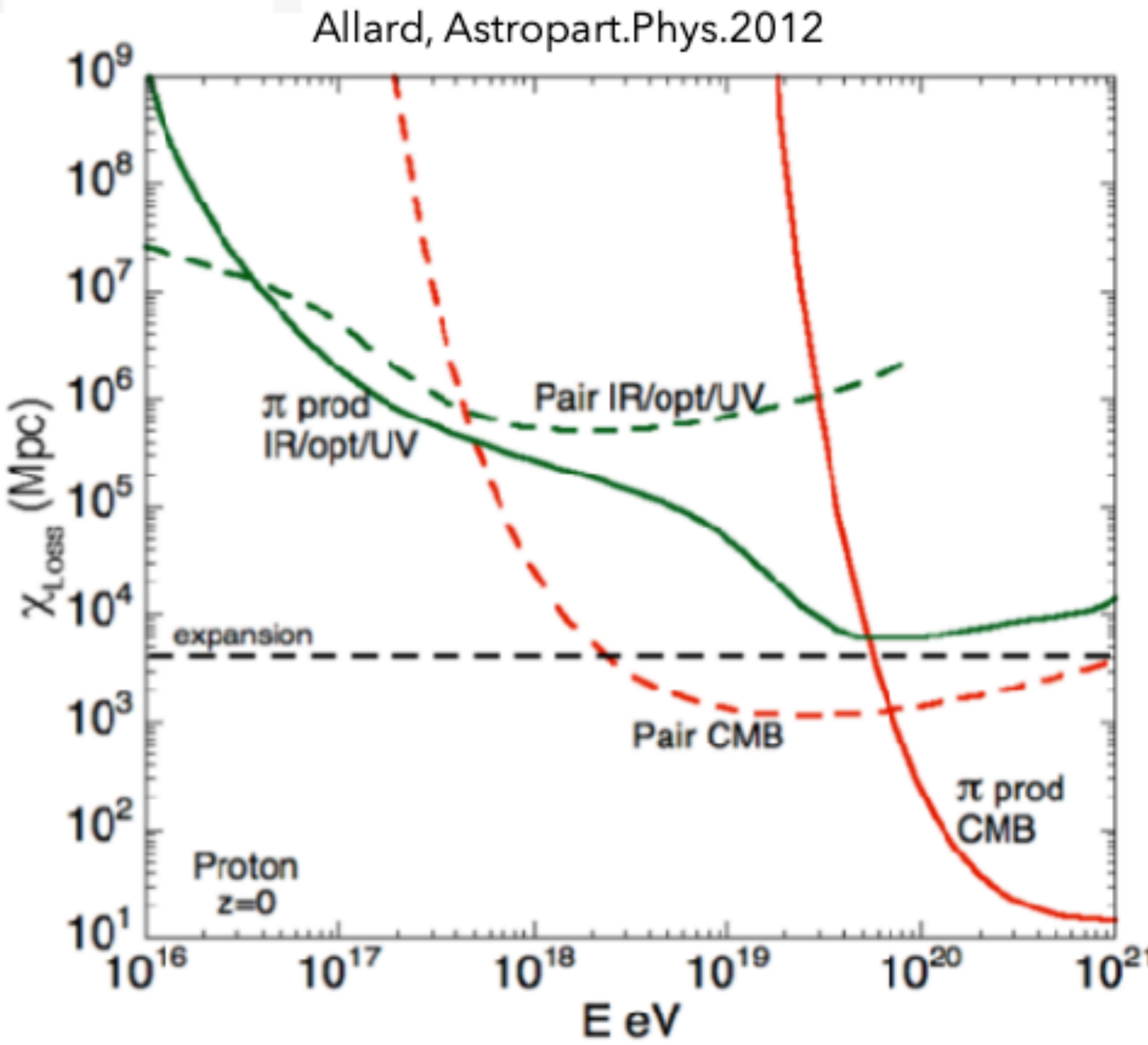

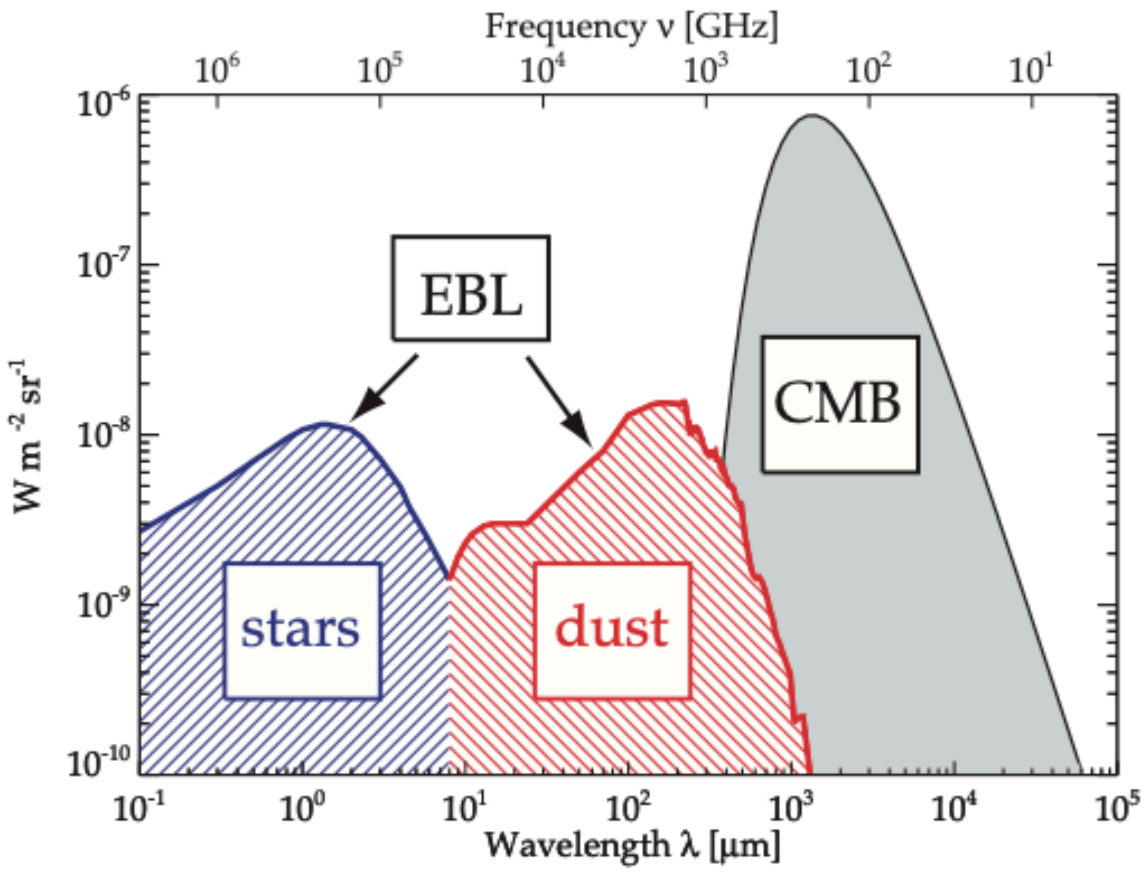

Energy losses in extragalactic space

- Adiabatic expansion of the Universe
- Electron-positron production, photo-pion production due to interactions with CMB and EBL.
- **Universe in UHECRs is not visible above a few hundreds of Mpc**

D. Mazin, AIP Conference Proceedings **1112**, 111 (2009)

IJCLab Irène Joliot-Curie Laboratoire de Physique des 2 Infinis

Indirect detection: Extensive Air Shower (EAS)

The collision of cosmic rays with the atmospheric molecules produces a cascade of particles, called Extensive Air Shower (EAS).

The particles of an EAS initiated by a proton or a nucleus can be roughly divided into three components:

- Hadronic (mostly pions)
- Electromagnetic (e^+, e^-, γ)
- Penetrant (muons and neutrinos)

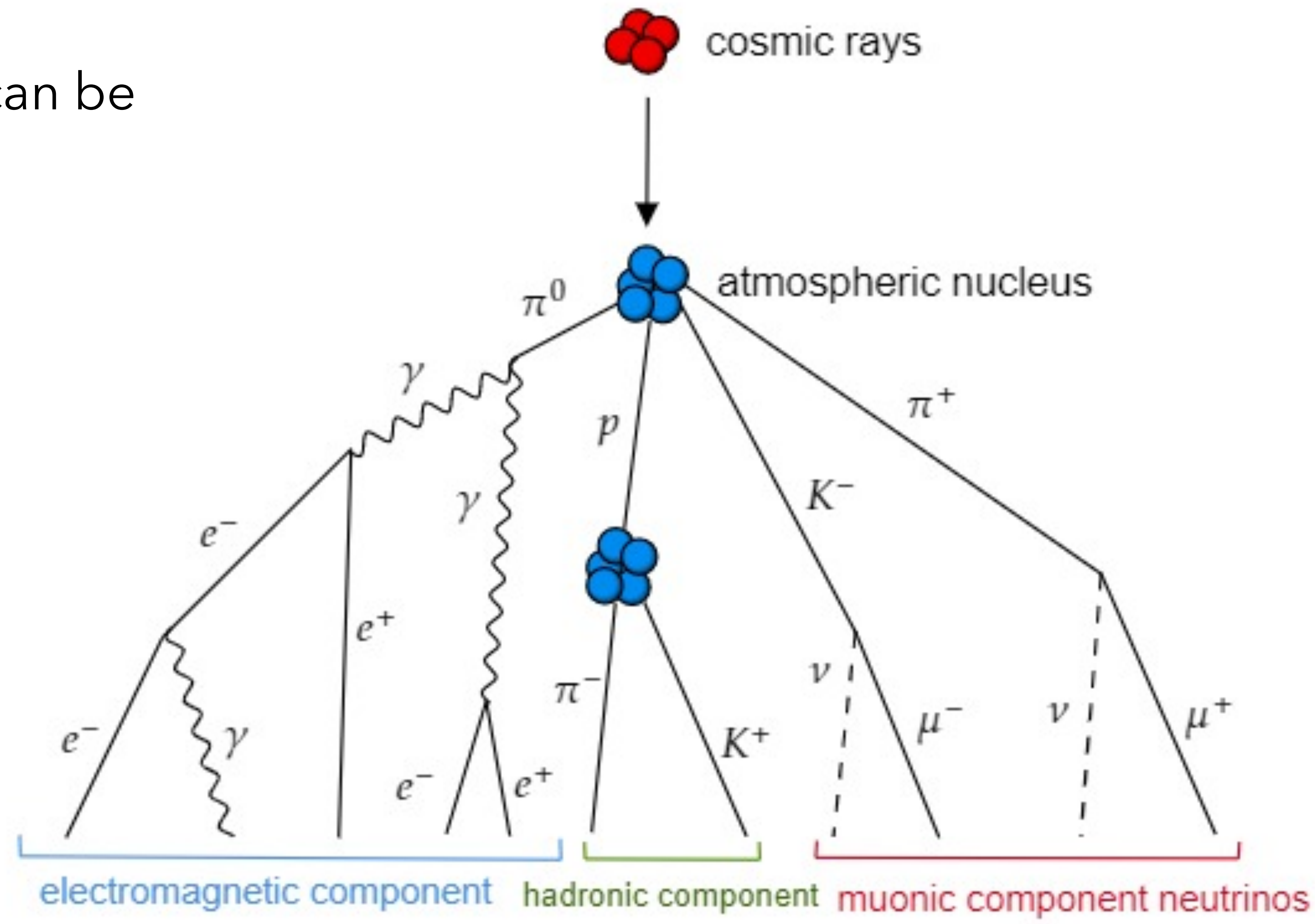

A key information to infer about properties of the primary particle is the depth of the shower maximum

$$X_{max} \propto lg(E/A)$$

https://www.youtube.com/watch?v=vTGSb8P90mc

Indirect detection: Extensive Air Shower (EAS)

https://www.youtube.com/watch?v=vTGSb8P90mc

Auger & TA

The Pierre Auger Observatory

Hybrid detector

Fluorescence detector (FD)
duty cycle 15%
24+3 fluorescence telescopes

Surface detector (SD)
duty cycle 100%
1660 water-Cherenkov detectors

Radio detector (RD)

The Pierre Auger Observatory

Hybrid detector

Fluorescence detector (FD)

duty cycle 15%

24+3 fluorescence telescopes

Surface detector (SD)

duty cycle 100%

1660 water-Cherenkov detectors

Radio detector (RD)

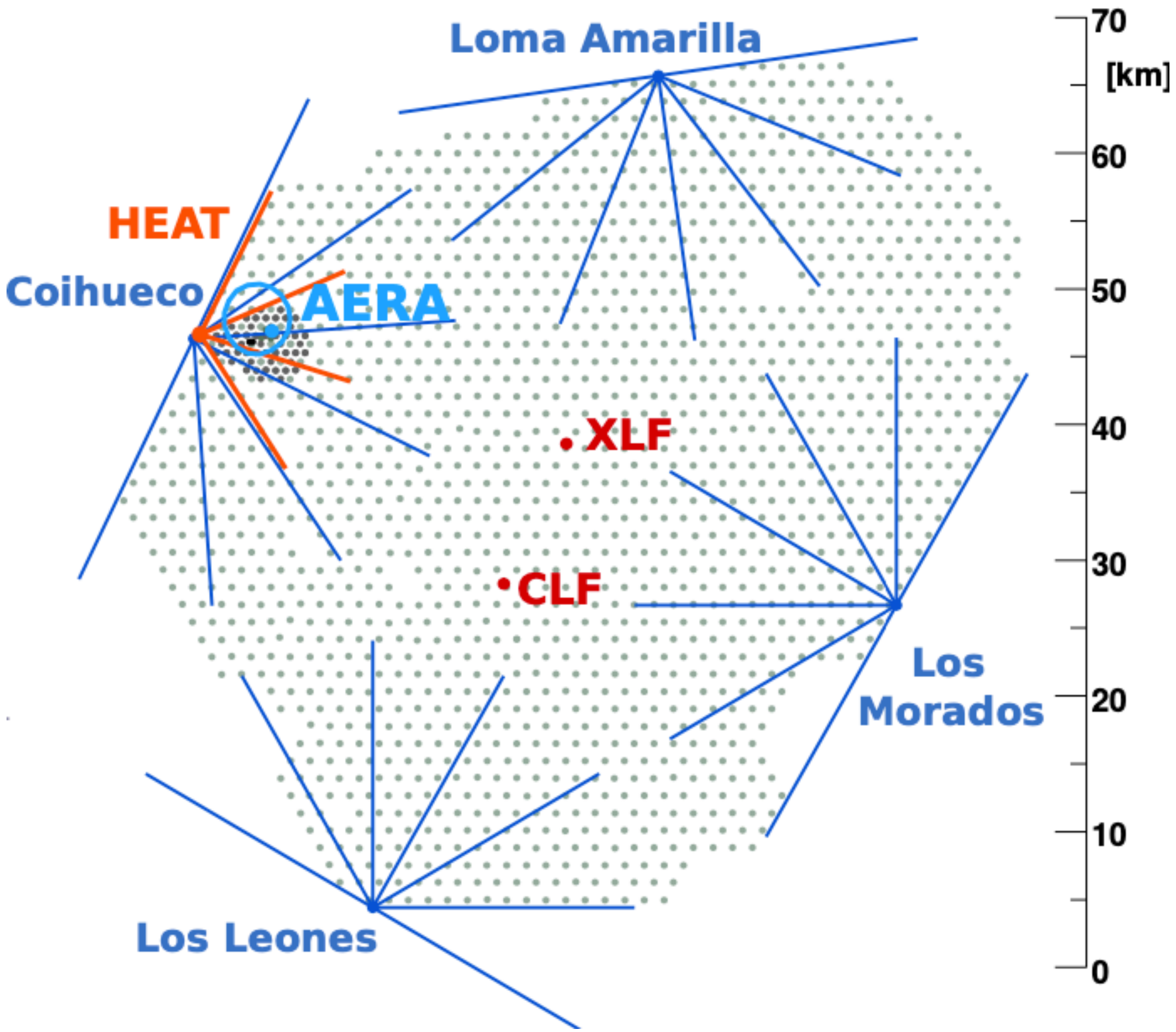

The hybrid detection

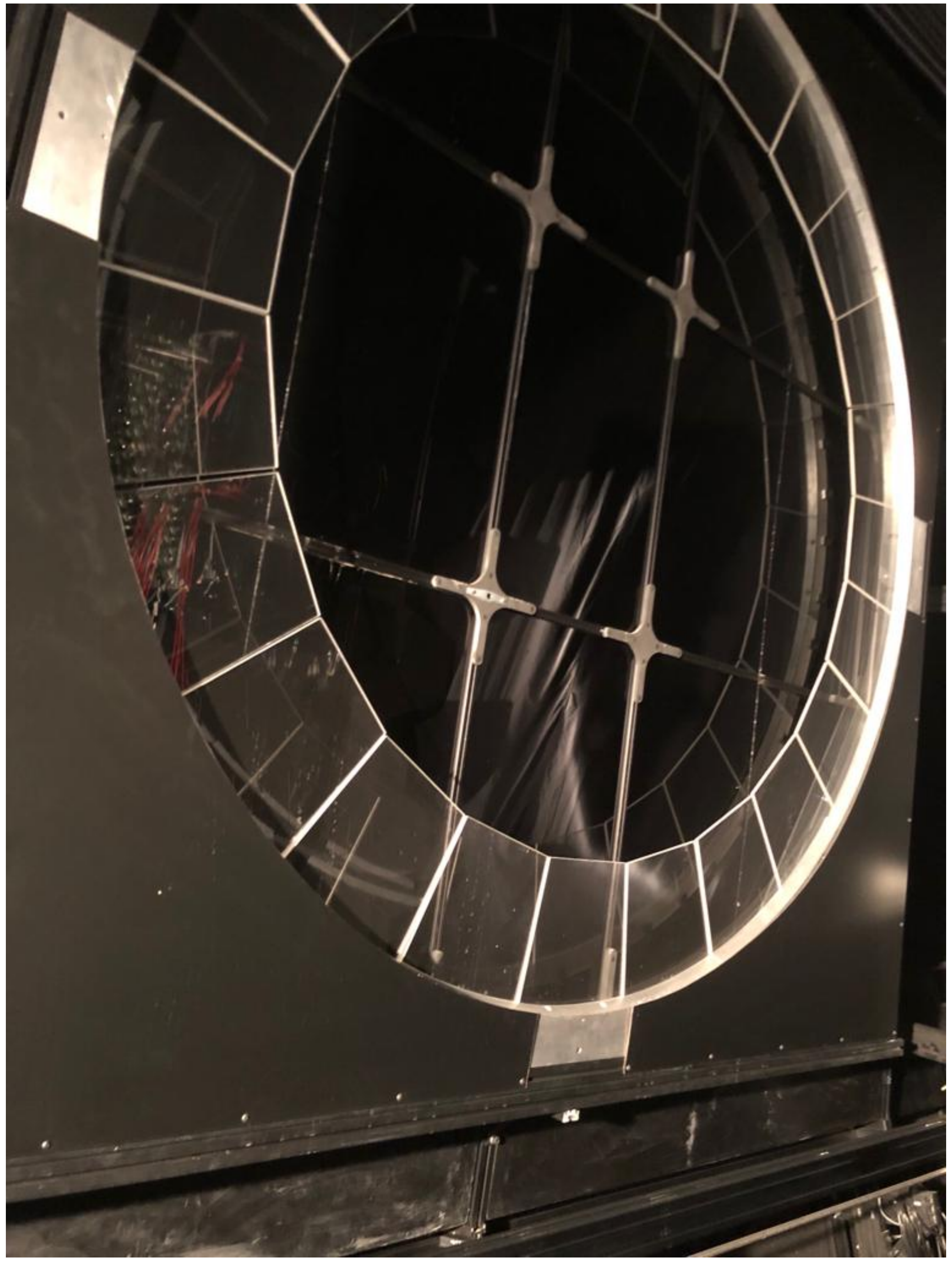
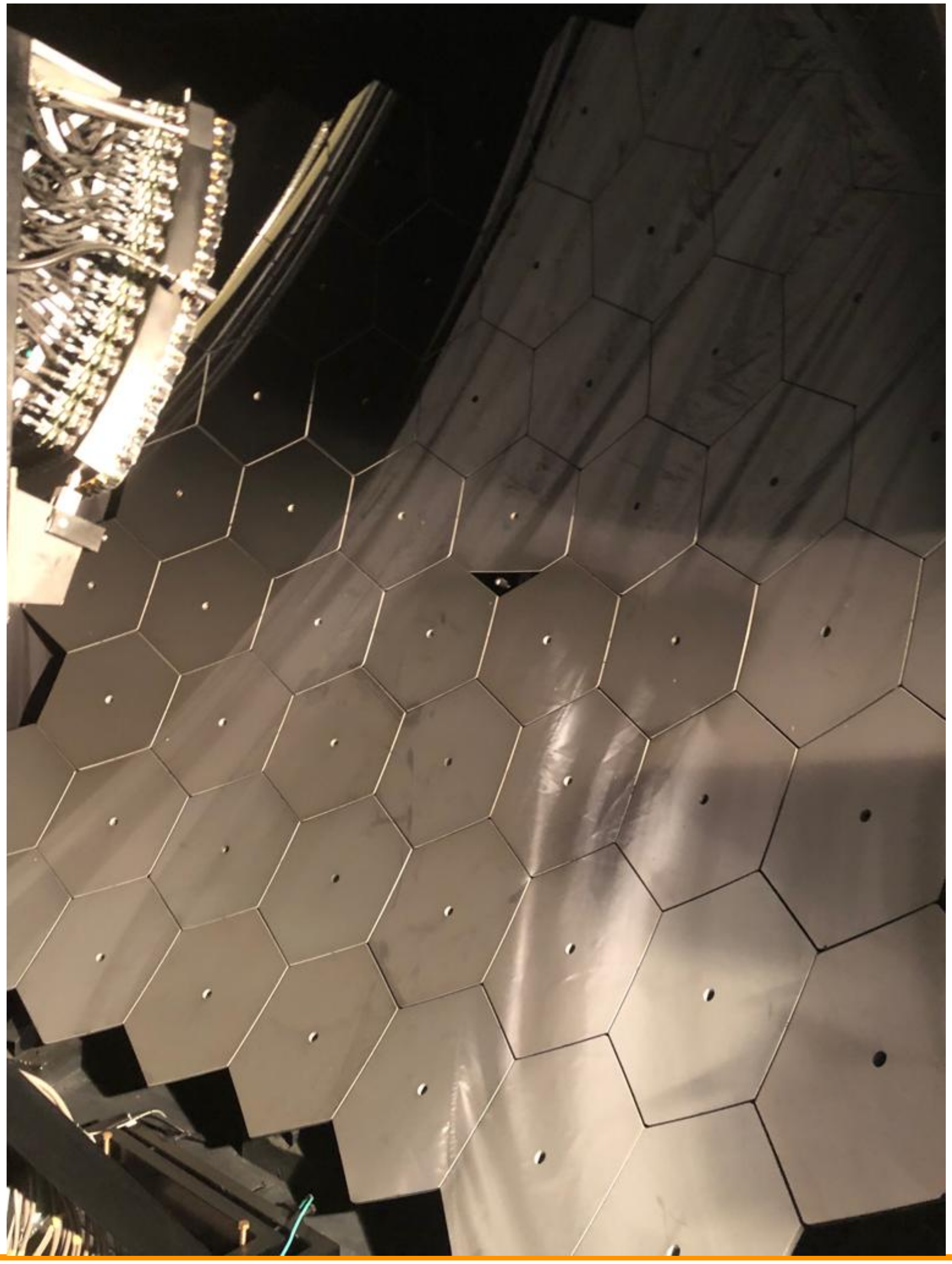
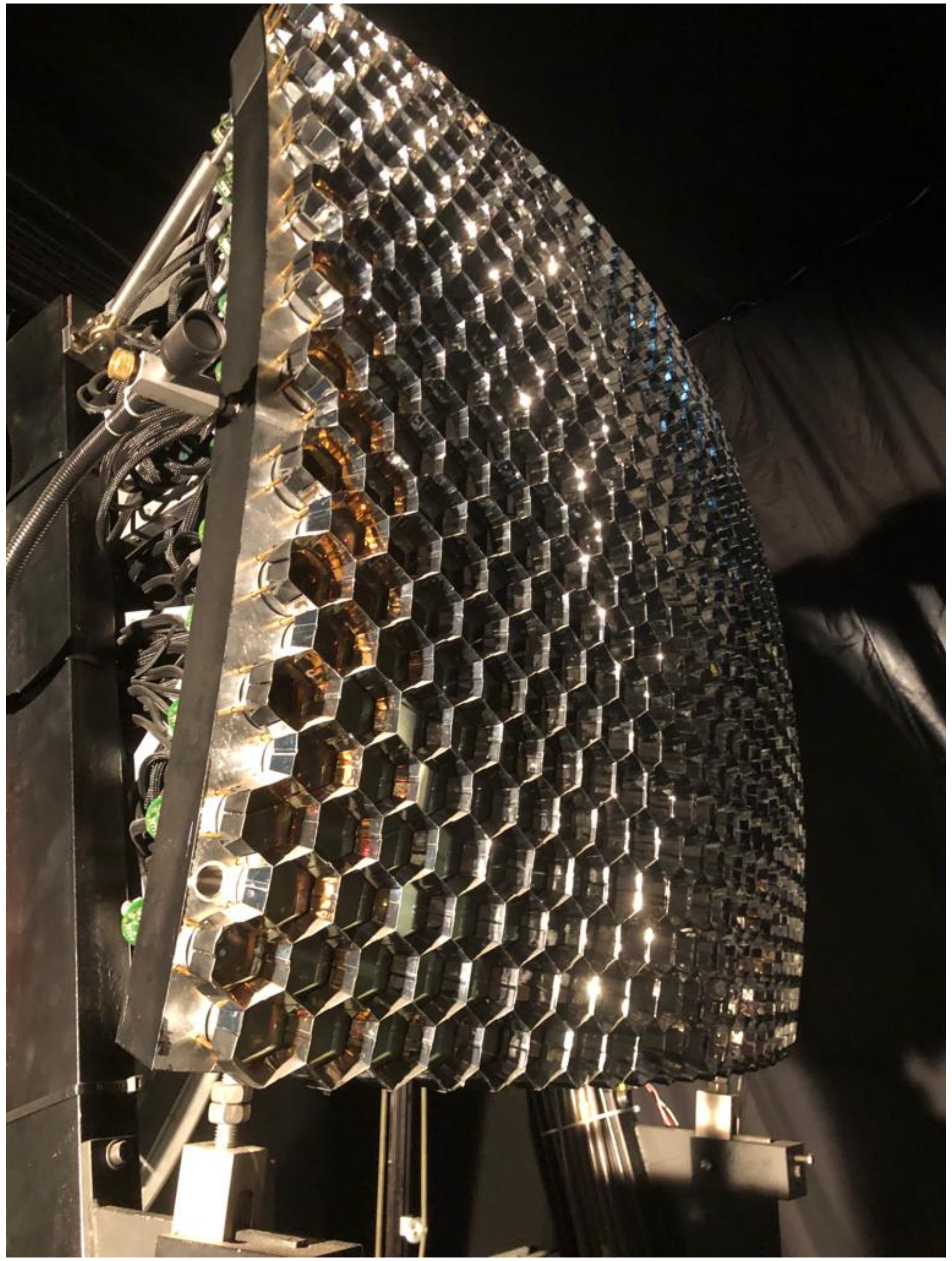

The hybrid detection

IJCLab Irène Joliot-Curie Laboratoire de Physique des 2 Infinis

The hybrid detection

FD telescopes at Los Morados

elevation 1.5° – 30°

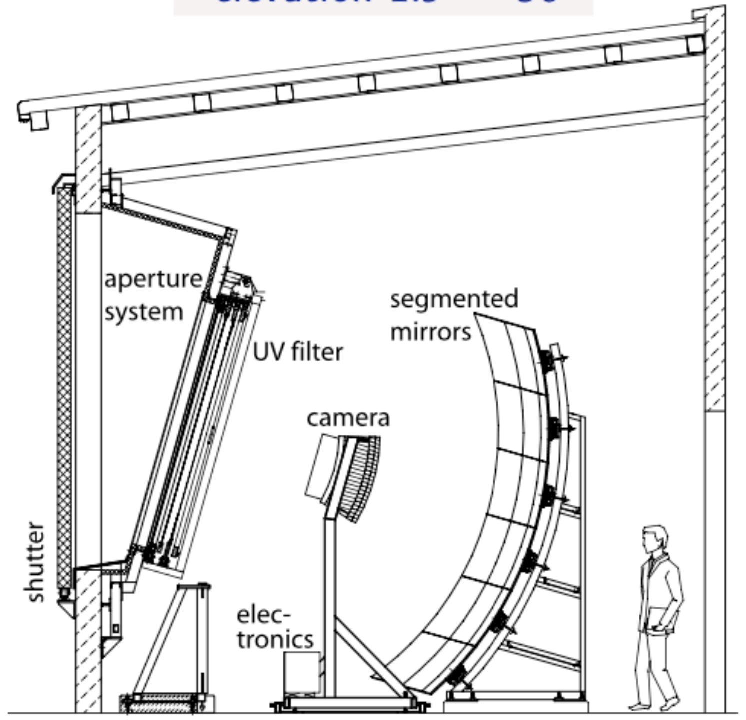

Water-Cherenkov station

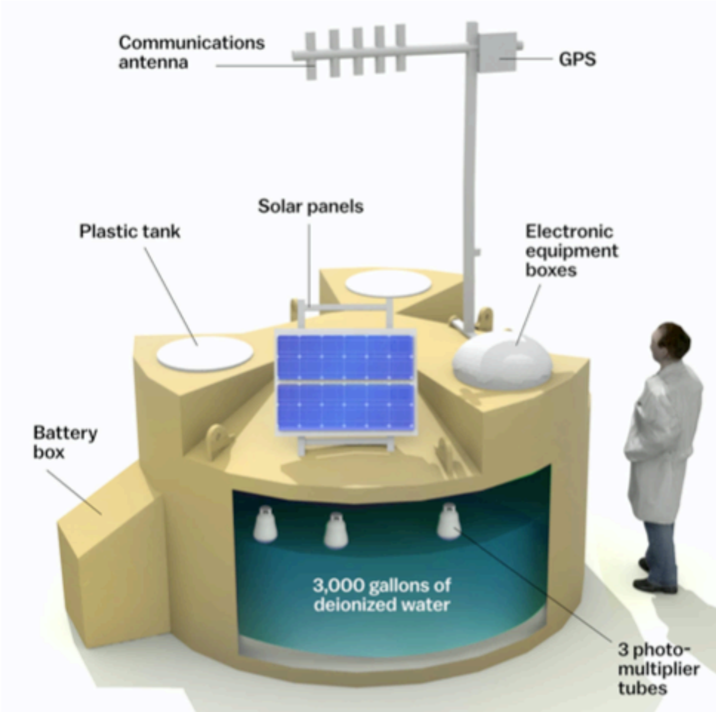

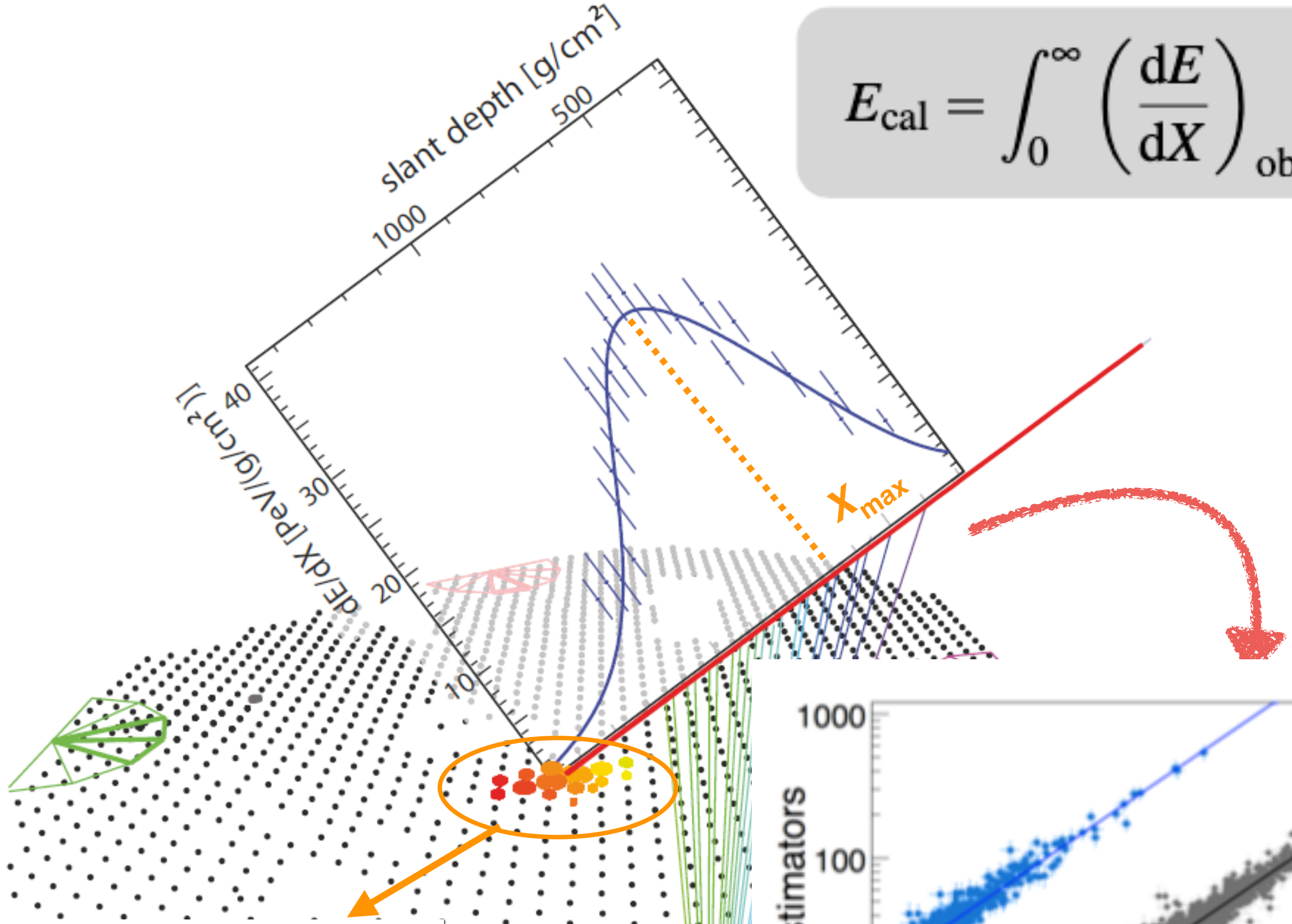

$$E_{\rm cal} = \int_0^\infty \left(\frac{dE}{dX}\right)_{\rm obs} dX$$

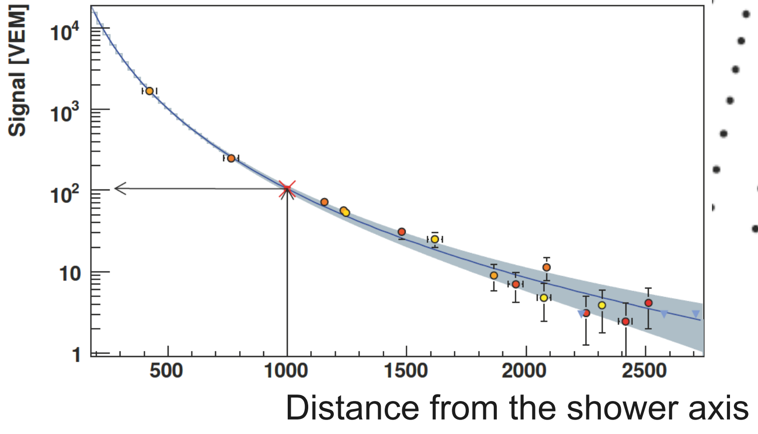

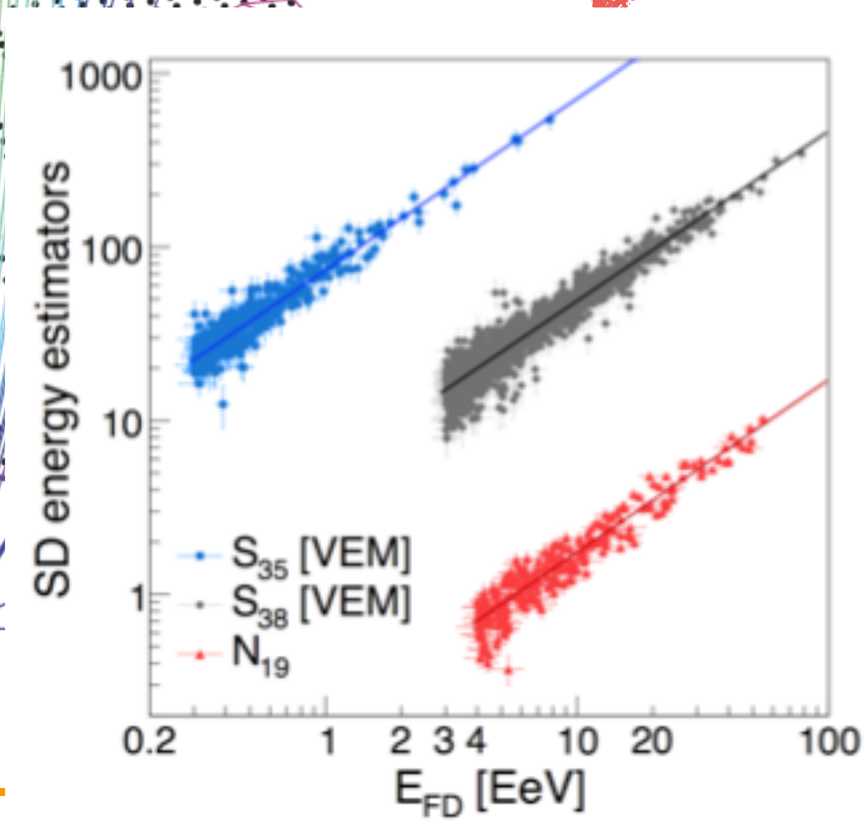

IJCLab Irène Joliot-Curie
Laboratoire de Physique des 2 Infinis

Telescope Array

- The largest cosmic ray observatory in the northern hemisphere

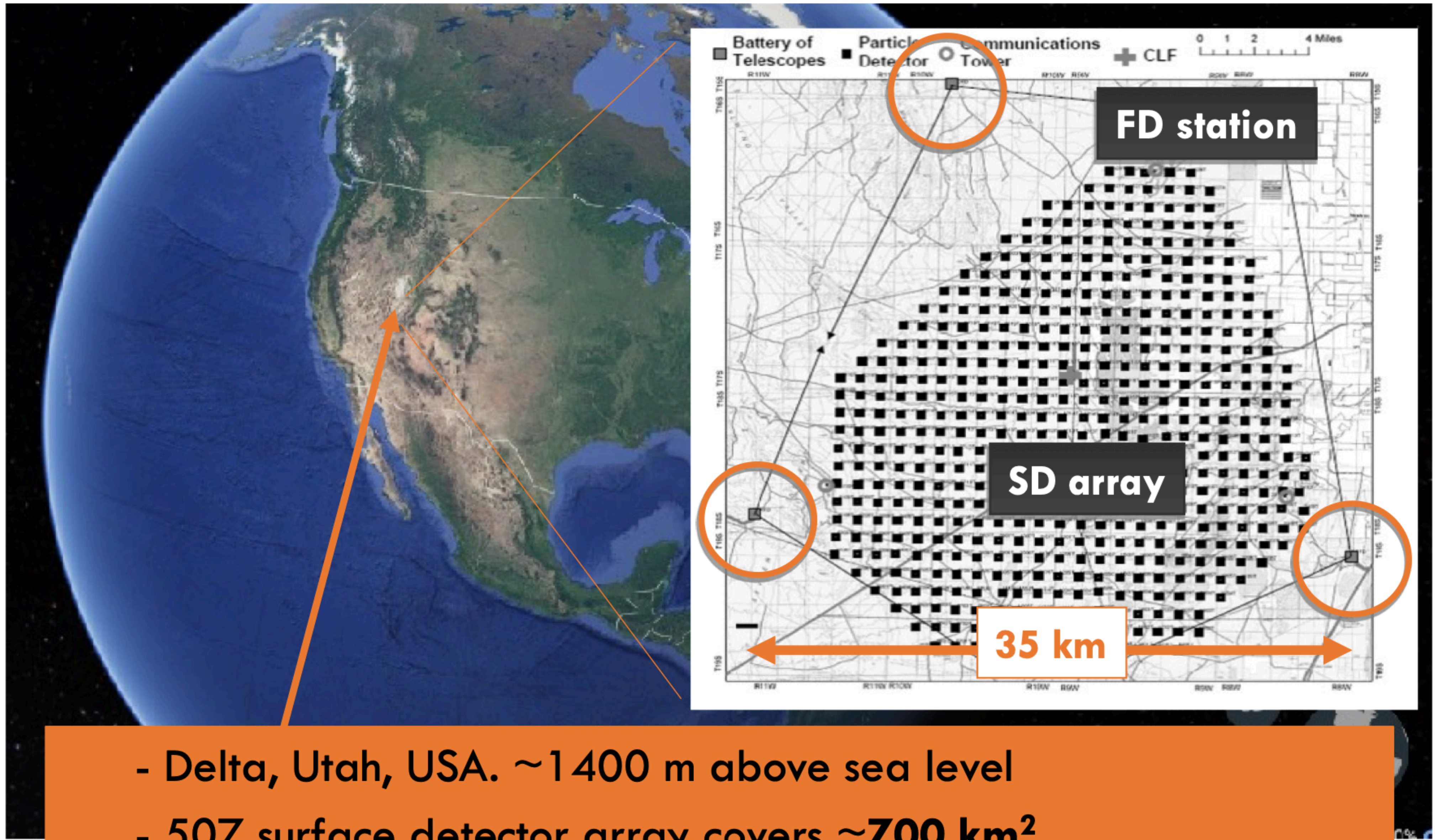

- Delta, Utah, USA. ~1400 m above sea level
- 507 surface detector array covers **~700 km²**
- 38 telescopes at 3 stations to observe the sky above the array

Surface Detector: Plastic Scintillator

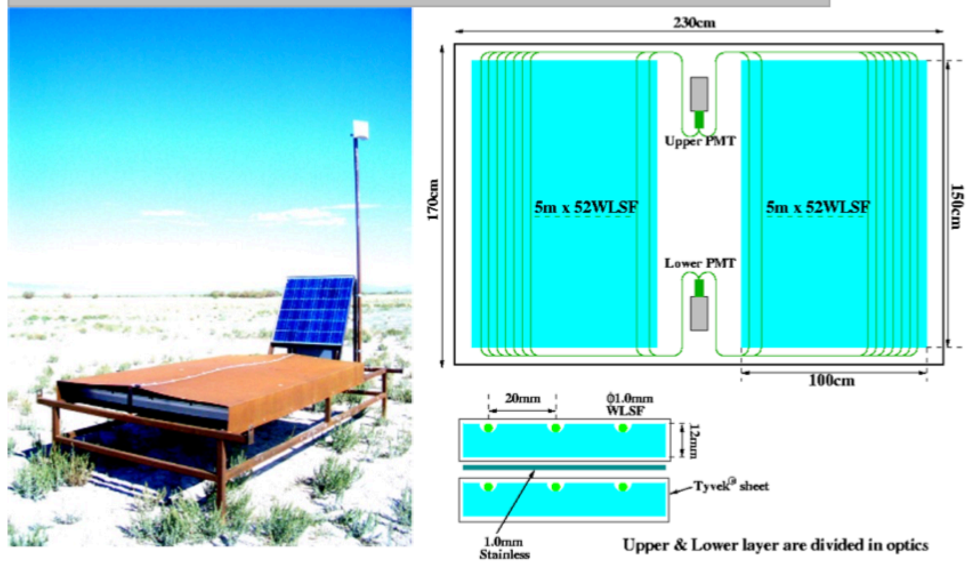

Fluorescence Detector: PMT camera

2022-10-03 UHECR2022 @ L'Aquila, Italy 4

Main results

UHECR spectrum

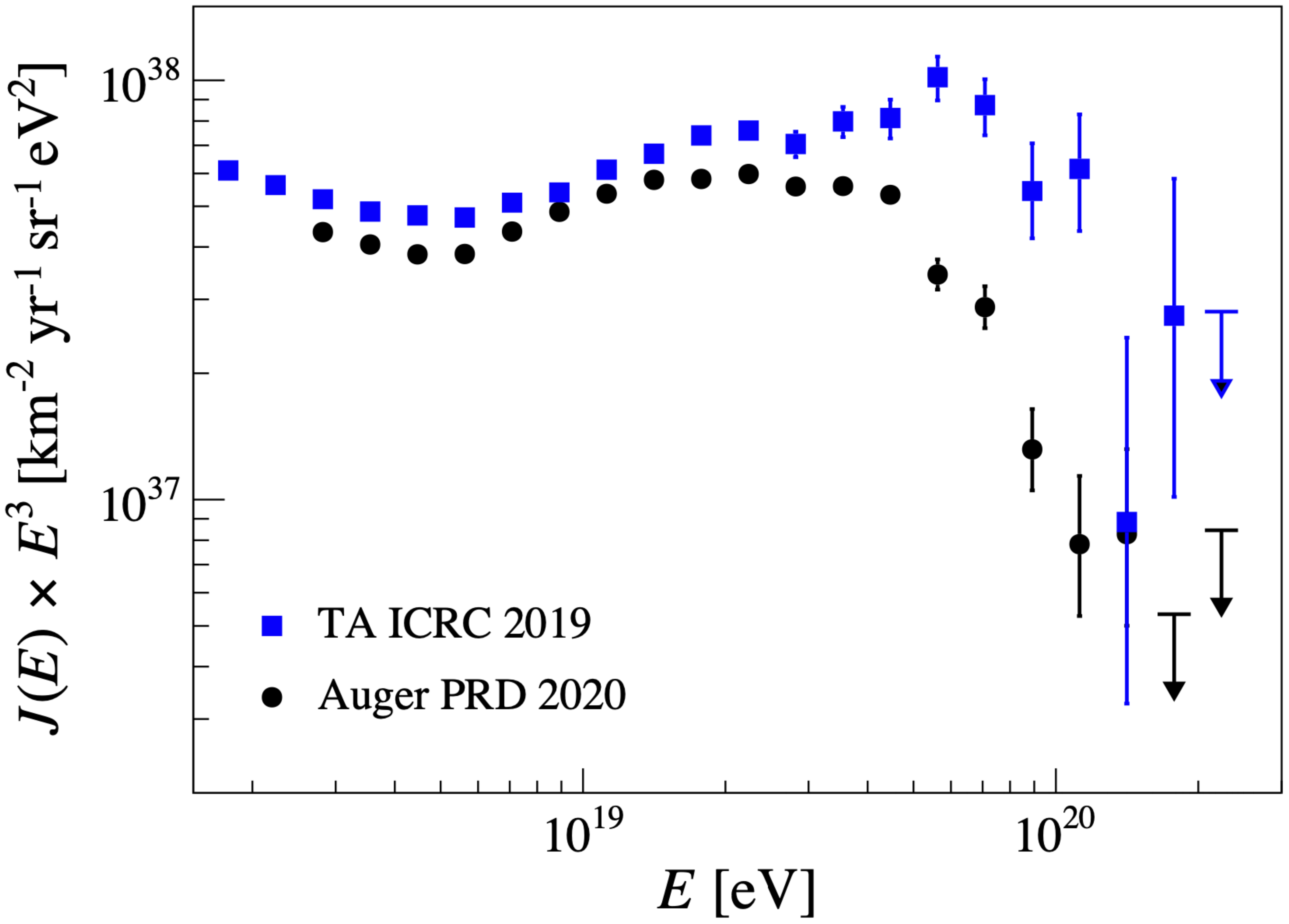

ratio of Auger to TA energy spectrum

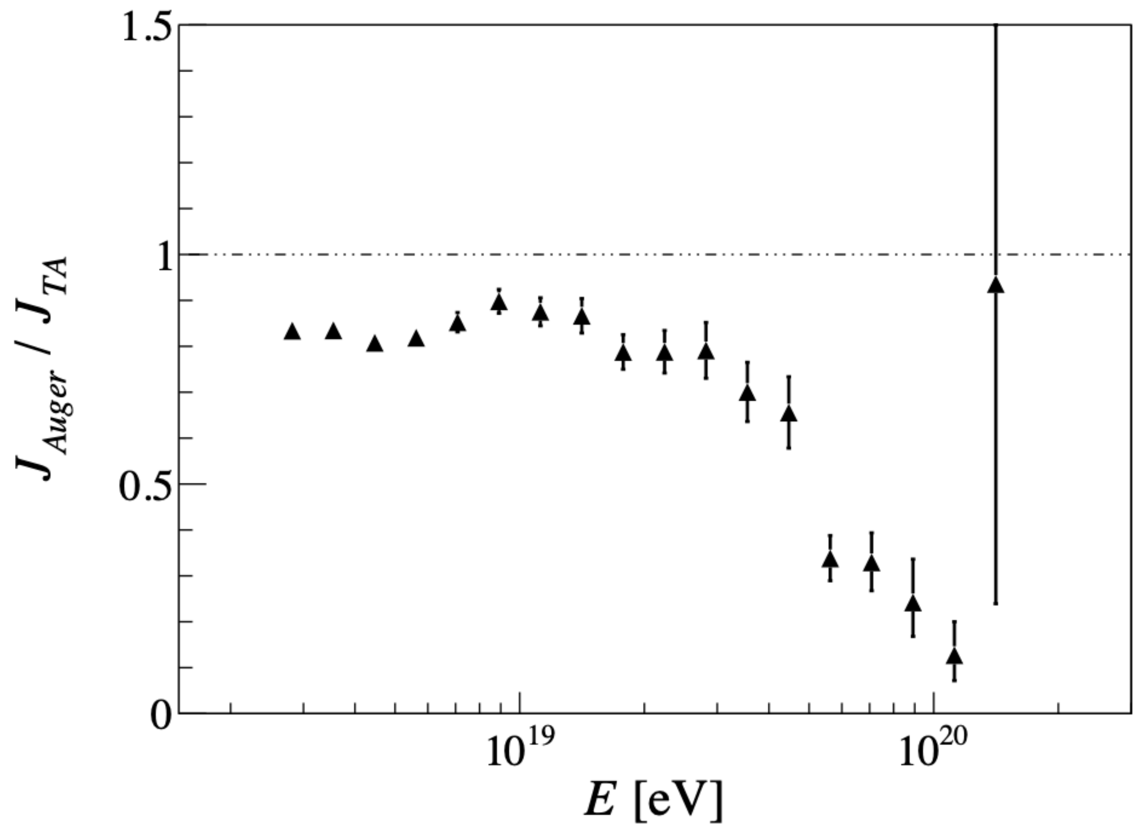

UHECR spectrum

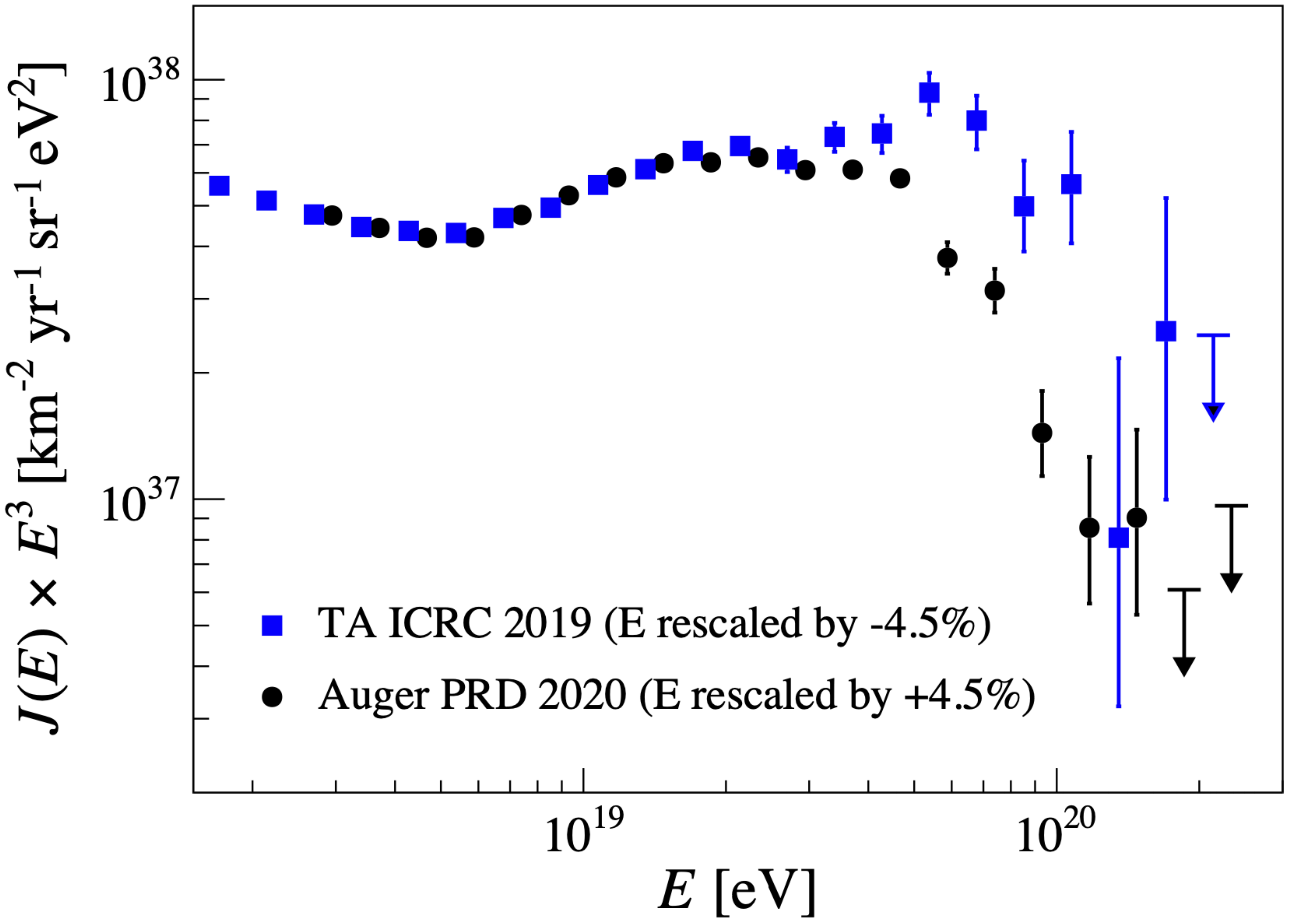

good agreement up to ≈ 10^{19} eV after an overall 9% rescaling of the energies

significant discrepancy at the highest energies

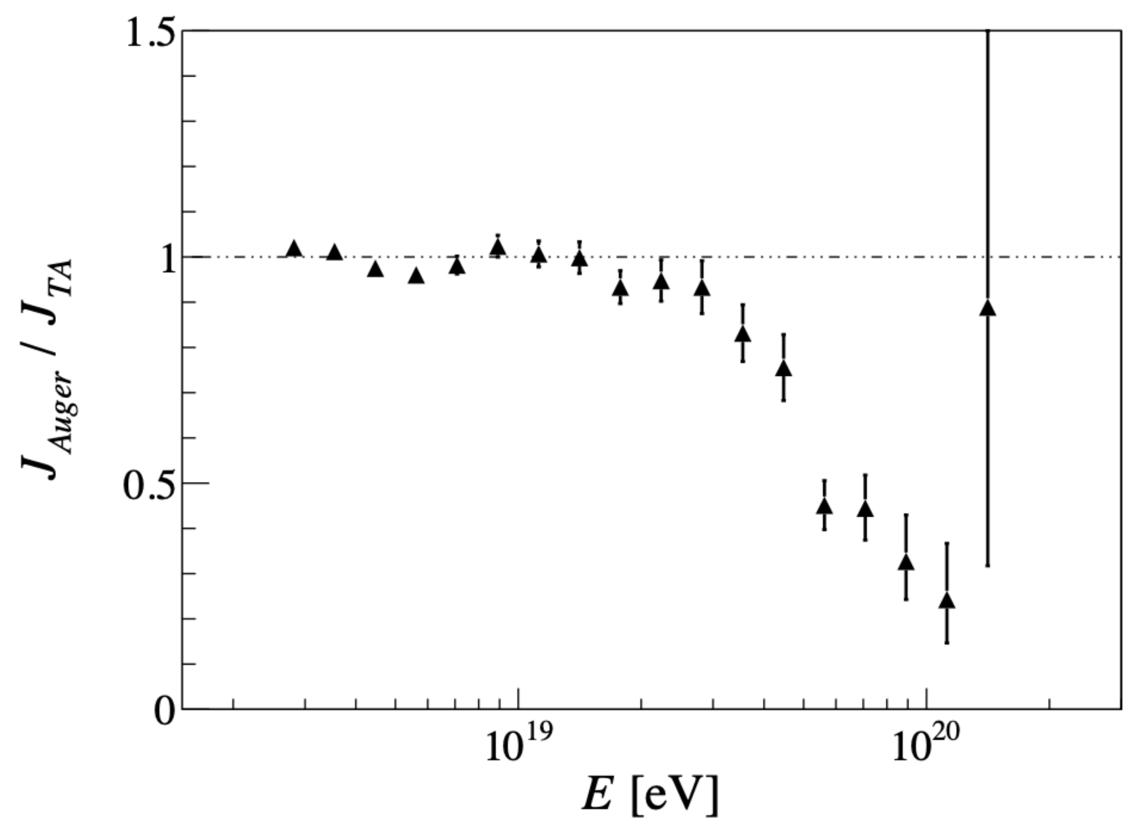

UHECR spectrum

note: TA full trigger efficiency E>$10^{18.8}$ eV

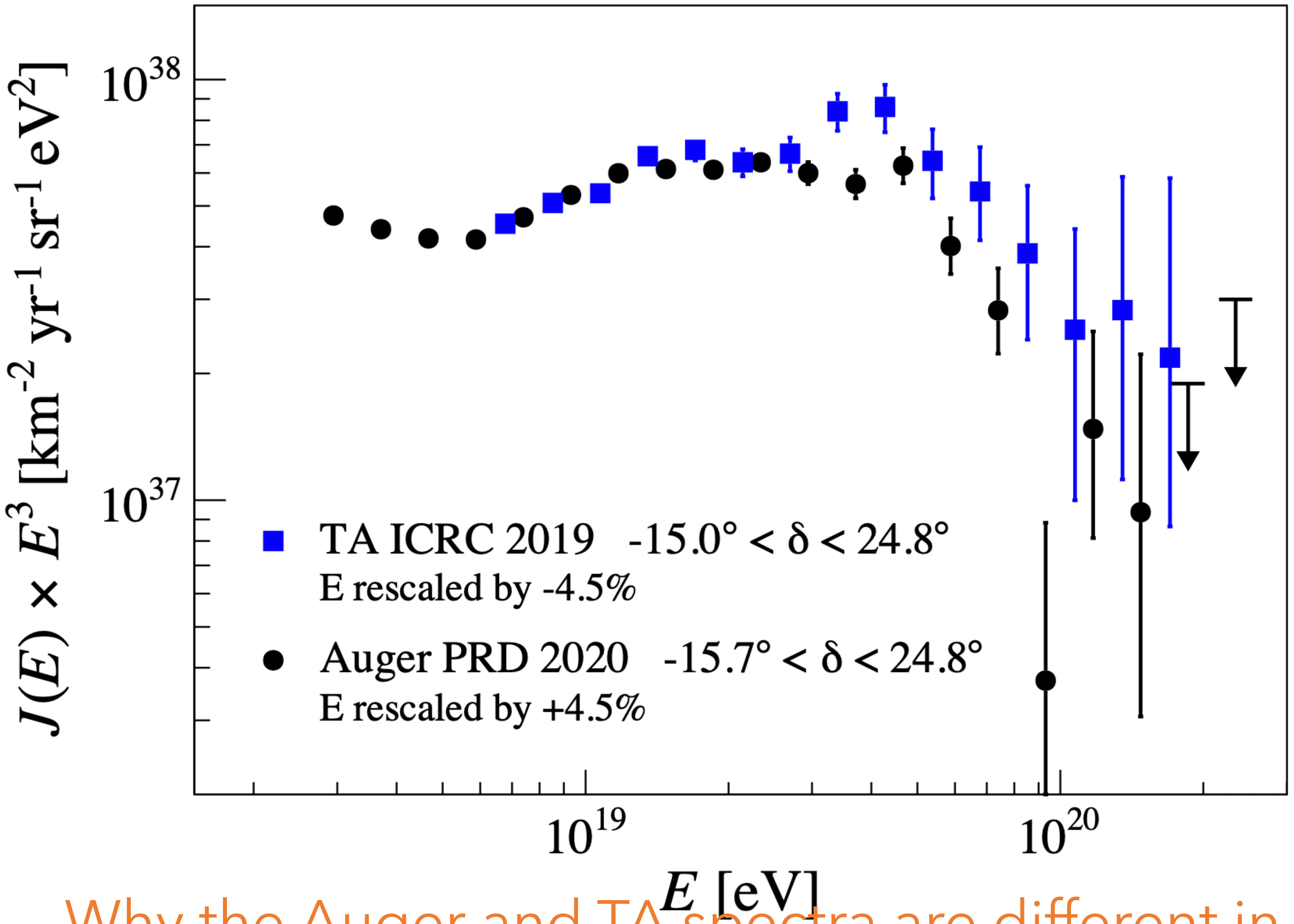

discrepancy at the highest energies persists in the common declination band

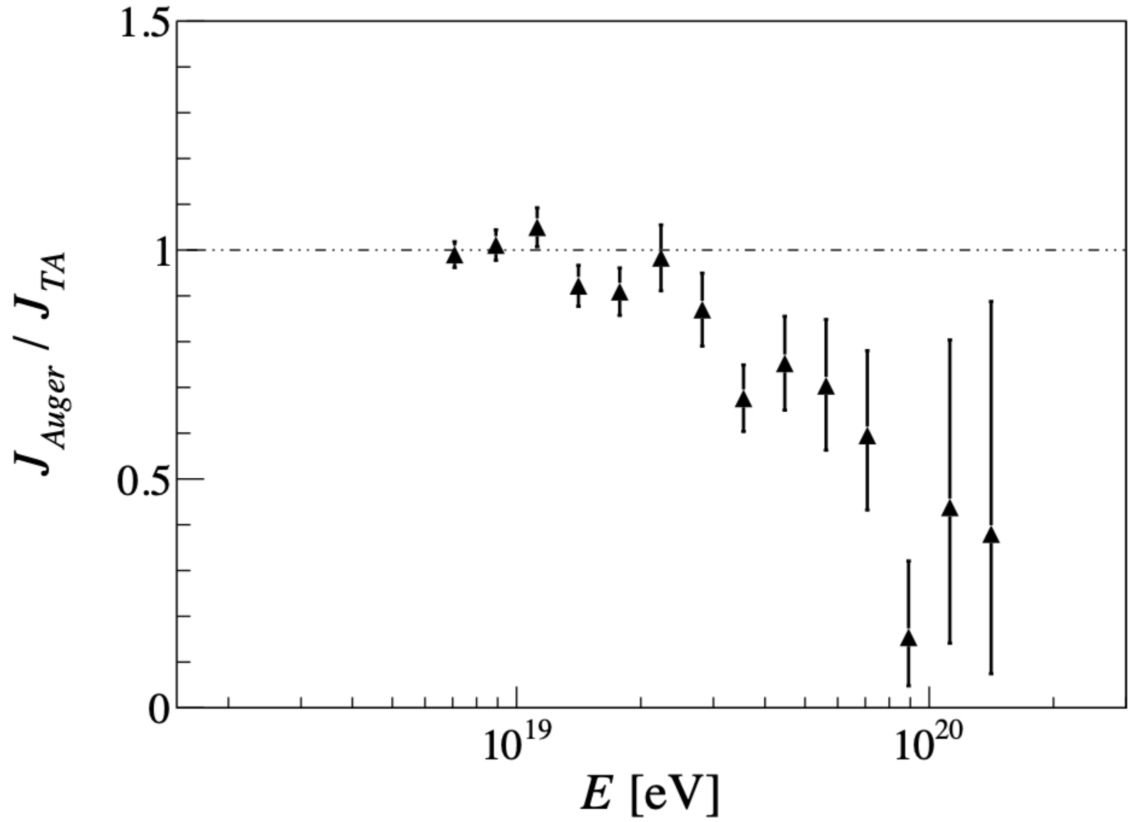

Why the Auger and TA spectra are different in the same declination band?

Possible systematics?

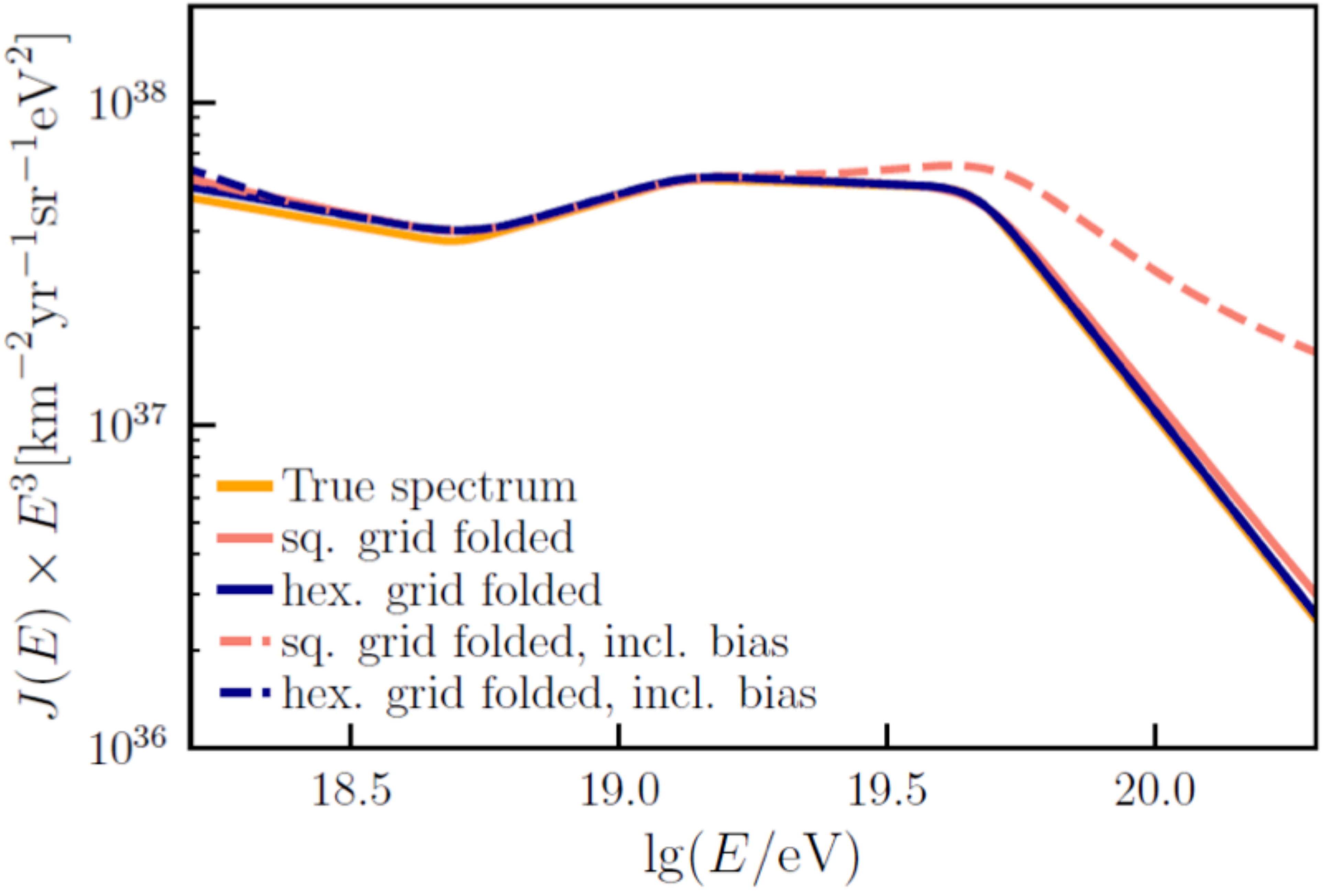

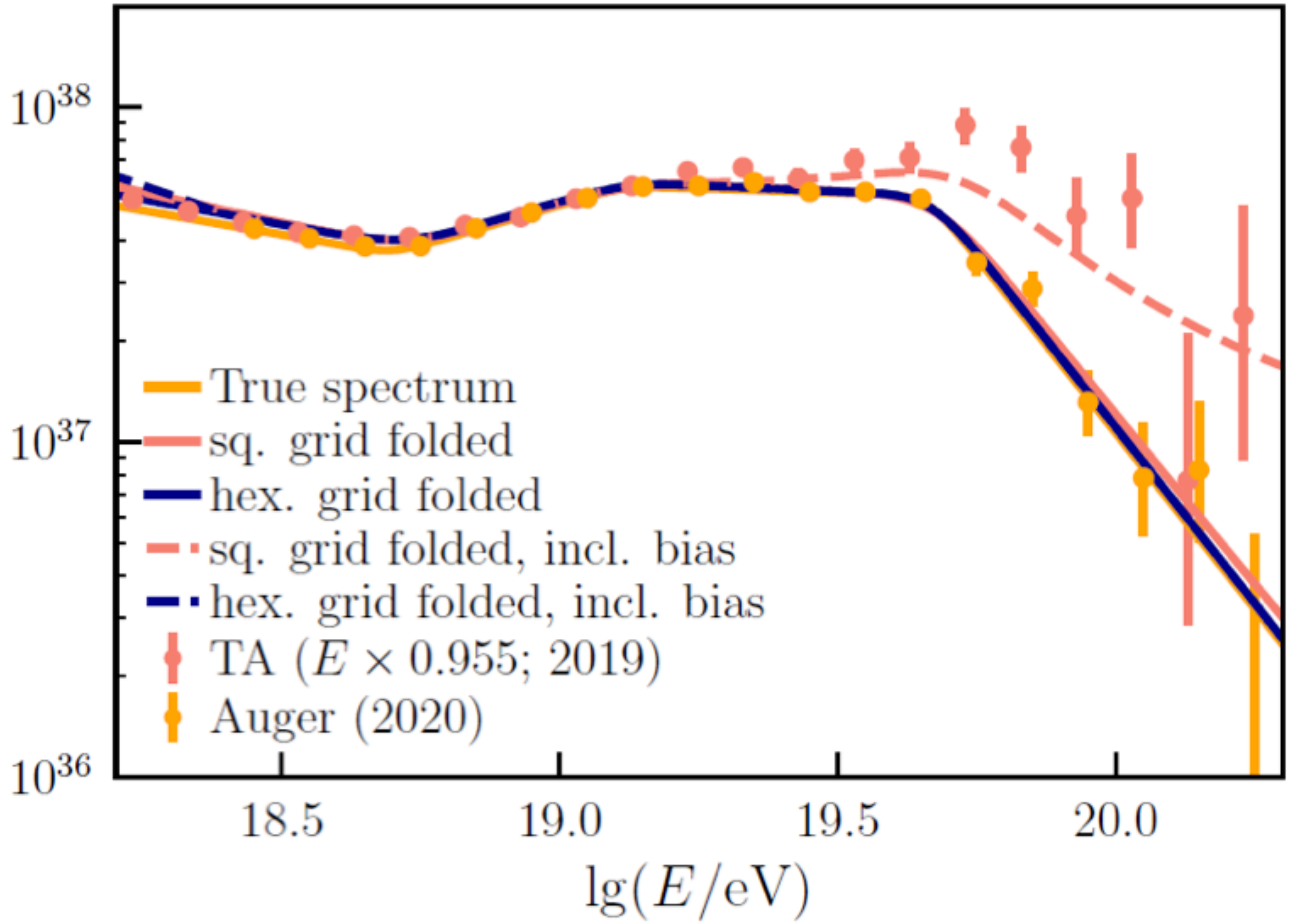

Possible explanation: different grid

IJCLab Irène Joliot-Curie Laboratoire de Physique des 2 Infinis

Mass composition

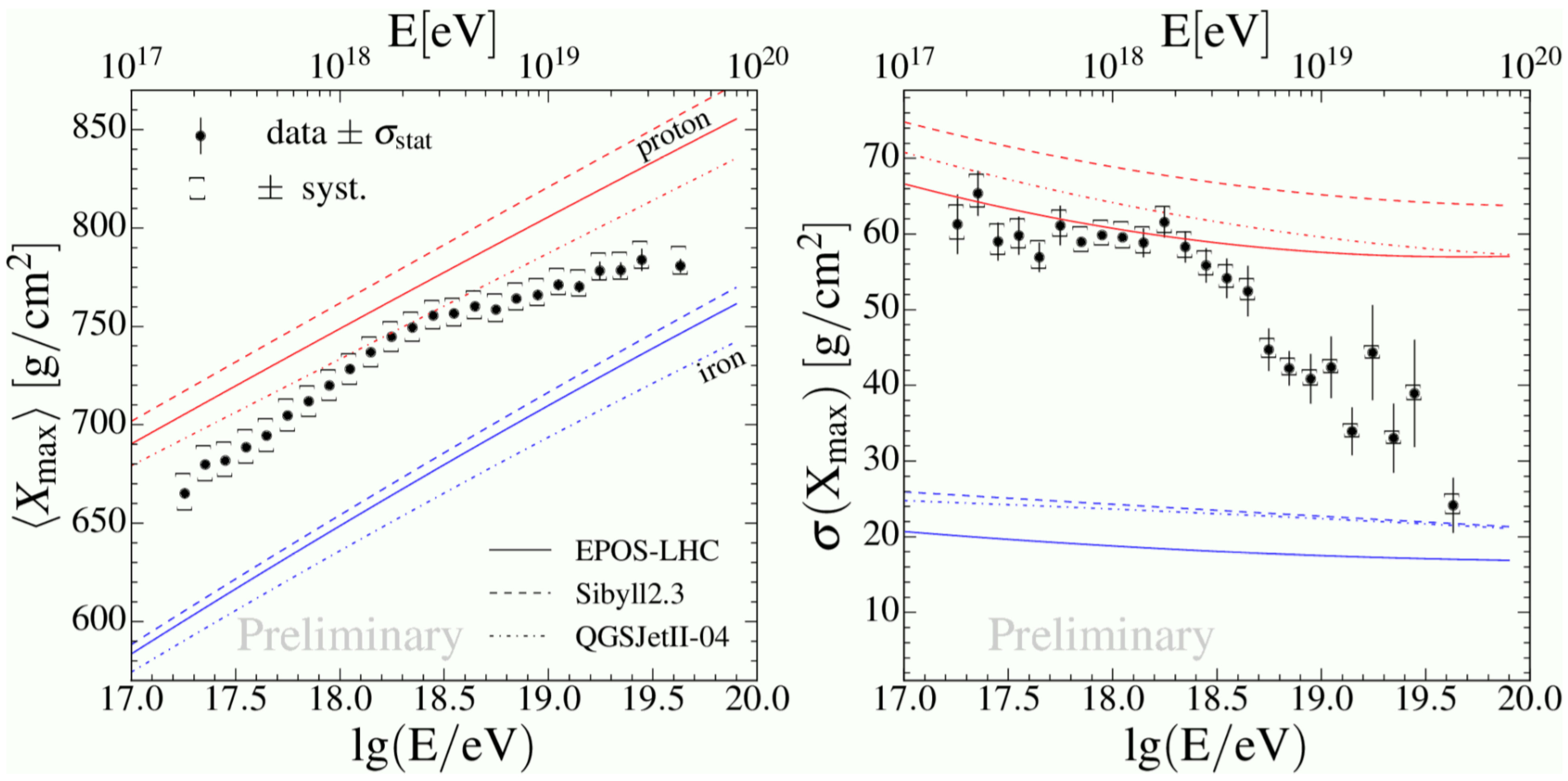

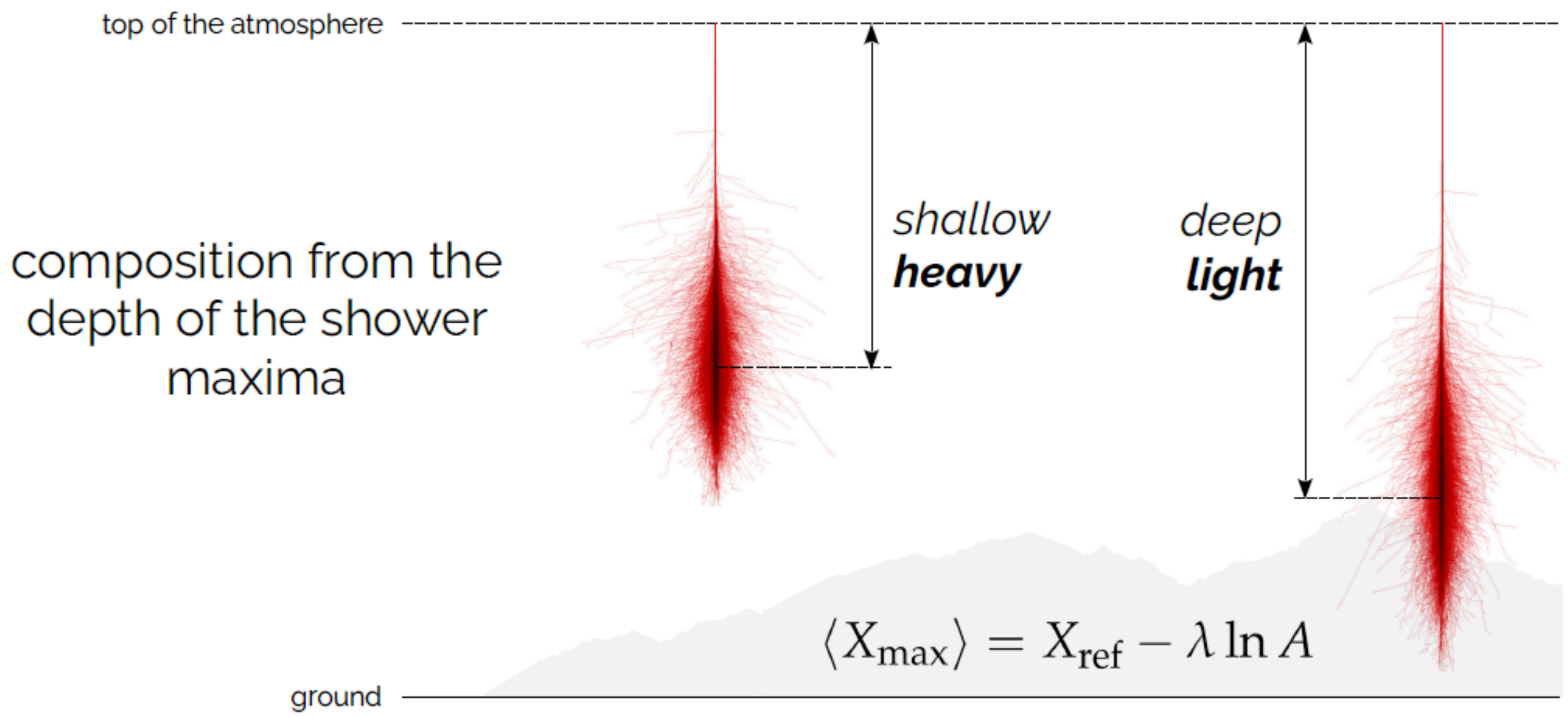

Mass composition

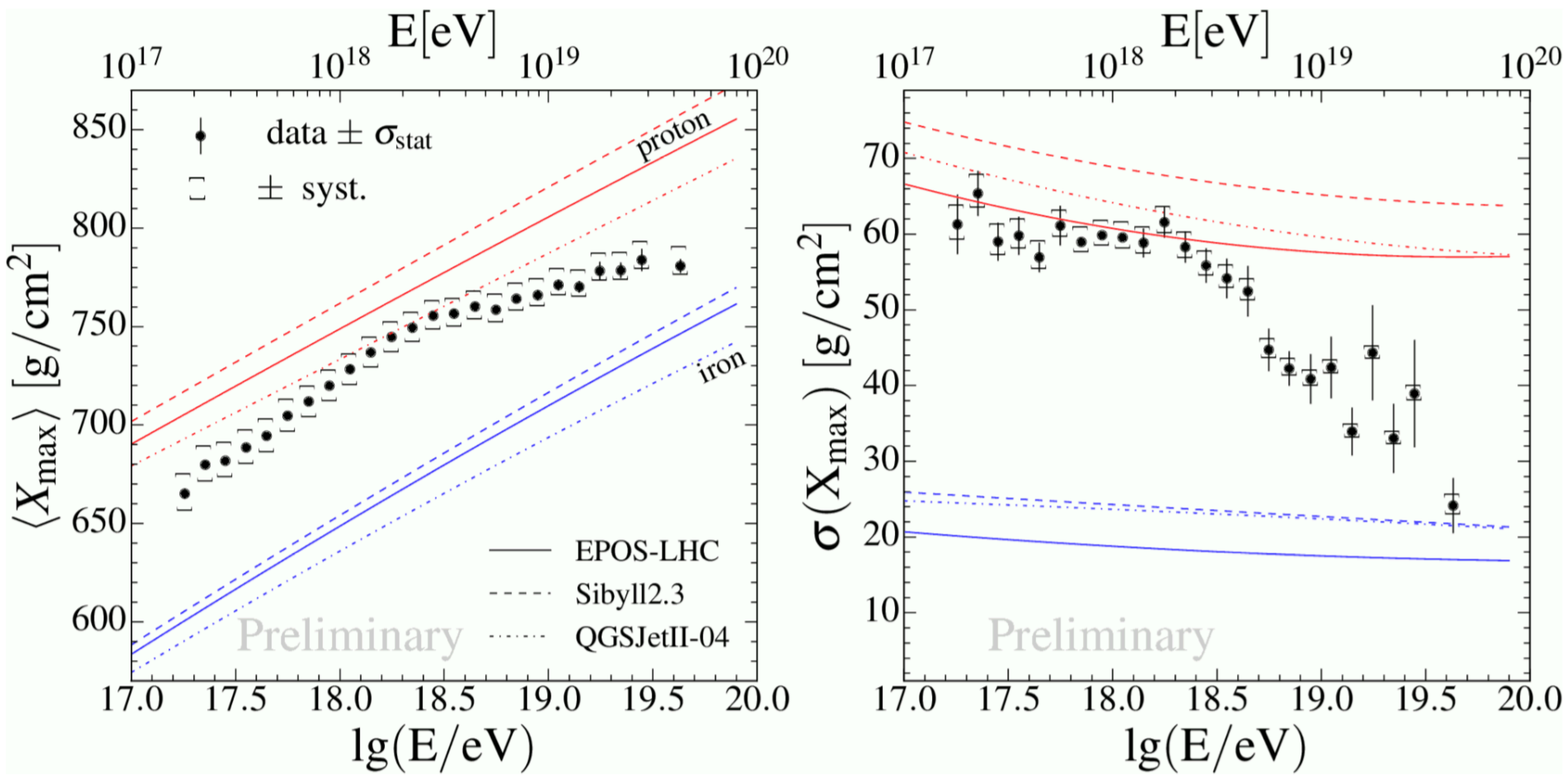

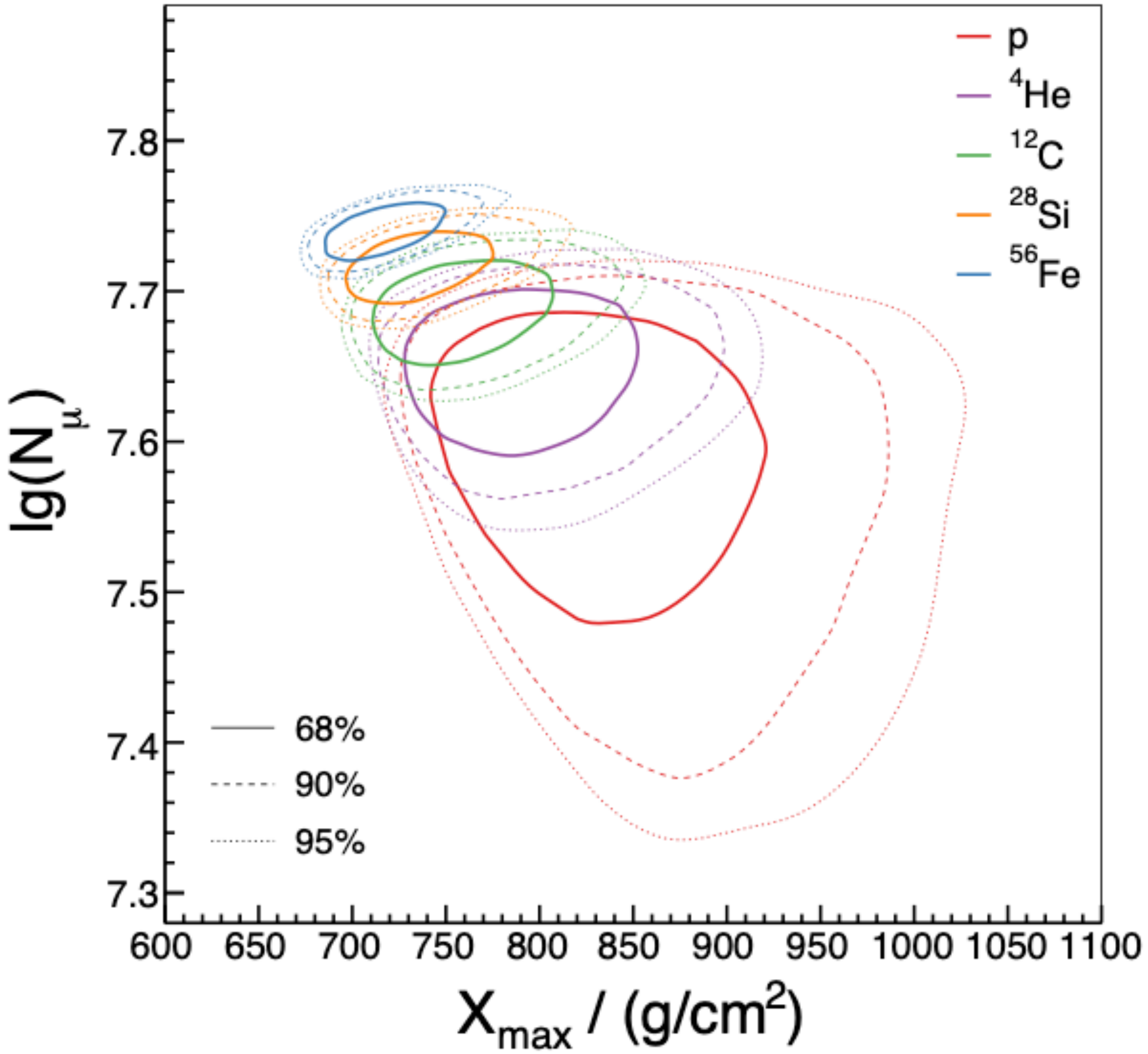

Muons have even better mass composition sensitivity than Xmax

A. Yushkov for the Pierre Auger collaboration, ICRC2019

R. Engel, UHECRs 2022

Mass composition

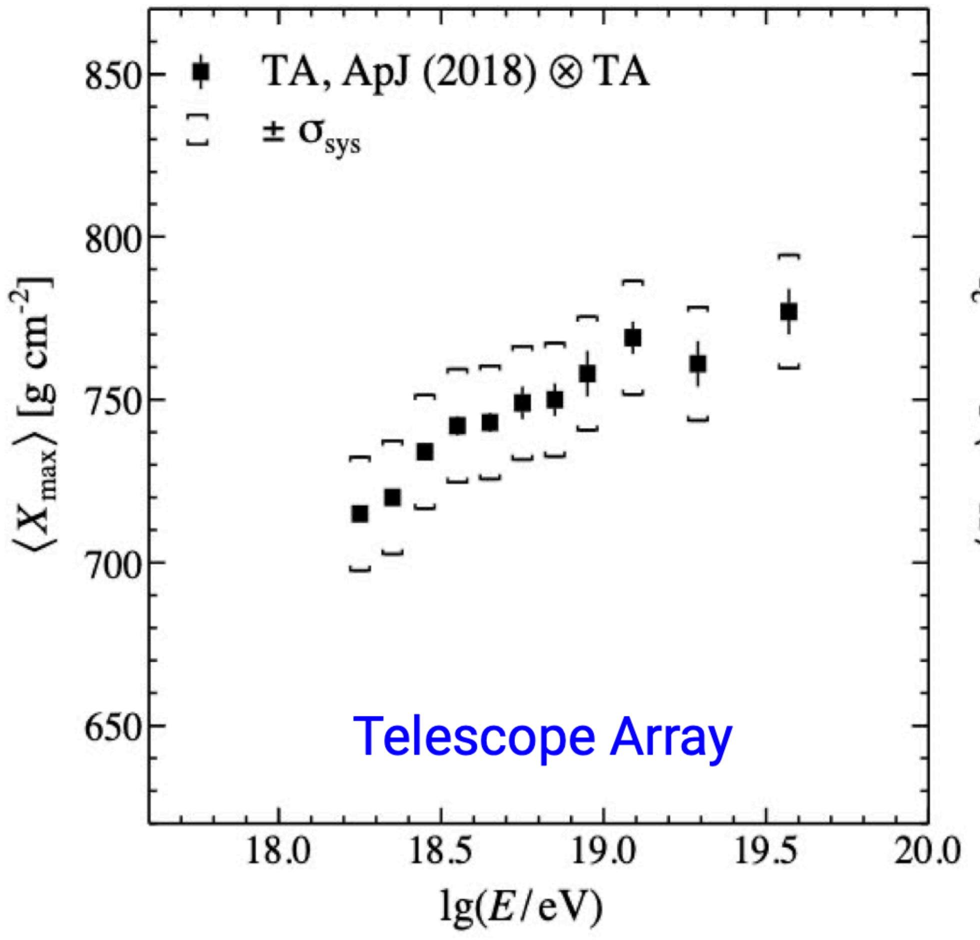

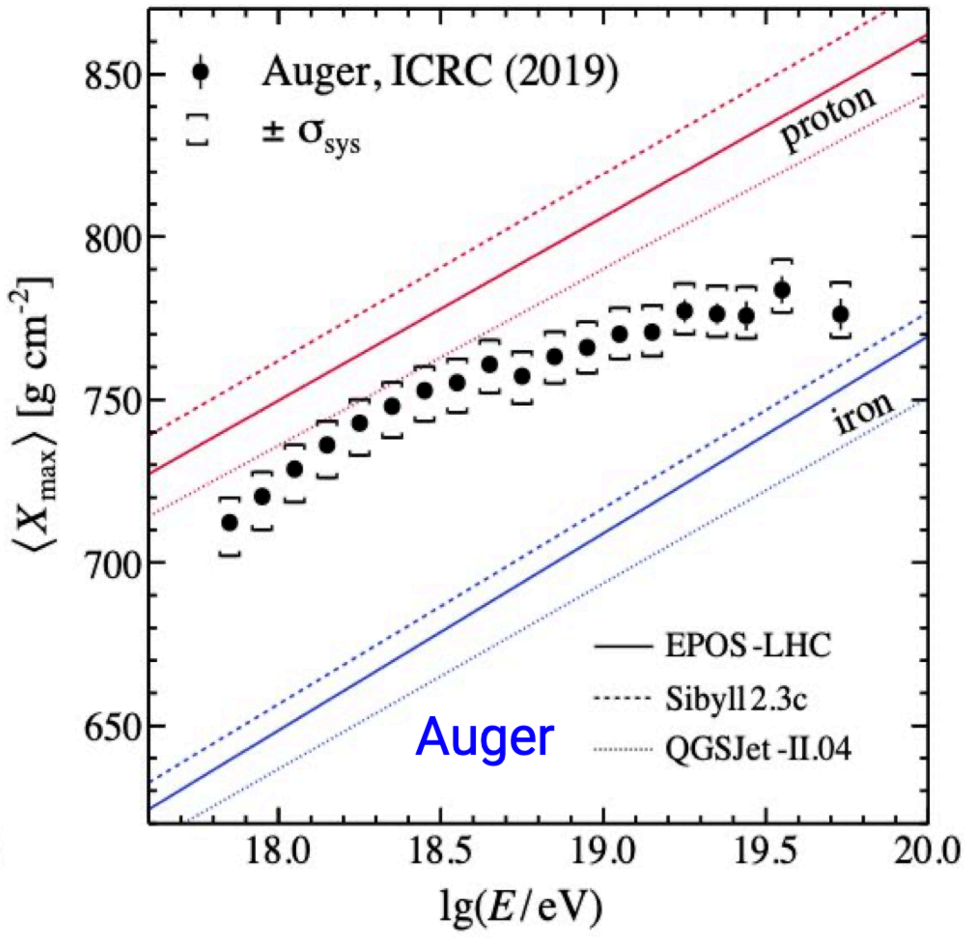

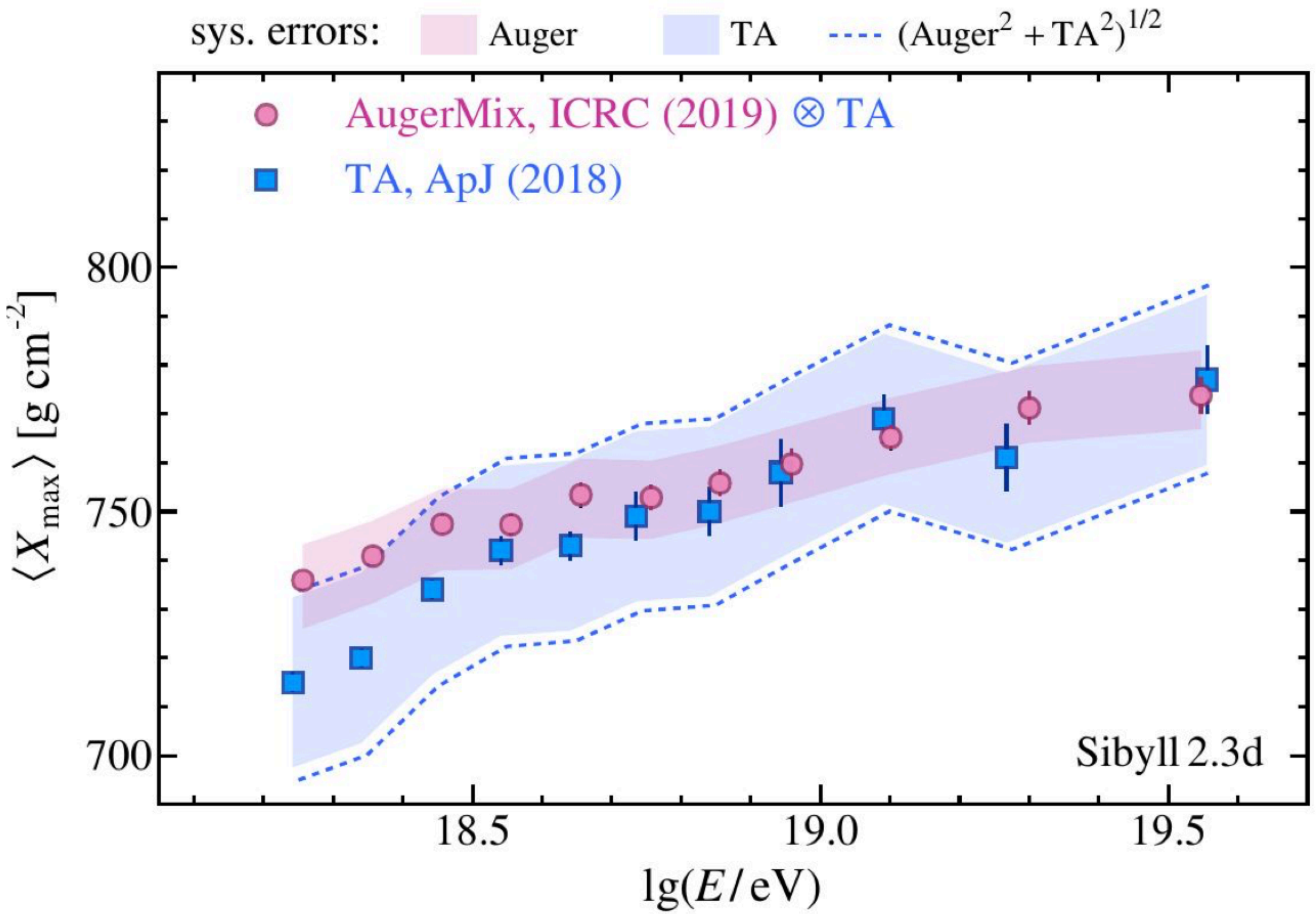

Large scale anisotropy

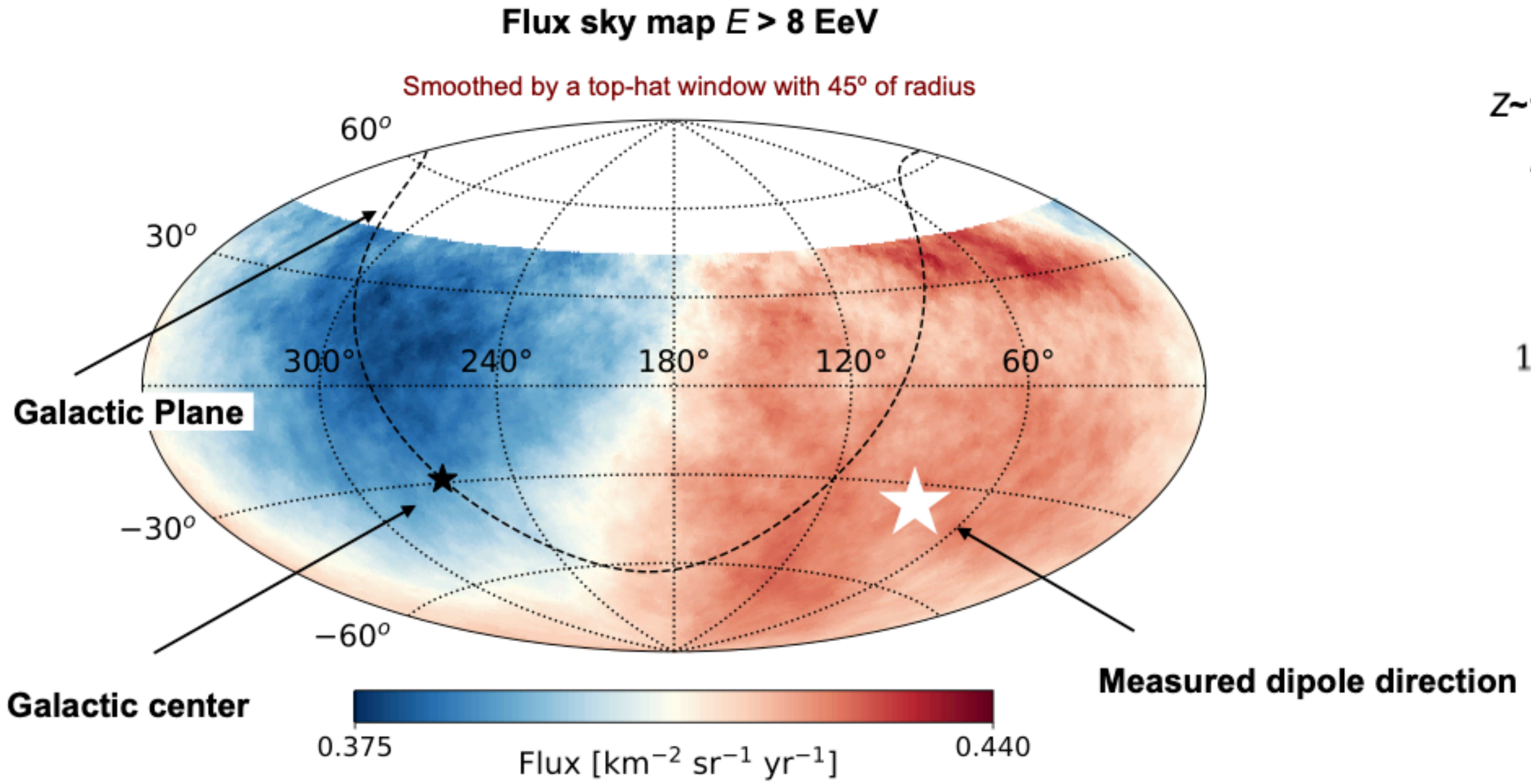

Equatorial coordinates

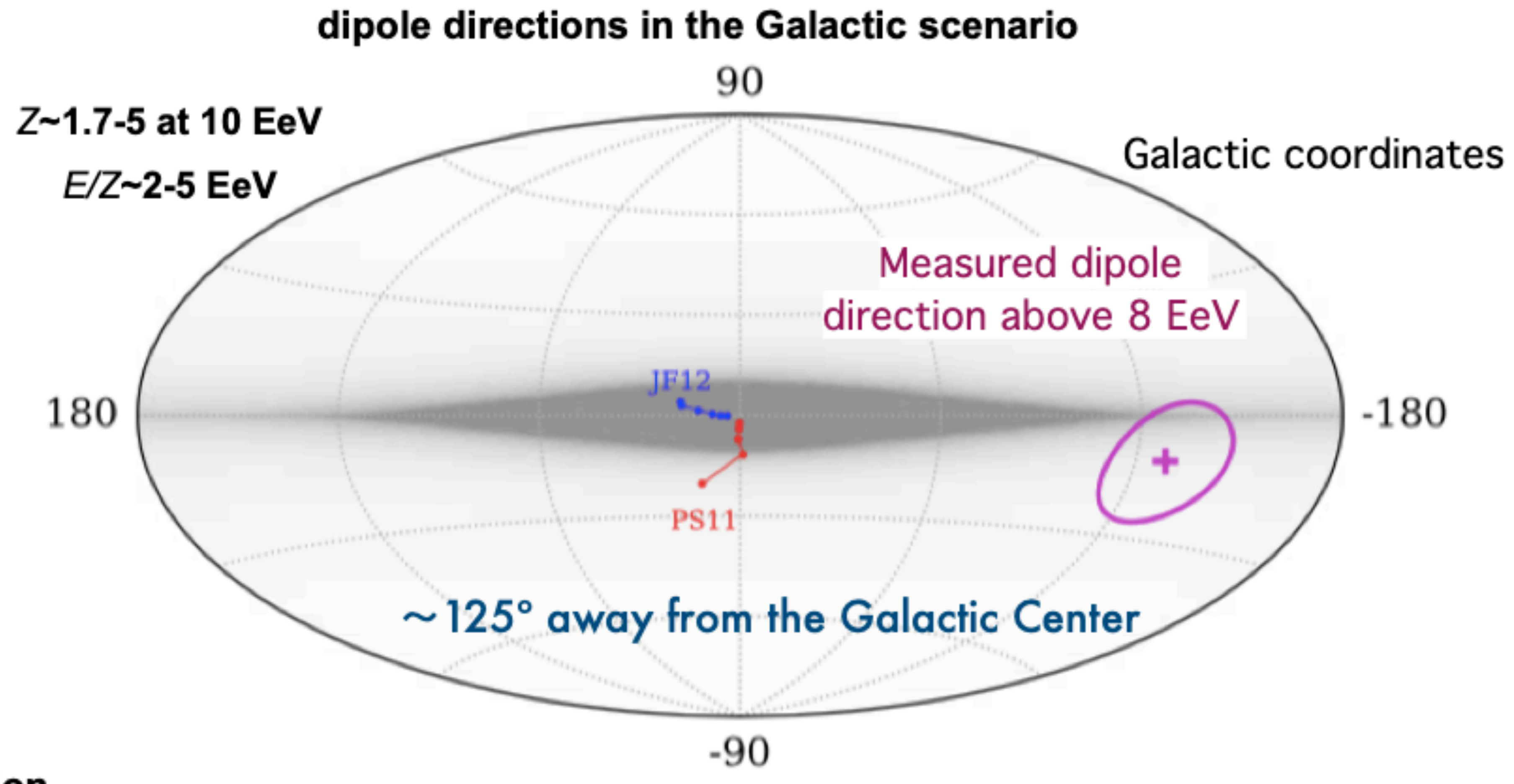

Extragalactic Origin

(Amplitude: factor 10 > CG effect due to the Earth motion in the CR rest frame)

7

Intermediate scale anisotropy

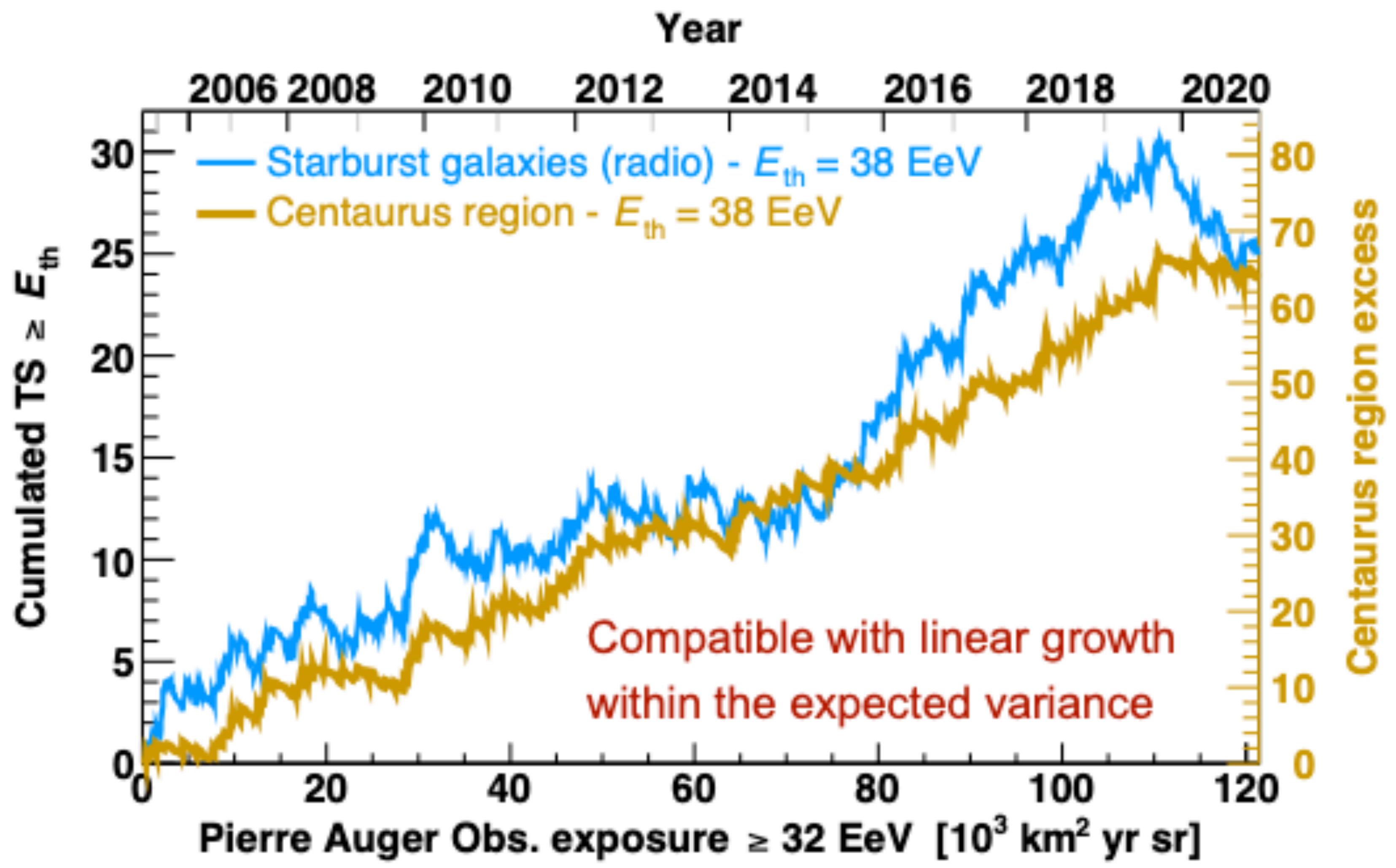

Best fit results at the global maximum

- **All galaxies,** *E*th = 40 EeV, Θ = 16°, f = 16%, TS = 18.0, post-trial *p*-value = 7.9e−4 **(3.2σ)**
- **Starburst,** *E*th = 38 EeV, Θ = 15°, f = 9%, TS = 25.0, post-trial *p*-value = 3.2e−5 **(4.0σ)**
- **All AGNs,** *E*th = 39 EeV, Θ = 16°, f = 7%, TS = 19.4, post-trial *p*-value = 4.2e−4 **(3.3σ)**
- **Jetted AGN,** *E*th = 39 EeV, Θ = 14°, f = 6%, TS = 17.9, post-trial *p*-value = 8.3e−4 **(3.4σ)**

Joint analysis Auger+TA

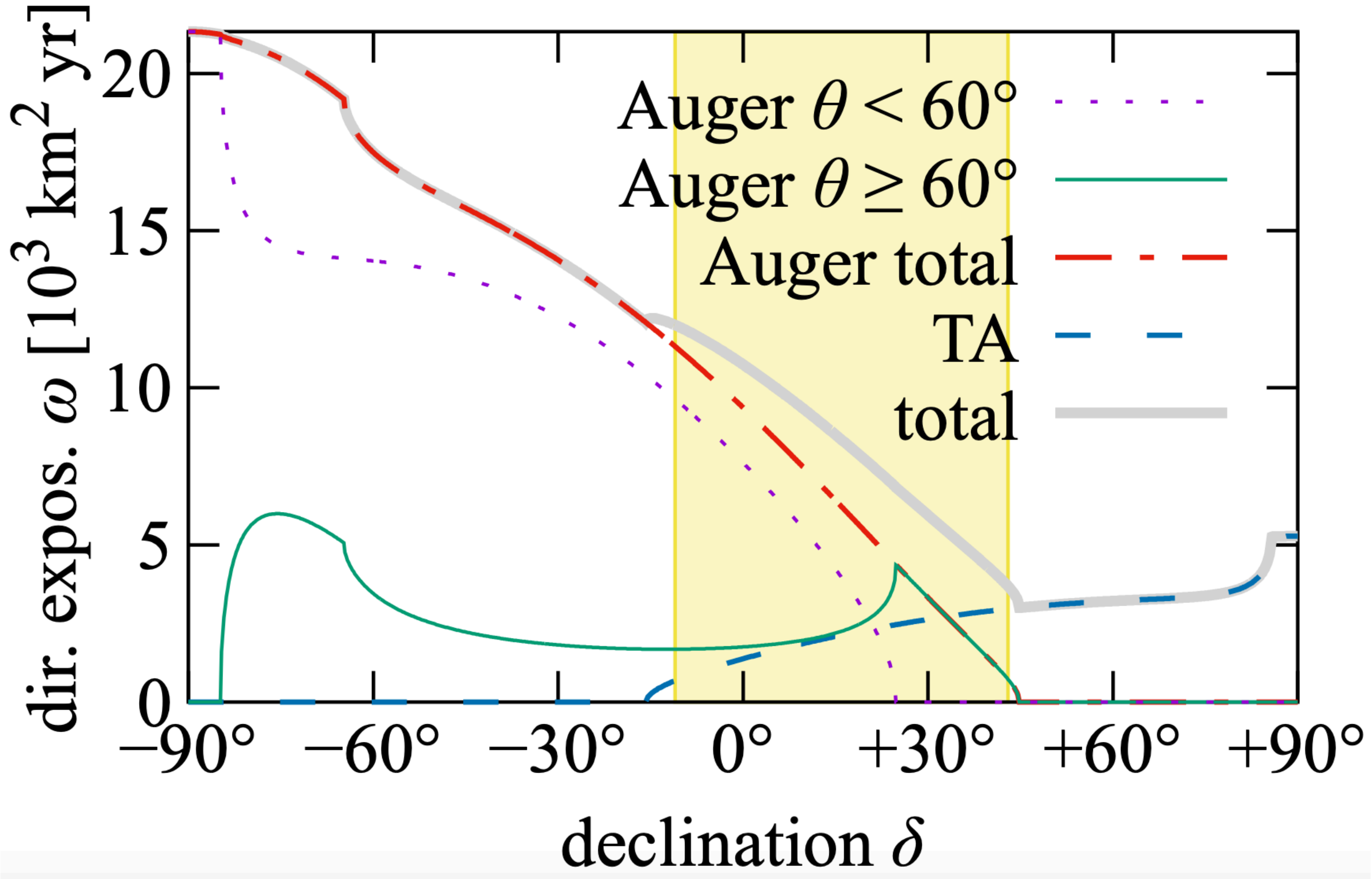

catalogue	$E_{min}^{(Auger)}$	$E_{min}^{(TA)}$	ψ [deg]	f [%]	TS	significance
all galaxies	40 EeV	51 EeV	29^{+11}_{-12}	41^{+29}_{-18}	14.3	$2.7\sigma_{global}$
starburst	38 EeV	49 EeV	$15.1^{+4.6}_{-3.0}$	$12.1^{+4.5}_{-3.1}$	31.1	$4.6\sigma_{global}$

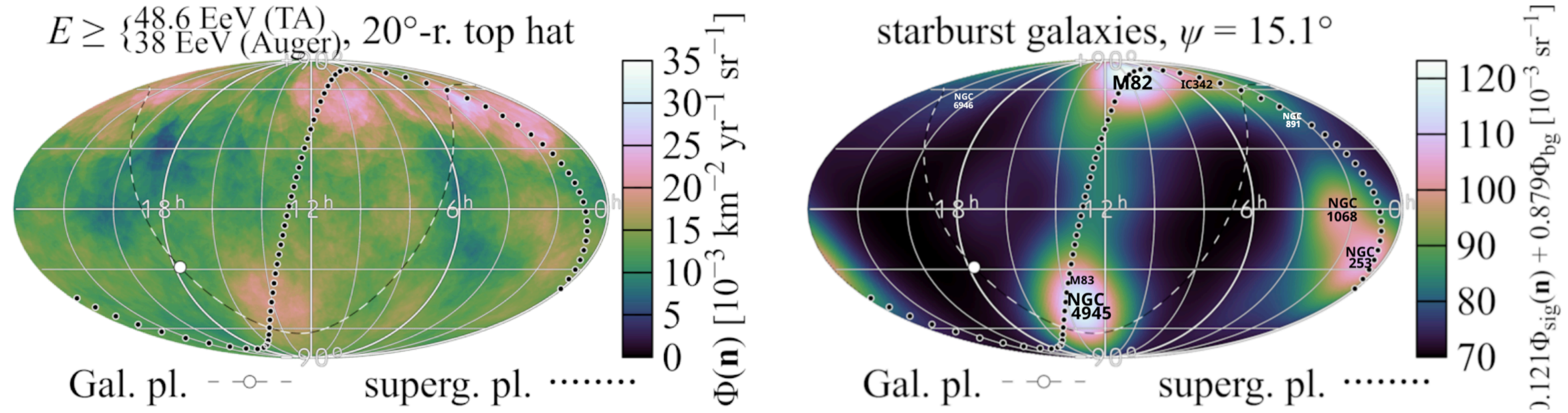

Contribution 10% with a isotropic flux!

Neglected magnetic fields!

Interpretation of results

Motivation: ankle interpretation

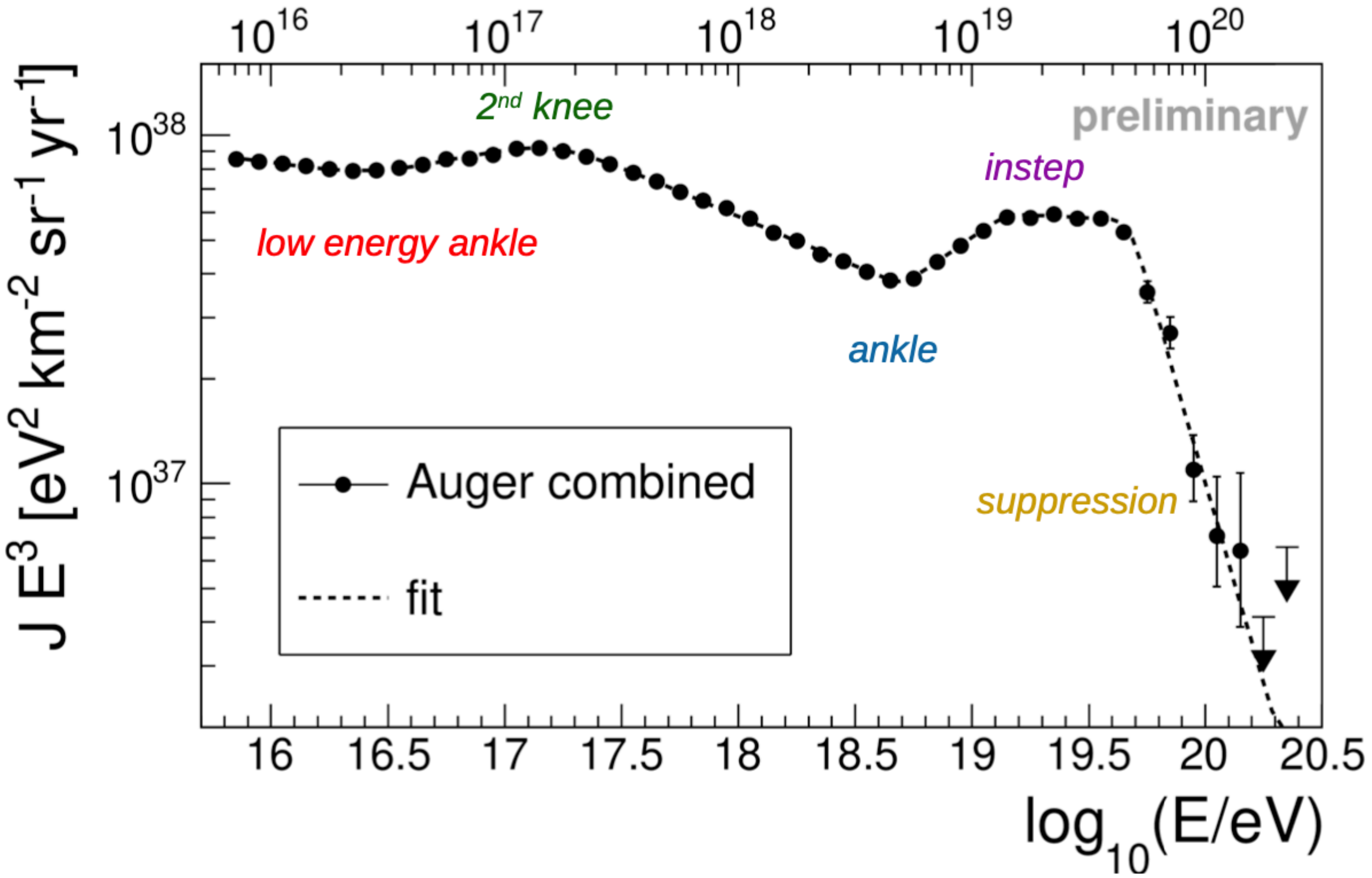

It is possible to link features in the UHECRs to astrophysical processes?

Several possible explanations:

- Transition model;
- Pure proton scenario;
- Mixed composition scenario;

How could the mass composition measurements help to understand these features?

Combined fit above the ankle: ingredients

- Assuming point-like sources identical and uniformly distributed;

Combined fit above the ankle: ingredients

- Assuming point-like sources identical and uniformly distributed;
- Acceleration of five representative masses: Hydrogen, Helium, Nitrogen, Silicon and Iron.

A.Aab et al. (The Pierre Auger Collaboration), JCAP04(2017)038

Combined fit above the ankle: ingredients

- Assuming point-like sources identical and uniformly distributed;
- Acceleration of five representative masses: Hydrogen, Helium, Nitrogen, Silicon and Iron.
- The injected flux for each mass is a power law with a broken-exponential cutoff.

$$J_k(E_i) = f_k J_0 \left(\frac{E_i}{E_0}\right)^{-\gamma} \cdot f_{\rm cut}(E_i, Z \cdot R_{\rm cut})$$

$$f_{\rm cut}(E_i, Z \cdot R_{\rm cut}) = \begin{cases} 1 & E_i < Z\ R_{\rm cut} \\ \exp\left(1 - \frac{E_i}{Z \cdot\ R_{\rm cut}}\right) & E_i > Z\ R_{\rm cut} \end{cases}$$

A.Aab et al. (The Pierre Auger Collaboration), JCAP04(2017)038

IJCLab Irène Joliot-Curie Laboratoire de Physique des 2 Infinis

Combined fit above the ankle: ingredients

- Assuming point-like sources identical and uniformly distributed;
- Acceleration of five representative masses: Hydrogen, Helium, Nitrogen, Silicon and Iron.
- The injected flux for each mass is a power law with a broken-exponential cutoff.

$$J_k(E_i) = f_k J_0 \left(\frac{E_i}{E_0}\right)^{-\gamma} \cdot f_{\rm cut}(E_i, Z \cdot R_{\rm cut})$$

$$f_{\rm cut}(E_i, Z \cdot R_{\rm cut}) = \begin{cases} 1 & E_i < Z\ R_{\rm cut} \\ \exp\left(1 - \dfrac{E_i}{Z \cdot\ R_{\rm cut}}\right) & E_i > Z\ R_{\rm cut} \end{cases}$$

- The injected flux are propagated through the extra-galactic space and fitted to the Auger energy spectrum and composition.

A.Aab et al. (The Pierre Auger Collaboration), JCAP04(2017)038

IJCLab Irène Joliot-Curie Laboratoire de Physique des 2 Infinis

Combined fit above the ankle: ingredients

- Assuming point-like sources identical and uniformly distributed;
- Acceleration of five representative masses: Hydrogen, Helium, Nitrogen, Silicon and Iron.
- The injected flux for each mass is a power law with a broken-exponential cutoff.

$$J_k(E_i) = f_k J_0 \left(\frac{E_i}{E_0}\right)^{-\gamma} \cdot f_{\rm cut}(E_i, Z \cdot R_{\rm cut})$$

$$f_{\rm cut}(E_i, Z \cdot R_{\rm cut}) = \begin{cases} 1 & E_i < Z\ R_{\rm cut} \\ \exp\left(1 - \frac{E_i}{Z \cdot\ R_{\rm cut}}\right) & E_i > Z\ R_{\rm cut} \end{cases}$$

- The injected flux are propagated through the extra-galactic space and fitted to the Auger energy spectrum and composition.
- Free parameters of the fit are: $J_0, \gamma, R_{\rm cut}$ and $(N-1)\ f_k$.

A.Aab et al. (The Pierre Auger Collaboration), JCAP04(2017)038

IJCLab Irène Joliot-Curie Laboratoire de Physique des 2 Infinis

Combined fit above the ankle: ingredients

- Assuming point-like sources identical and uniformly distributed;
- Acceleration of five representative masses: Hydrogen, Helium, Nitrogen, Silicon and Iron.
- The injected flux for each mass is a power law with a broken-exponential cutoff.

$$J_k(E_i) = f_k J_0 \left(\frac{E_i}{E_0}\right)^{-\gamma} \cdot f_{\rm cut}(E_i, Z \cdot R_{\rm cut})$$

$$f_{\rm cut}(E_i, Z \cdot R_{\rm cut}) = \begin{cases} 1 & E_i < Z\ R_{\rm cut} \\ \exp\left(1 - \frac{E_i}{Z \cdot\ R_{\rm cut}}\right) & E_i > Z\ R_{\rm cut} \end{cases}$$

- The injected flux are propagated through the extra-galactic space and fitted to the Auger energy spectrum and composition.
- Free parameters of the fit are: $J_0, \gamma, R_{\rm cut}$ and $(N-1)\ f_k$.
- The total deviance is considered as the sum of the deviance of the spectrum and the deviance of the composition.

A.Aab et al. (The Pierre Auger Collaboration), JCAP04(2017)038

IJCLab Irène Joliot-Curie Laboratoire de Physique des 2 Infinis

Astrophysical interpretation of Auger data

Fitting both the spectrum and composition, one can infer information about the source scenarios which are compatible to data.

- ✴Nuclei are accelerated at the sources.
- ✴ A hard injection spectrum at the sources is required.
- ✴ Suppression due to photo-interactions and by limiting acceleration at the sources, while the ankle feature is not easy to accomodate.

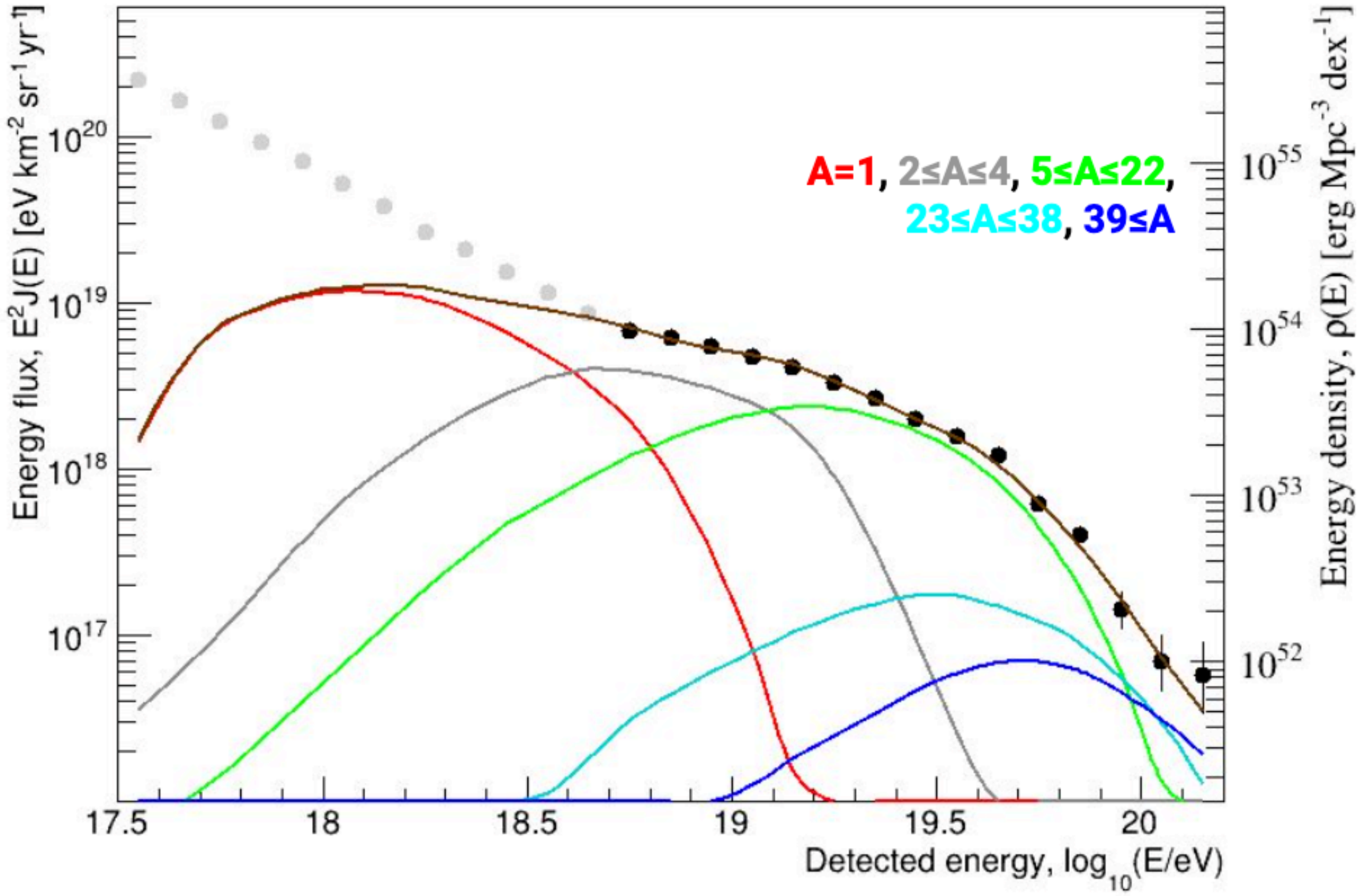

A.Aab et al. (The Pierre Auger Collaboration), JCAP04(2017)038

Including arrival direction

- ✴Assumption: UHECR production rate follows matter (ex: Star Formation Rate)
- ✴Fit of energy spectrum and composition using a catalogue which reconstructs the 3D distribution of the most extreme sources in the Universe.

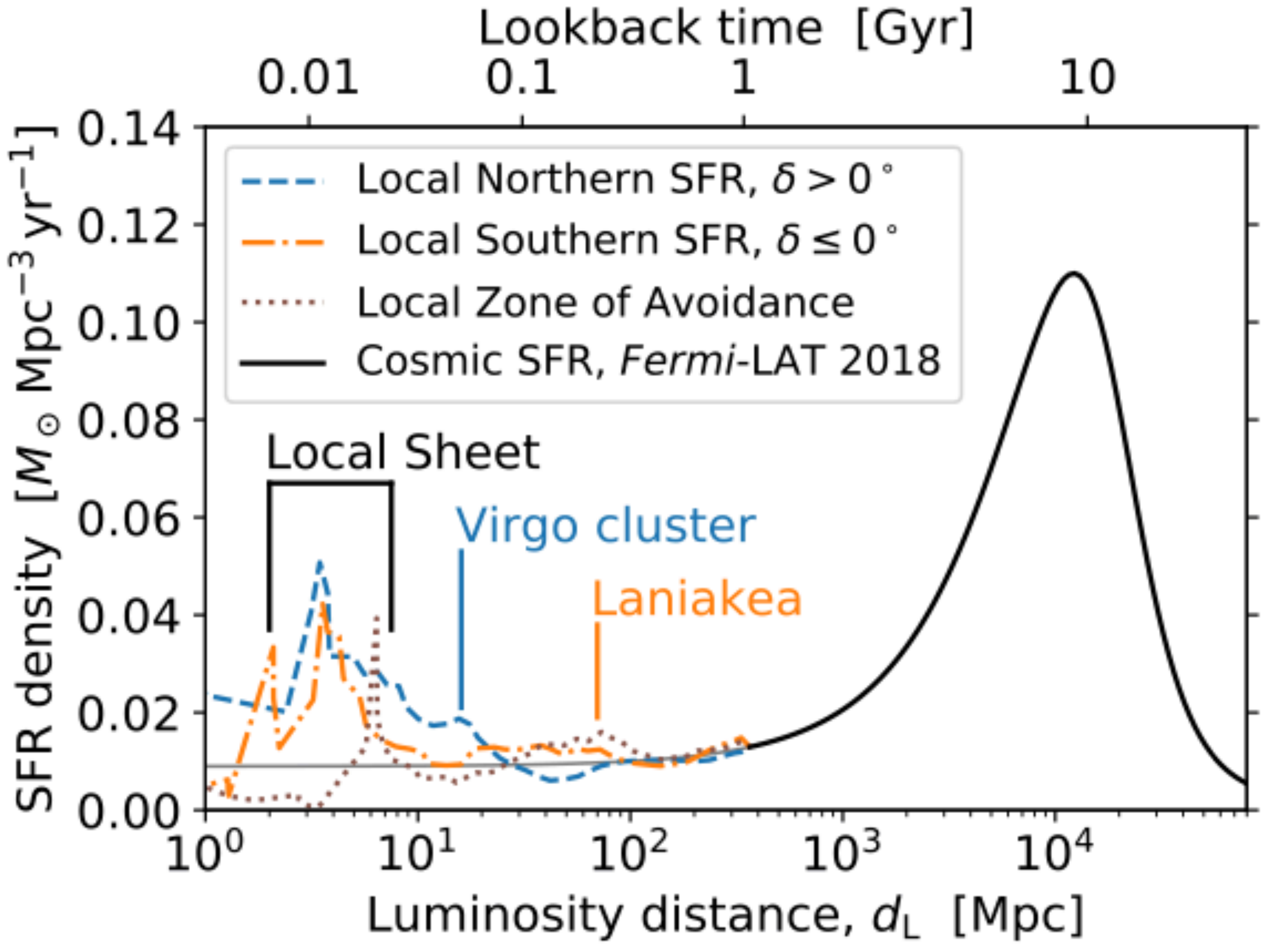

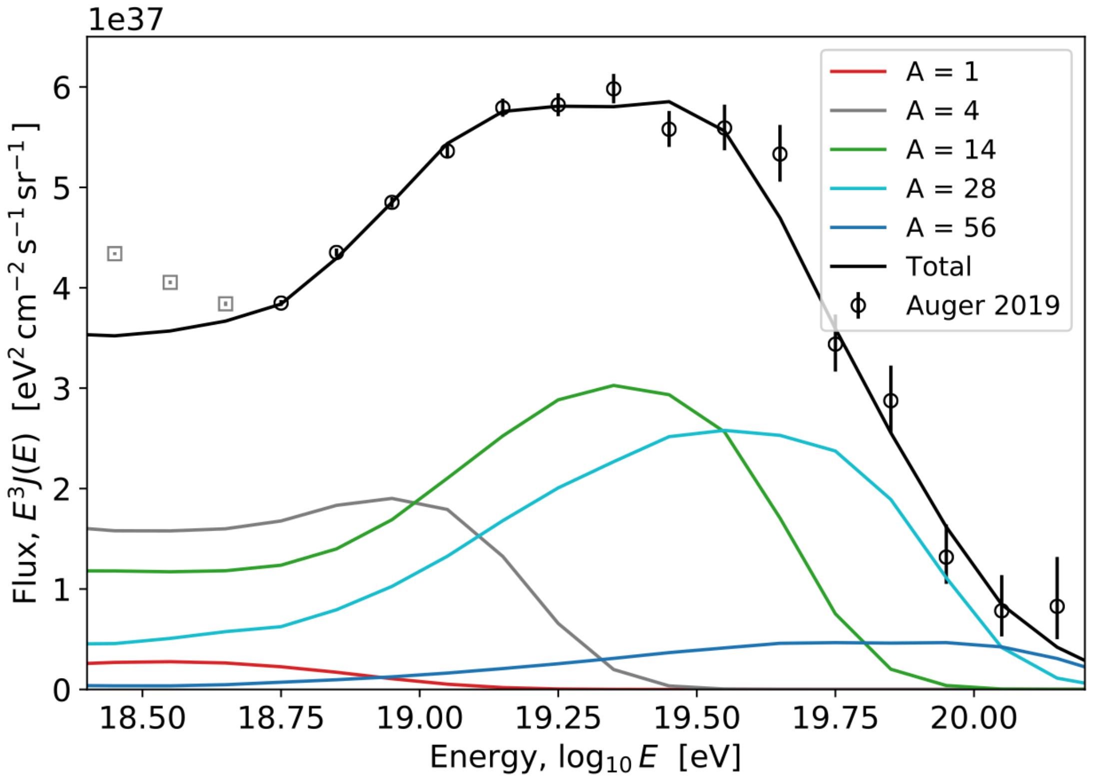

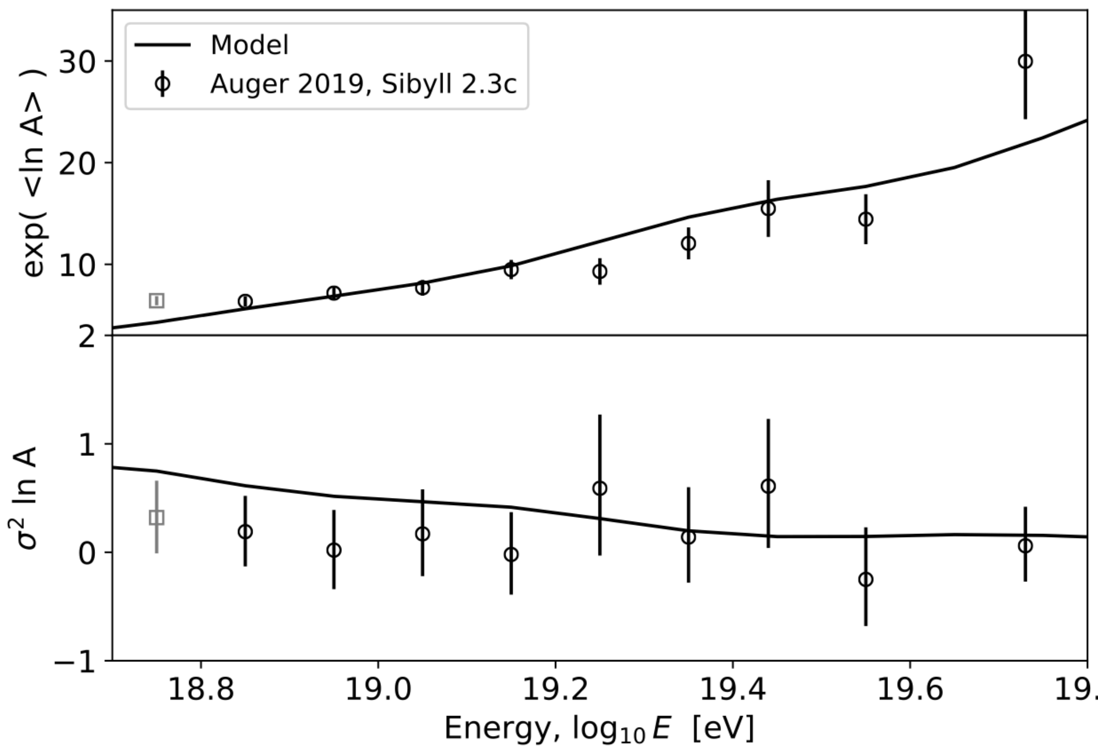

J. Biteau et al., *PoS* ICRC2021 (2021) 1012

A. Aab *et al* JCAP04(2017)038

IJCLab Irène Joliot-Curie Laboratoire de Physique des 2 Infinis

Including arrival direction

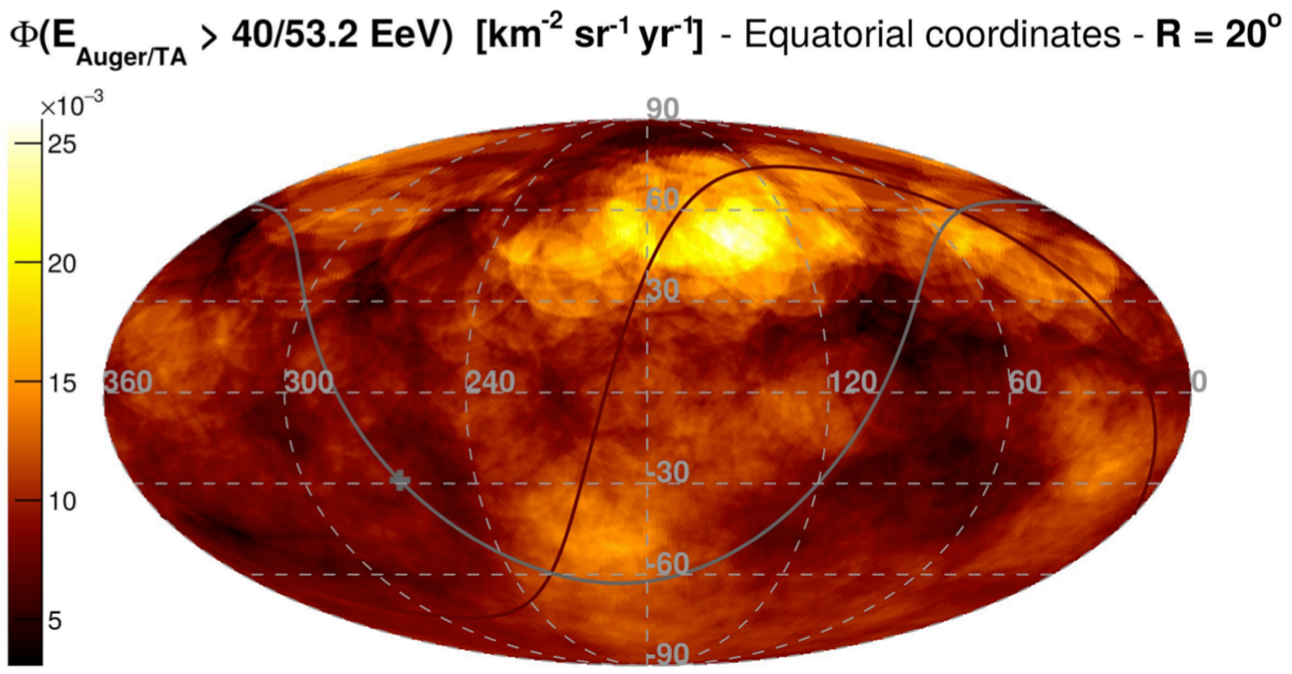

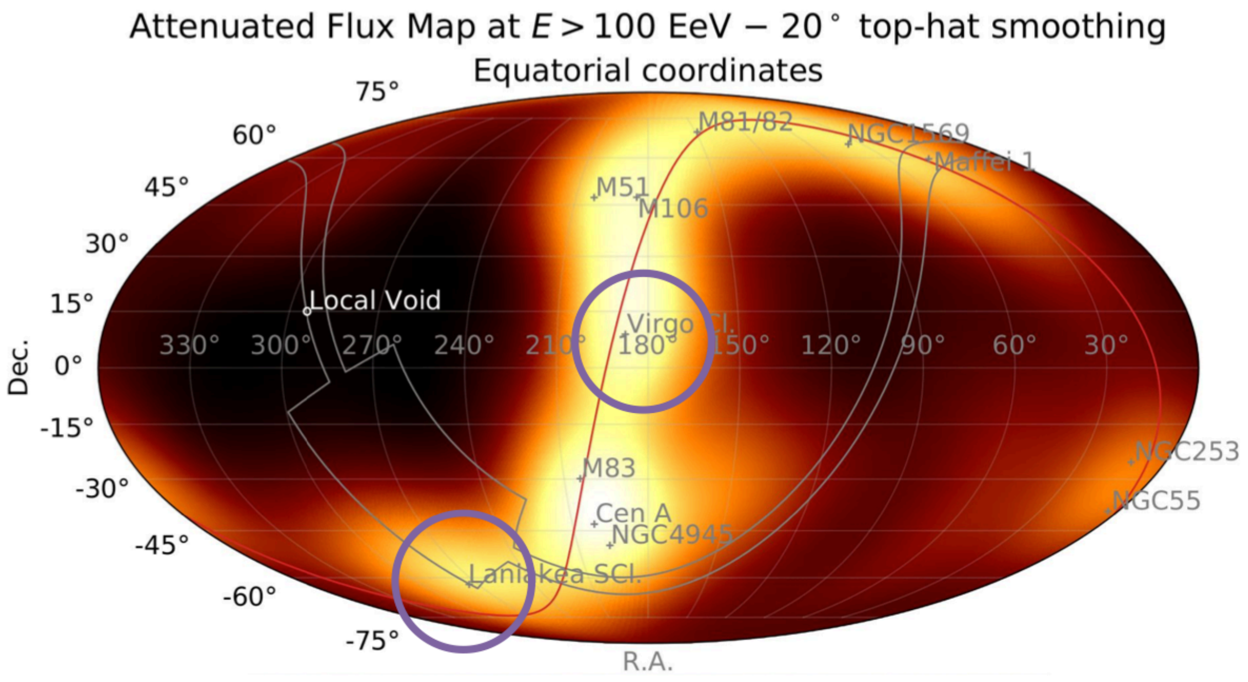

Why don't we see nearby clusters or superclusters?

Including arrival direction

→ Study the propagation of UHECRs in Galaxy Clusters' environment!

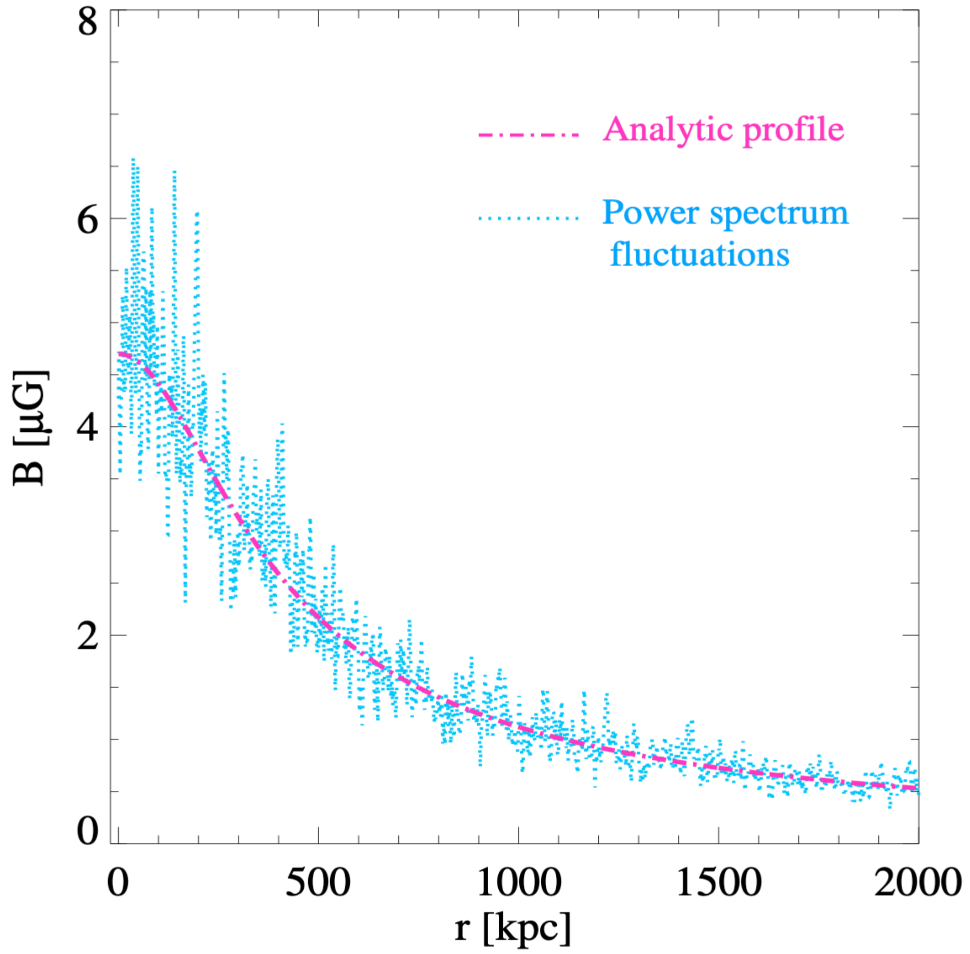

$$\frac{L_{eff}}{L}(E,Z) \simeq \cos\theta \simeq 1 + \frac{\theta^2}{2} \simeq 65\left(\frac{10^{20}\ \mathrm{eV}}{E}\right)^2\left(\frac{L}{1\ \mathrm{Mpc}}\right)\left(\frac{L_{coh}}{10\ \mathrm{kpc}}\right)\left(\frac{B}{1\ \mu\mathrm{G}}\right)^2\left(\frac{Z}{26}\right)^2$$

→ Possible trapping due to clusters' magnetic field!

A. Bonafede et al., A&A 513, A30 (2010)

D. Hooper, et al., Phys. Rev. D **77**, 103007

The universal galaxy cluster pressure profile

- ✳ Self-similarity: approximation all their properties depend only on mass and redshift;
- ✳ (M, z) –> pressure profile for any cluster.

$$P(r) = \frac{P_0 \cdot P_{500} \cdot f(M,z)}{(x/r_p)^\gamma \cdot (1 + (x/r_p)^\alpha)^{\frac{\beta - \gamma}{\alpha}}}$$

with P_0 normalisation factor

α, β, γ and r_p are fitted parameters.

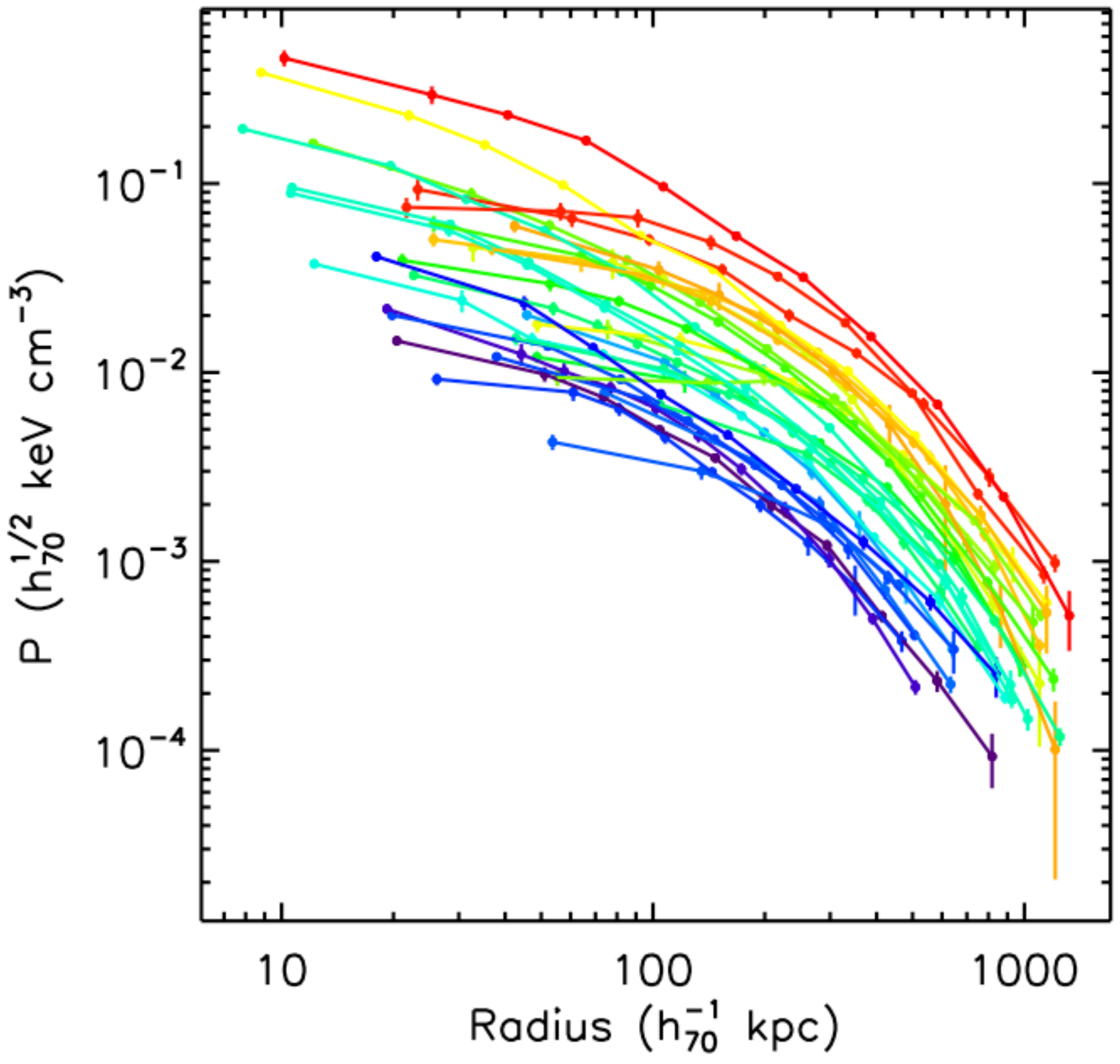

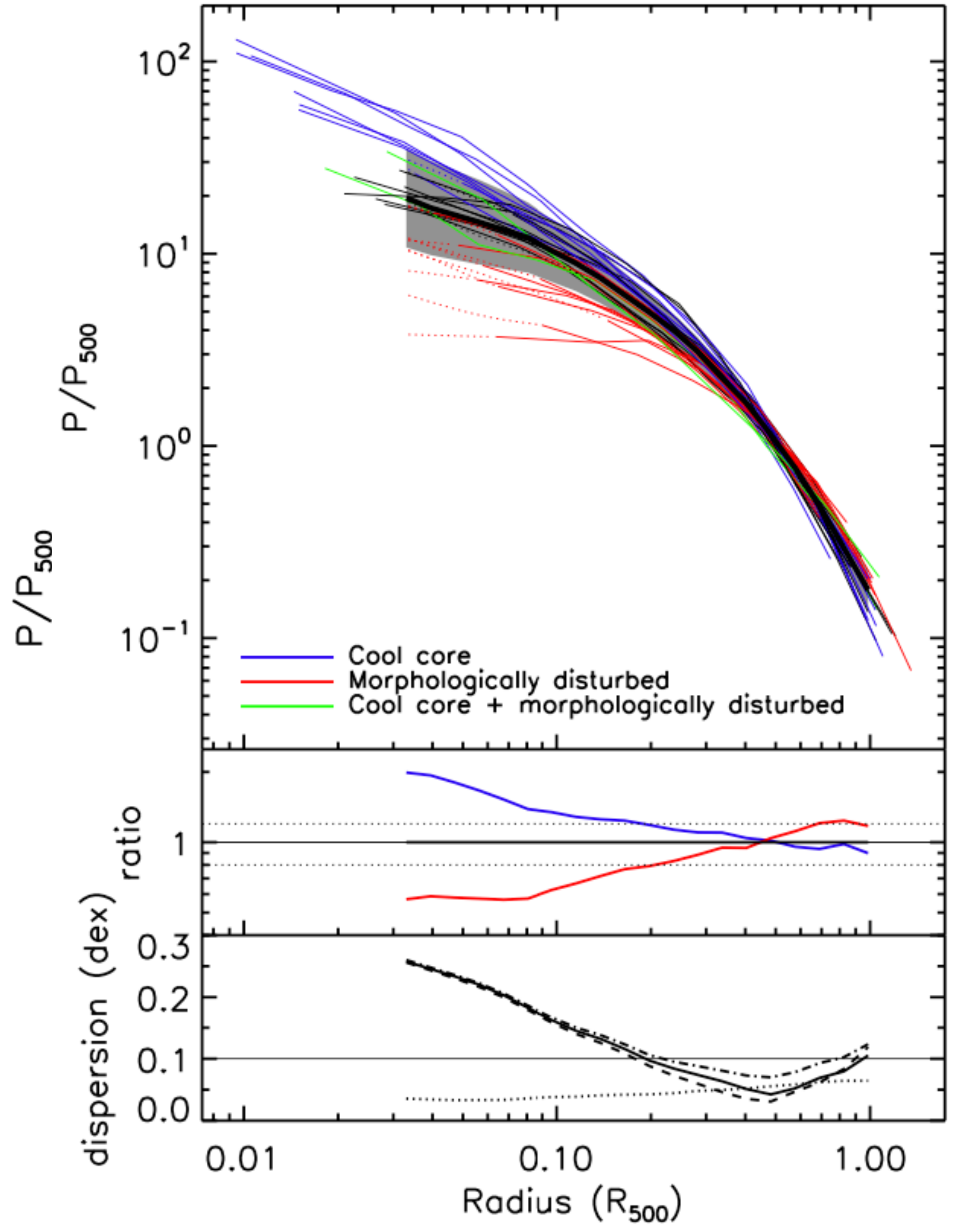

Arnaud et al, A&A 517, A92 (2010).

IJCLab Irène Joliot-Curie Laboratoire de Physique des 2 Infinis

Virgo Cluster

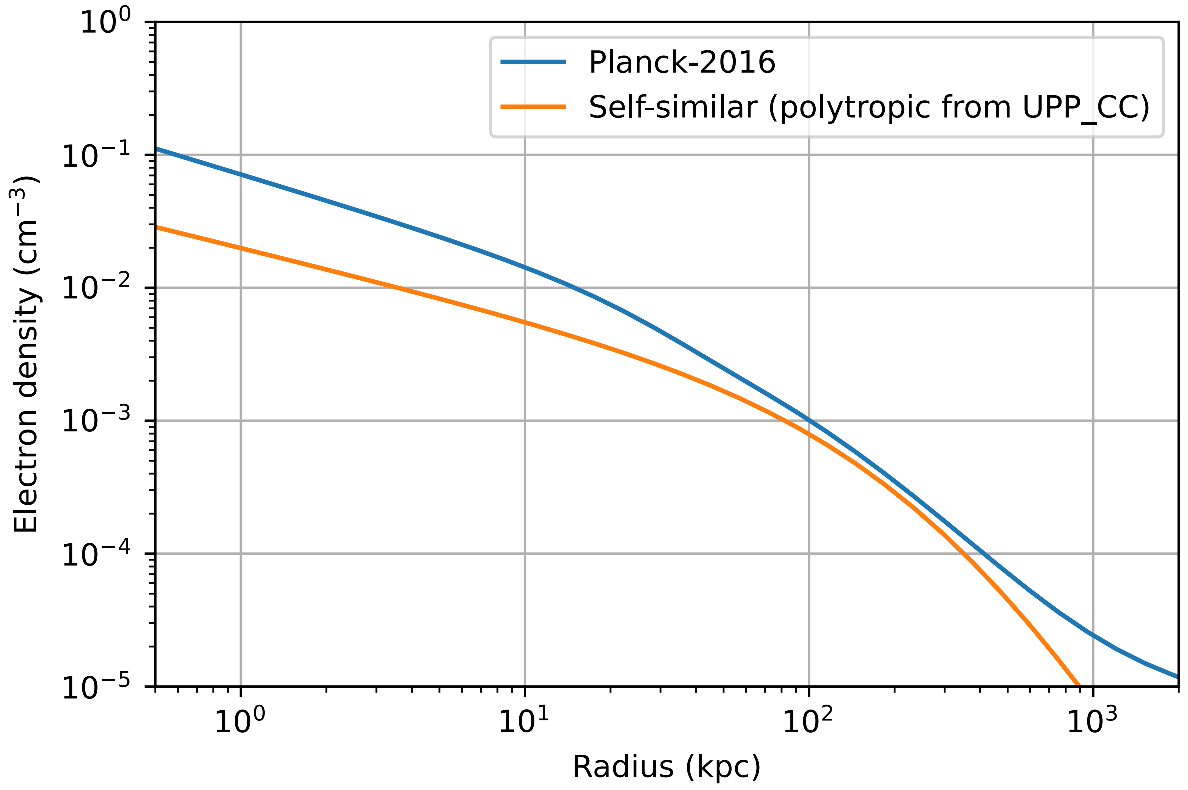

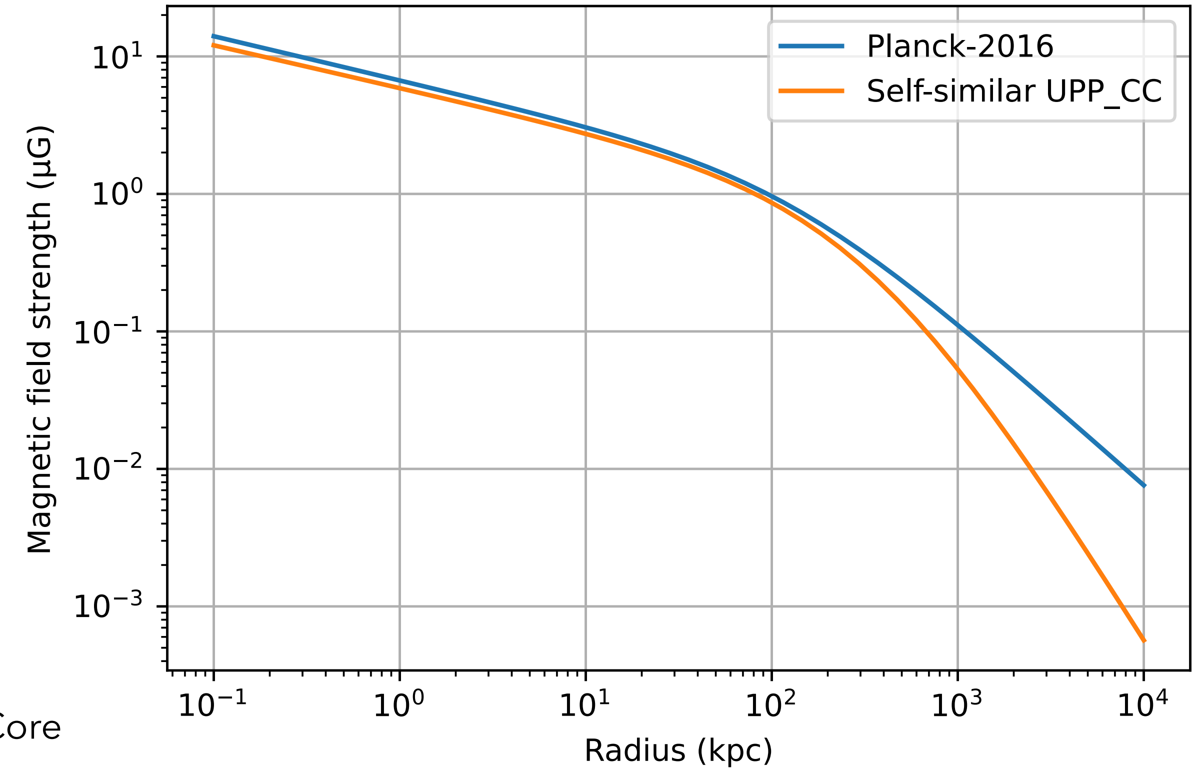

*UPP_CC = Universal Pressure Profile for Cool Core

Planck collaboration, A&A 596, A101 (2016)

R. Adam et al, A&A 644, A70 (2020)

Source-propagation in Galaxy Clusters

✴Propagation in source computed using SimProp;

✴Computation of interaction and diffusion times;

✴Inclusion of magnetic field effect on propagation; **New!**

✴Including radial dependence. **New!**

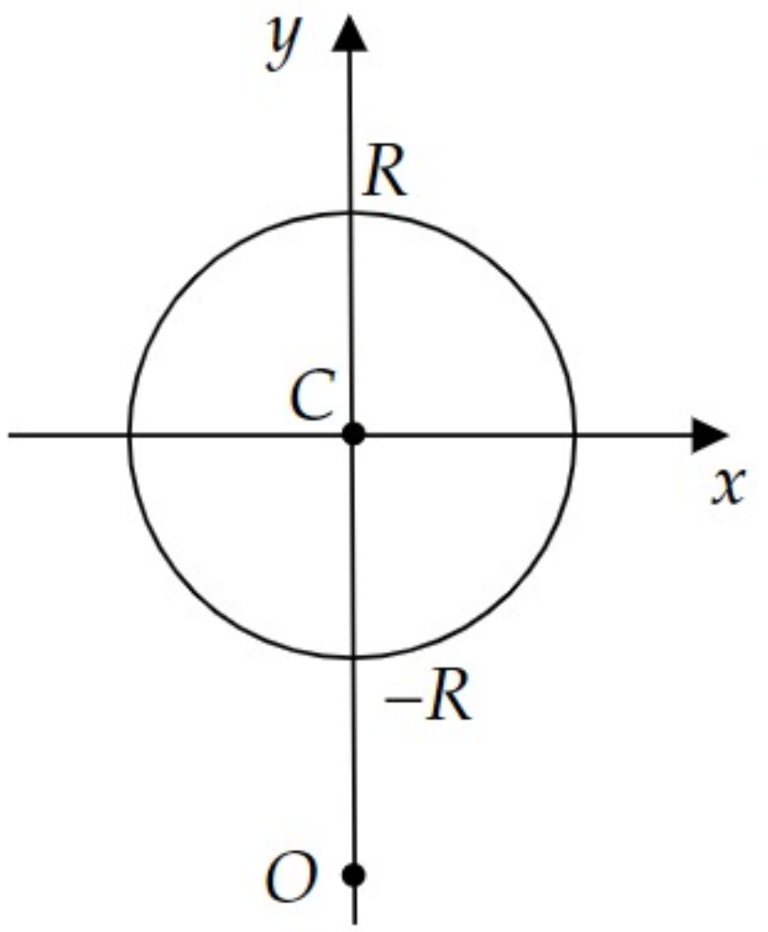

$R = 1\,Mpc$

Filtering

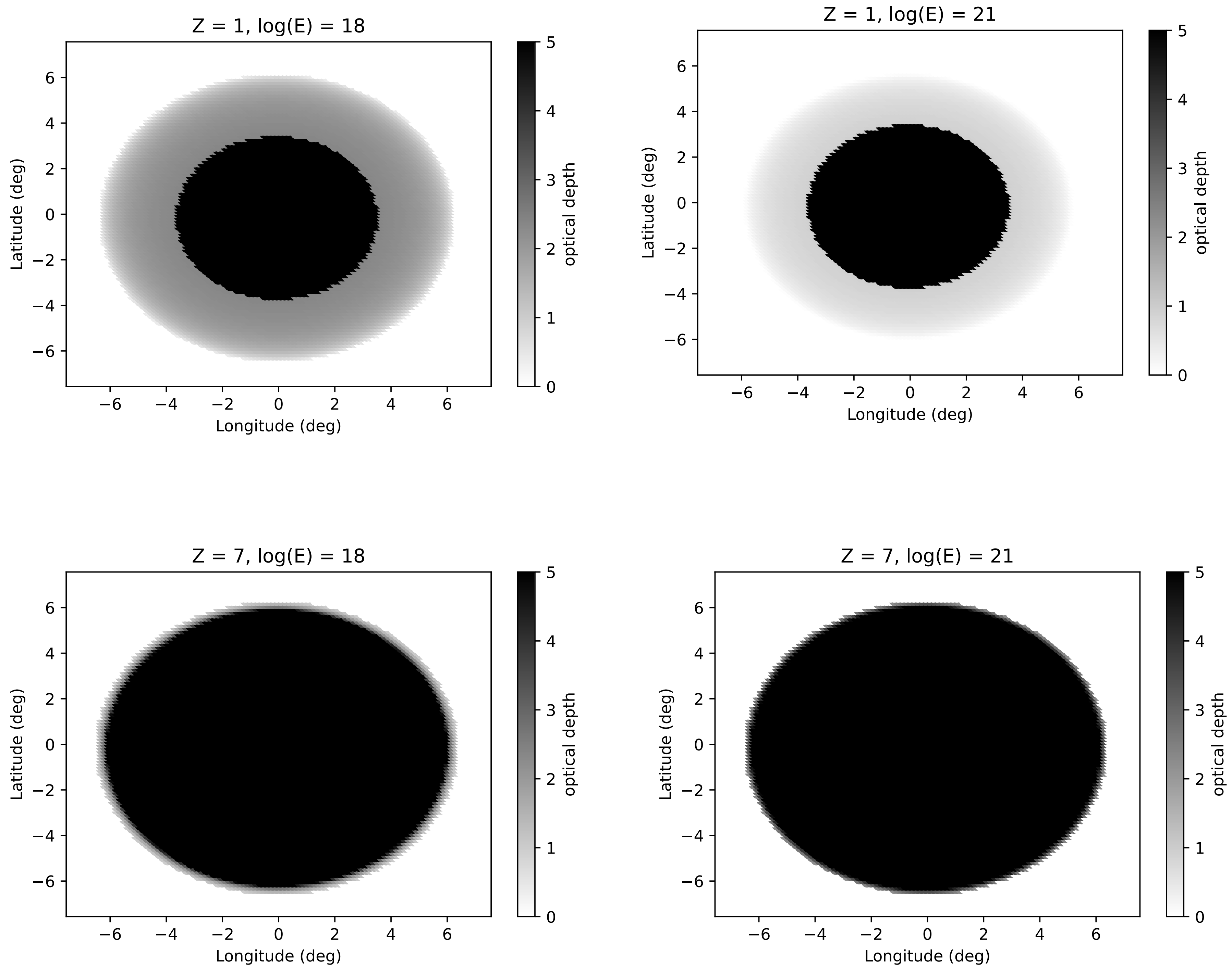

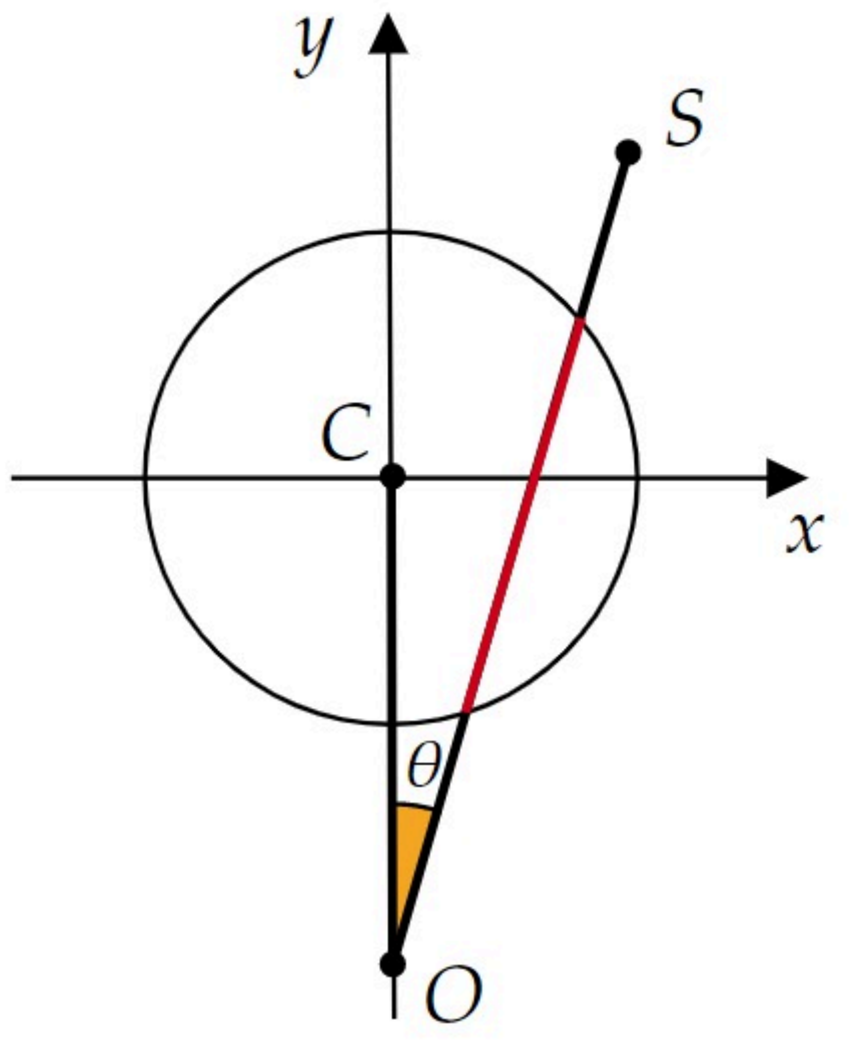

= 1 *Mpc*

We should not see Virgo Cluster!

Condorelli et al., in prep.

IJCLab Irène Joliot-Curie Laboratoire de Physique des 2 Infinis

Summary and future perspectives

- ☑ Energy spectrum Auger vs TA: Is there really a disagreement? Is there a difference in the spectrum in the Northern and Southern sky?
- ☑ Mass Composition: Agreement between the two experiments. Need to increase statistics at the highest energies.
- ☑ Arrival direction: Dipolar anisotropy above 8 EeV confirmedEGCR at E>8 EeV, amplitude increasing with energy as expected in the case of transition GCR-EGCR between 0.1-1.0 EeV. How to include magnetic field effects?
- ☑ Combined fit: which are the sources of UHECRs? (AGNs, TDE, SBG, GRB,etc..)
- ☑ Need for a clear-cut understanding of the dynamics inside EG sources: in-source backgrounds and UHECR interactions.

Summary and future perspectives

- ☑ Energy spectrum Auger vs TA: Is there really a disagreement? Is there a difference in the spectrum in the Northern and Southern sky?
- ☑ Mass Composition: Agreement between the two experiments. Need to increase statistics at the highest energies.
- ☑ Arrival direction: Dipolar anisotropy above 8 EeV confirmedEGCR at E>8 EeV, amplitude increasing with energy as expected in the case of transition GCR-EGCR between 0.1-1.0 EeV. How to include magnetic field effects?
- ☑ Combined fit: which are the sources of UHECRs? (AGNs, TDE, SBG, GRB,etc..)
- ☑ Need for a clear-cut understanding of the dynamics inside EG sources: in-source backgrounds and UHECR interactions.

Thanks for your attention!

Back-up slides!

Highlight results

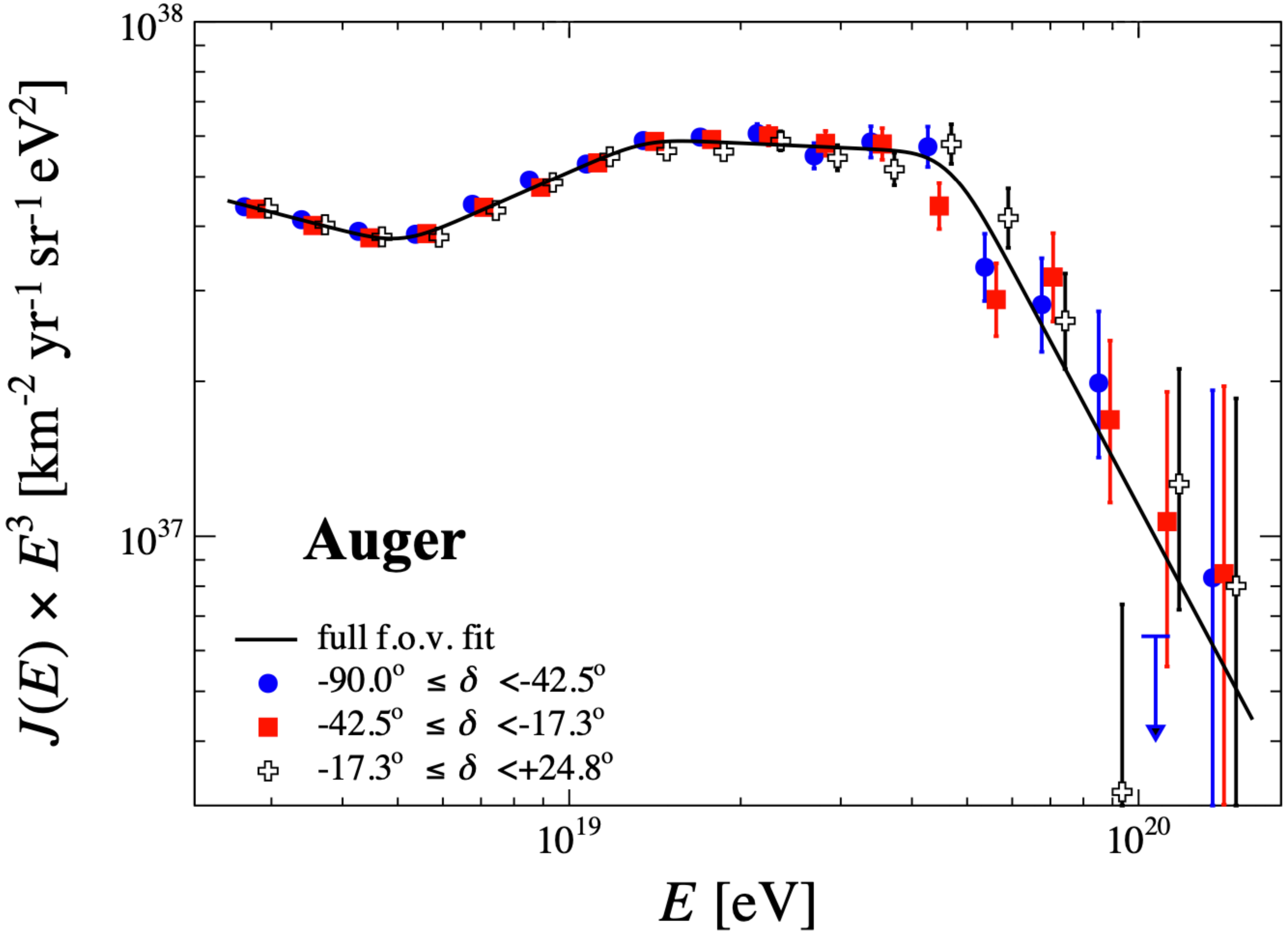

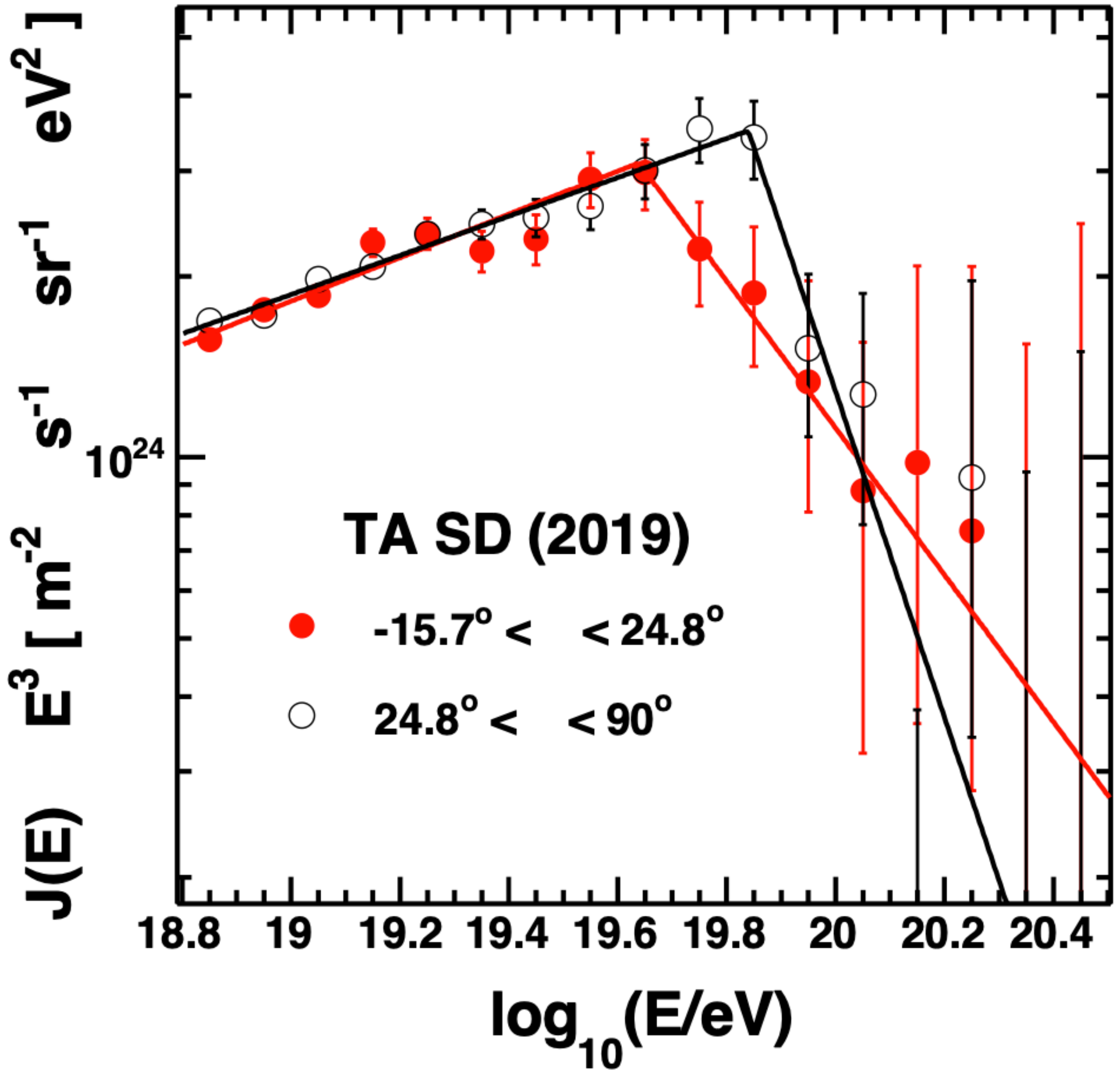

Source-propagation model

- Accelerated particles confined in the environment surrounding the source;
- Presence of photon and gas density;
- High energy particles–> escape with no interaction;
- Low energy particles –> Pile-up of nucleons at lower energies.

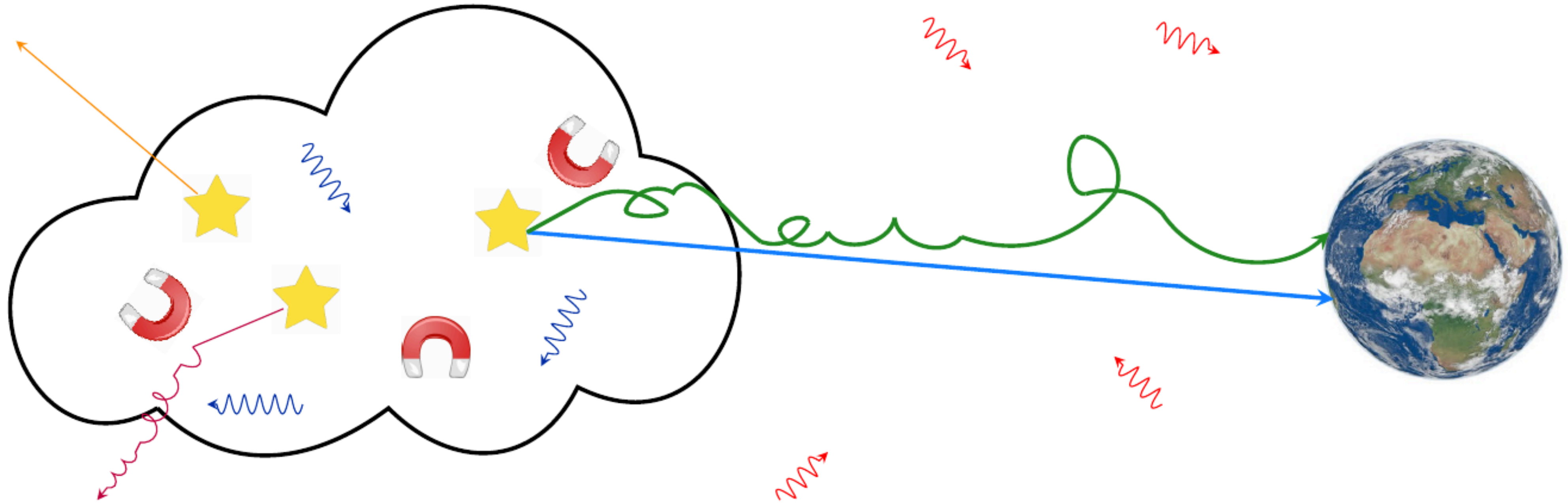

IJCLab Irène Joliot-Curie Laboratoire de Physique des 2 Infinis

Application to Starburst Galaxies

- Motivation: Acceleration & Correlation.
- Leaky box model: computation of interaction and escape times.

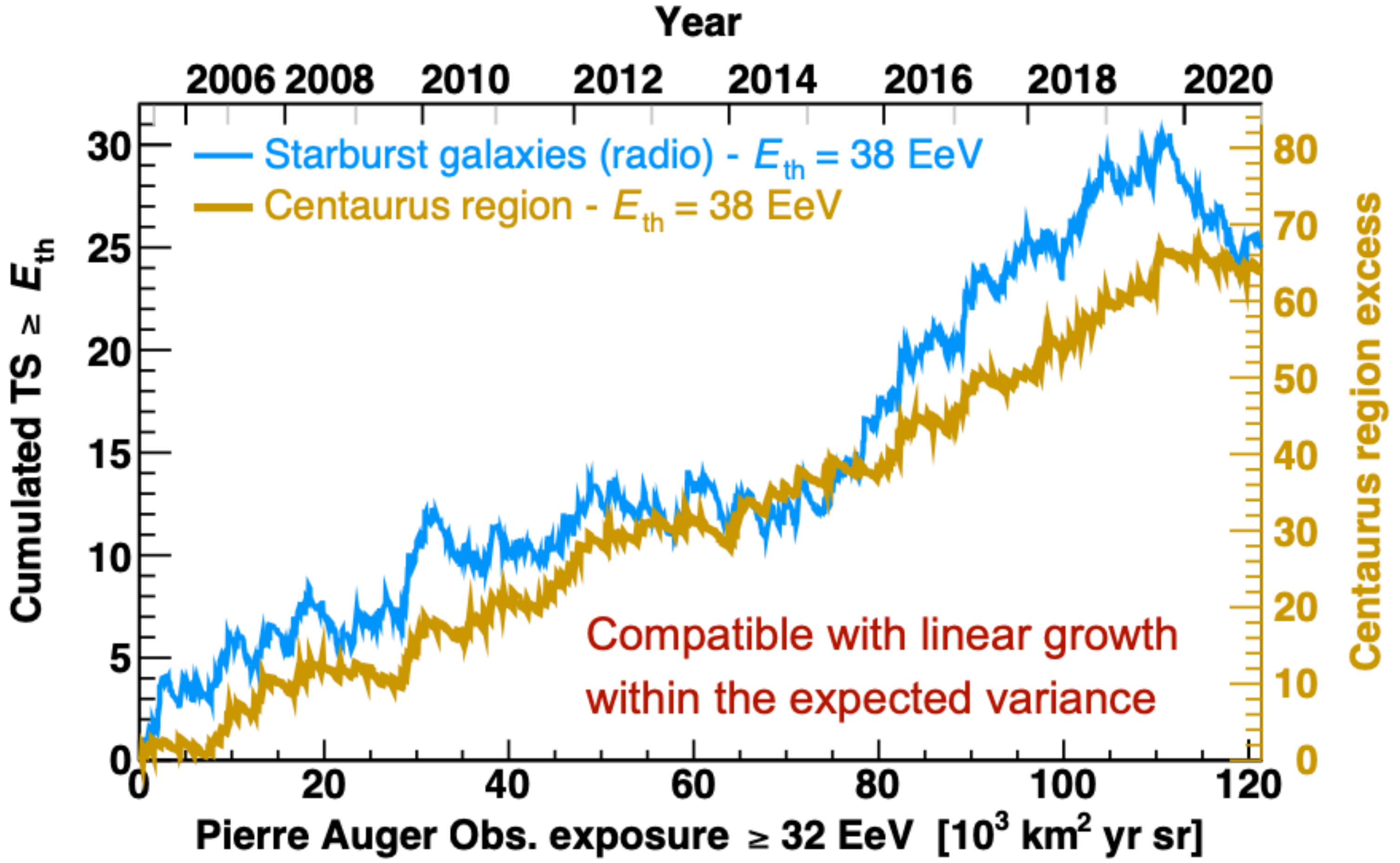

Photo-interaction time

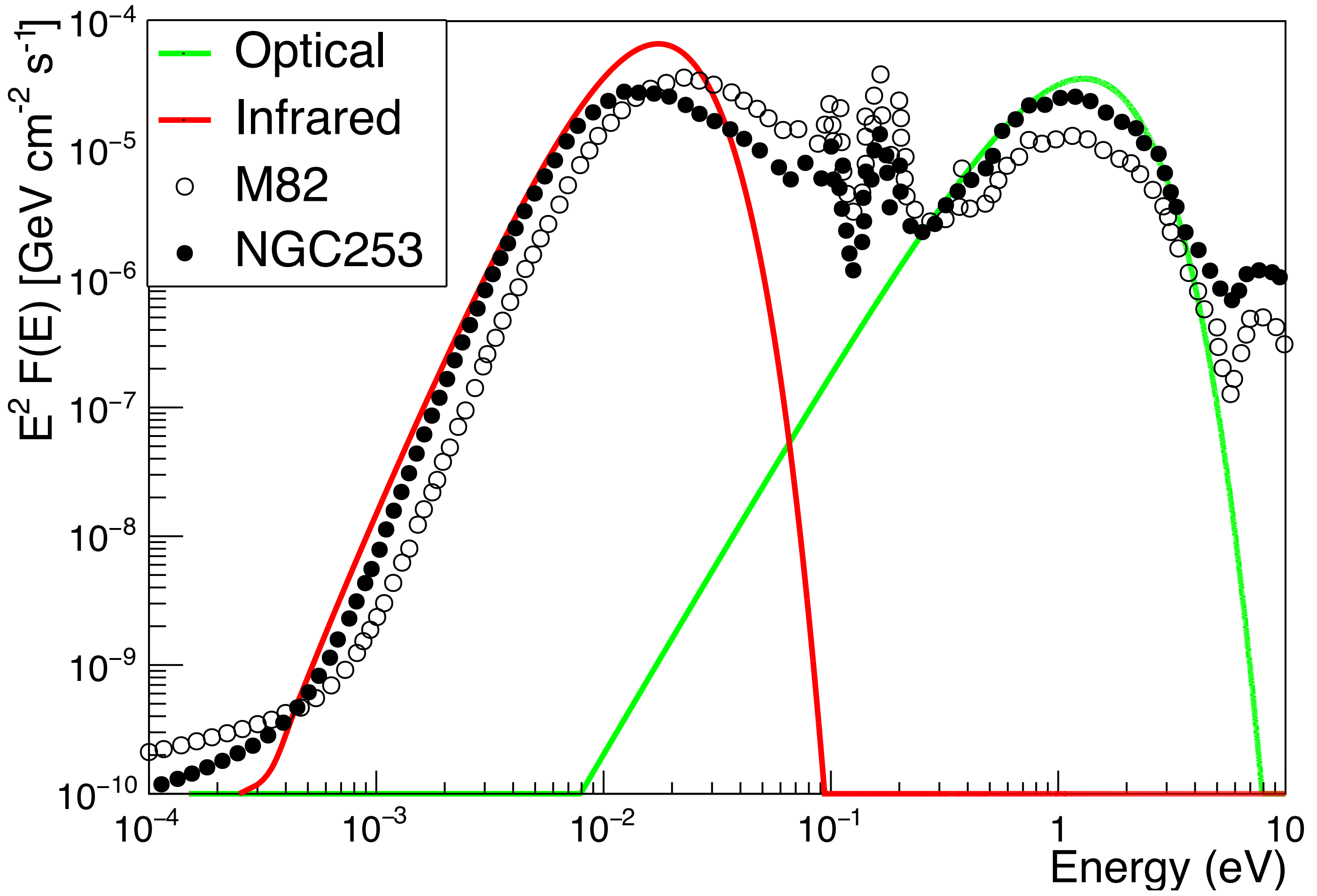

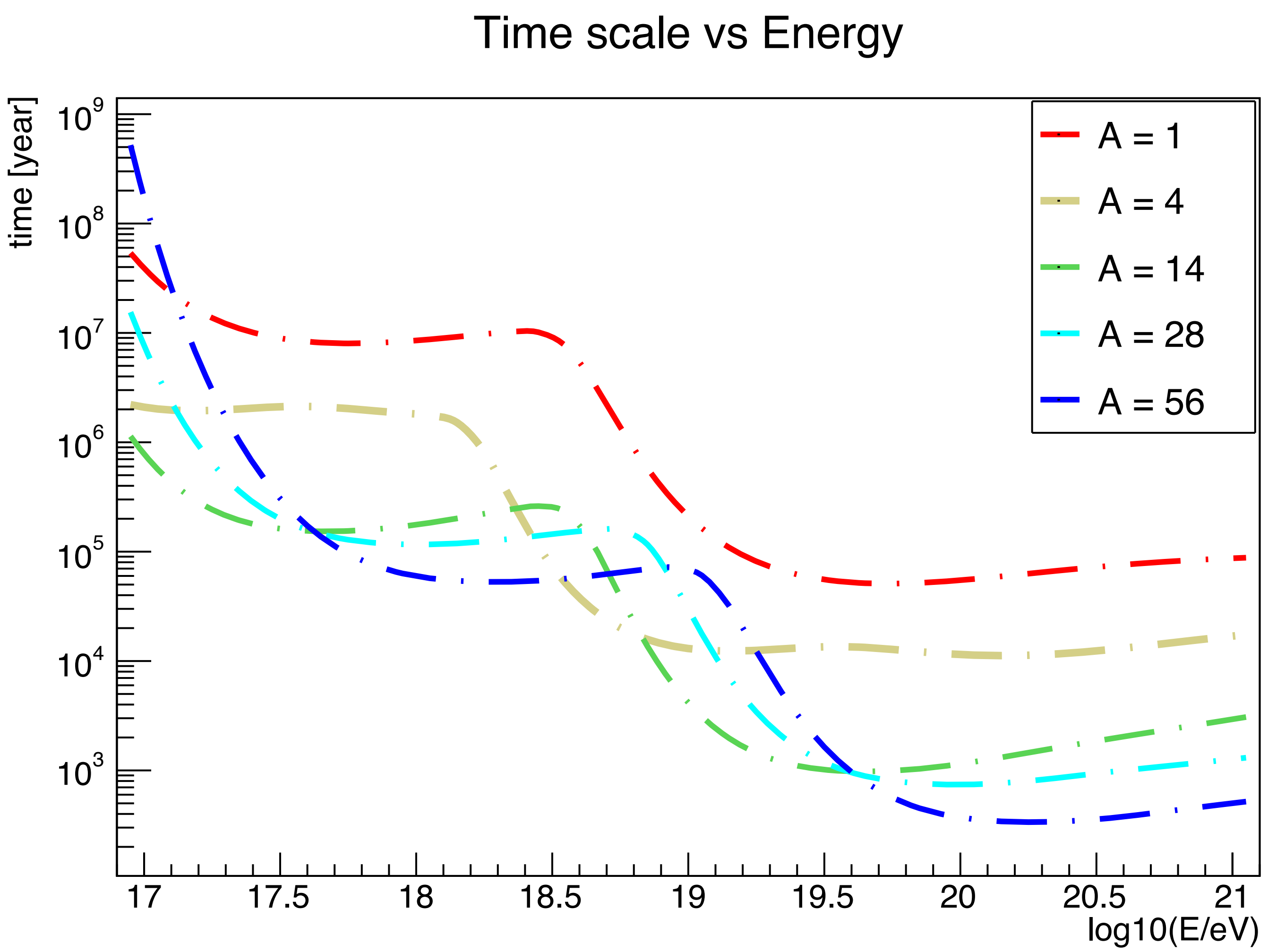

$$\frac{dN}{dt} = \frac{c}{2\Gamma} \int_{\epsilon'_{th}}^{\infty} \sigma_{A\gamma}(\epsilon')\epsilon' \int_{\epsilon'/2\Gamma}^{\infty} \frac{n_\gamma(\epsilon)}{\epsilon^2} d\epsilon \, d\epsilon'$$

Adapting SimProp (software for UHECRs propagation in extra-galactic space):

- Implementation of the photon field in the source;

Frédéric Galliano et al., 2008 ApJ 672 214
E. Peretti et al. Mon. Not. Roy. Astron. Soc. 487 (2019) no.1, 168-180

R. Aloisio et al. JCAP11(2017)009

Spallation time

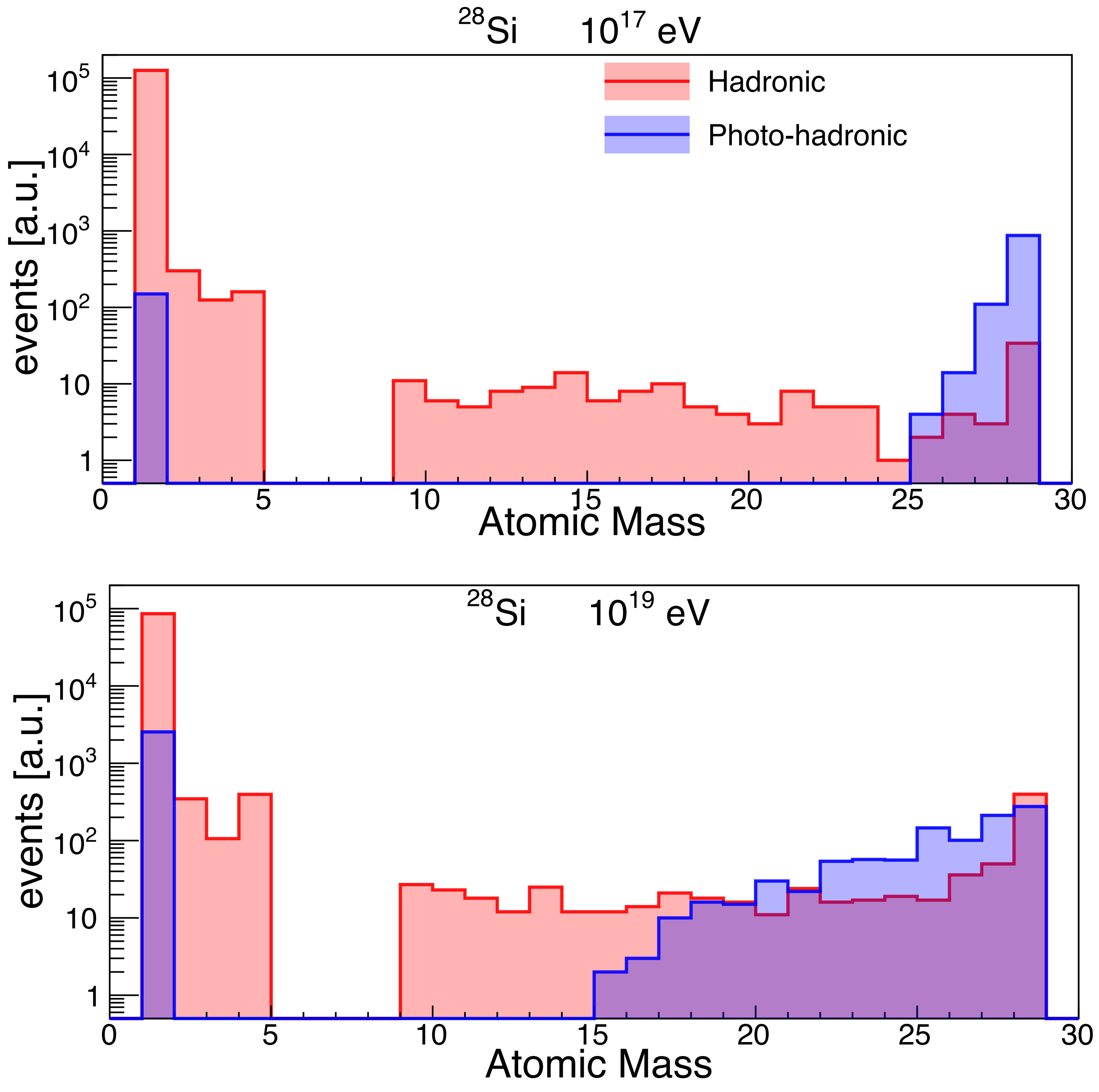

$$\tau_{\rm spal}(E) = \frac{1}{n_{\rm ISM} \cdot \sigma(E) \cdot c}$$

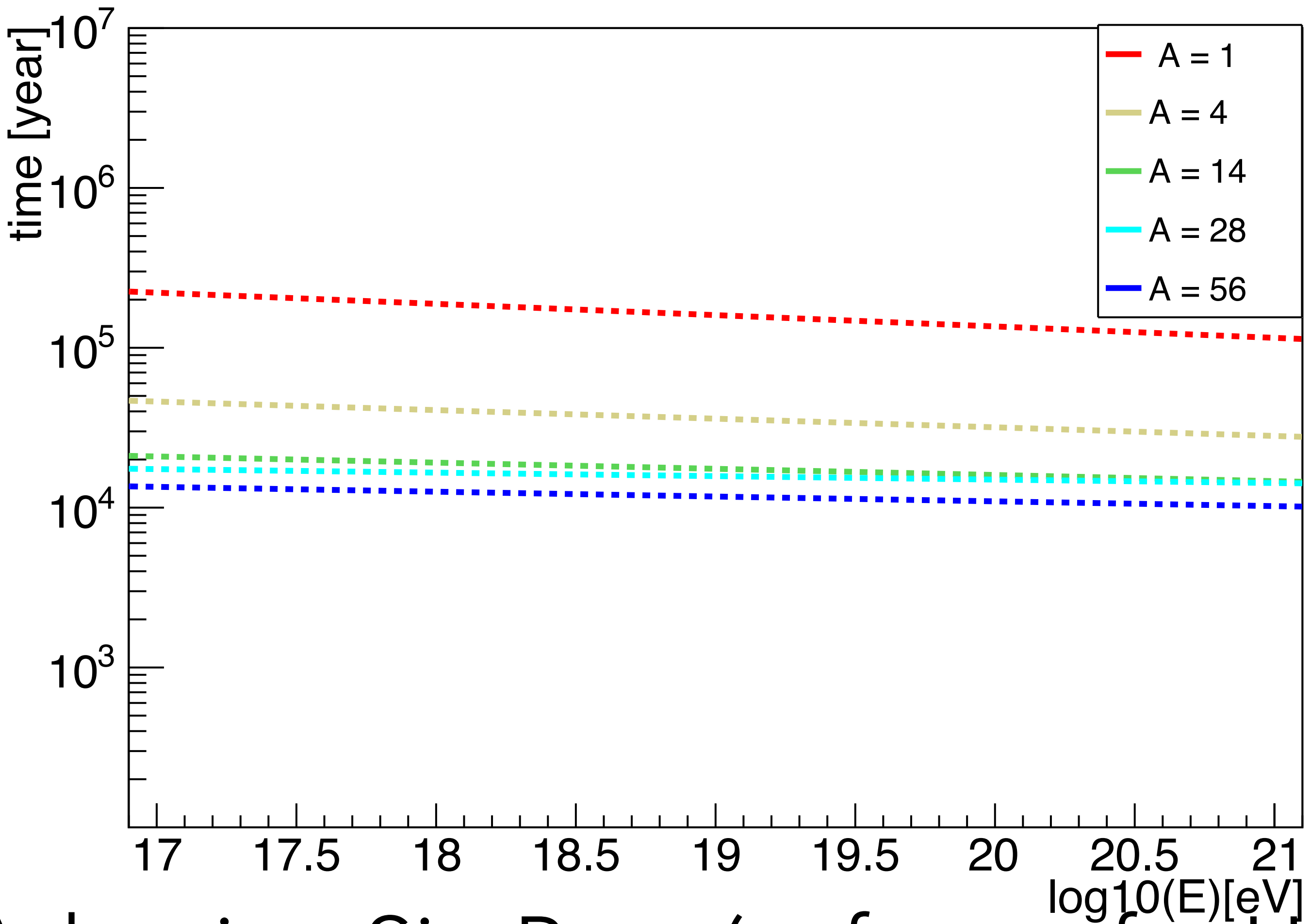

Adapting SimProp (software for UHECRs propagation in extra-galactic space):

- ✴ Implementation of the photon field in the source;
- ✴ Implementation of the spallation process;

IJCLab Irène Joliot-Curie Laboratoire de Physique des 2 Infinis

Escape time

Diffusion

$$\tau_D = \frac{R^2}{D}$$

Depends on the slope in energy and on the coherence lenght l_c

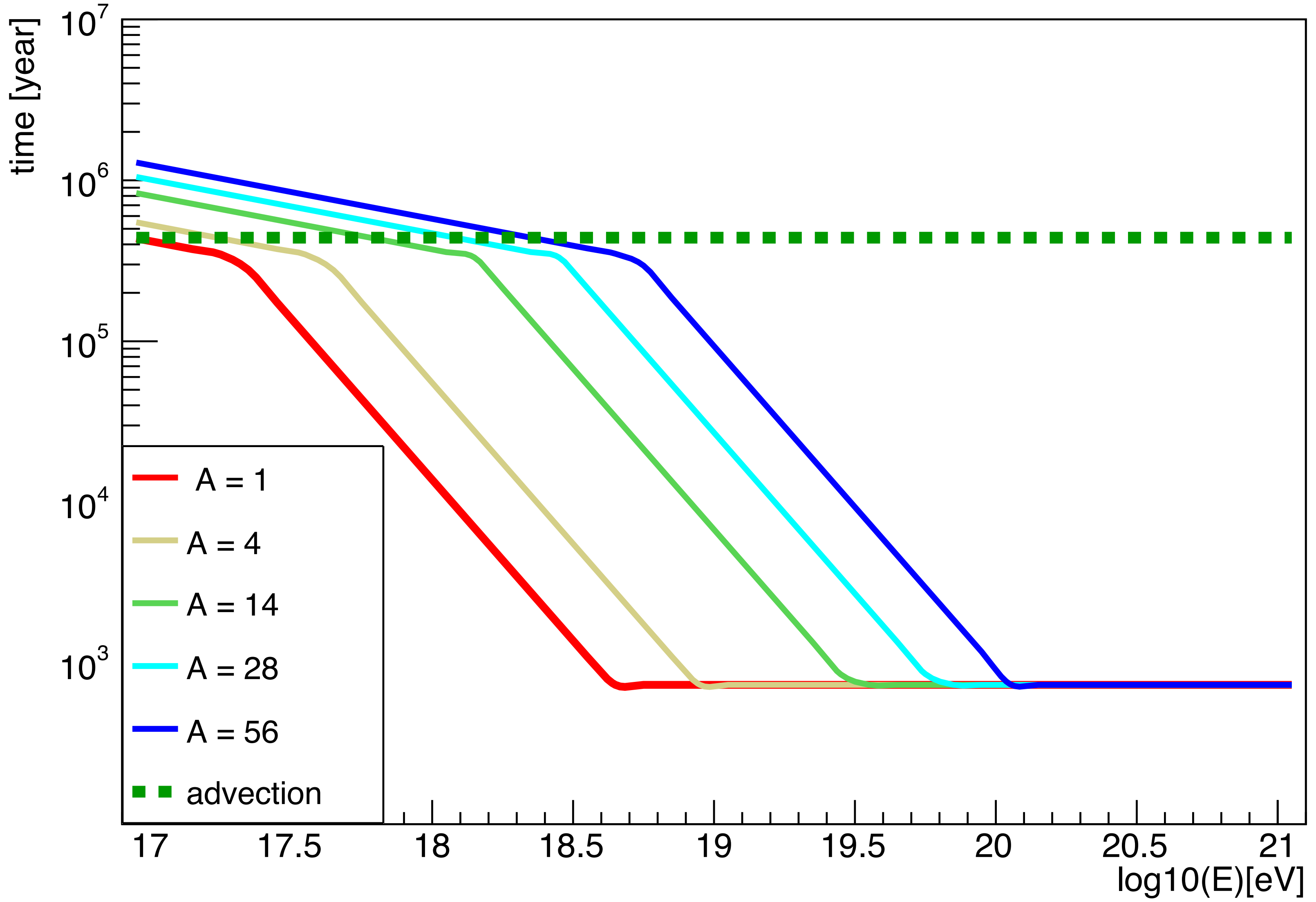

Advection

$$\tau_{\mathrm{adv}} = \frac{R}{v_w}$$

P. Subedi et al 2017 ApJ 837 140

IJCLab Irène Joliot-Curie Laboratoire de Physique des 2 Infinis

Total timescale

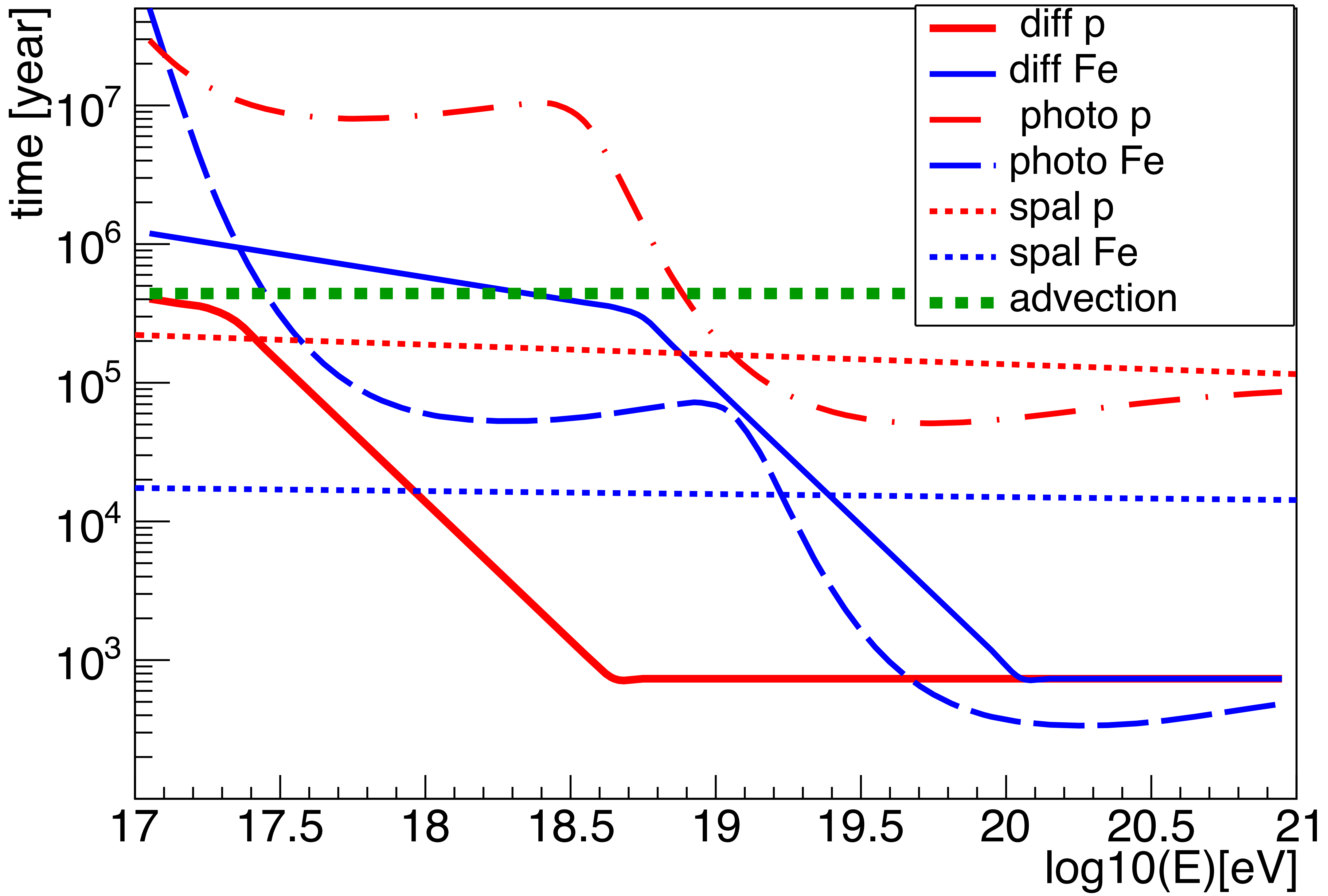

IJCLab Irène Joliot-Curie Laboratoire de Physique des 2 Infinis

Comparison to the experimental data

- A single nuclear specie is propagated inside the source. Sources are considered identical.
- The escaping fluxes are propagated through the Universe.
- The fluxes arriving in atmosphere are compared to the experimental data.
- Within the parameter space, a set of parameters at the source that can describe energy spectrum and composition at Earth was found.

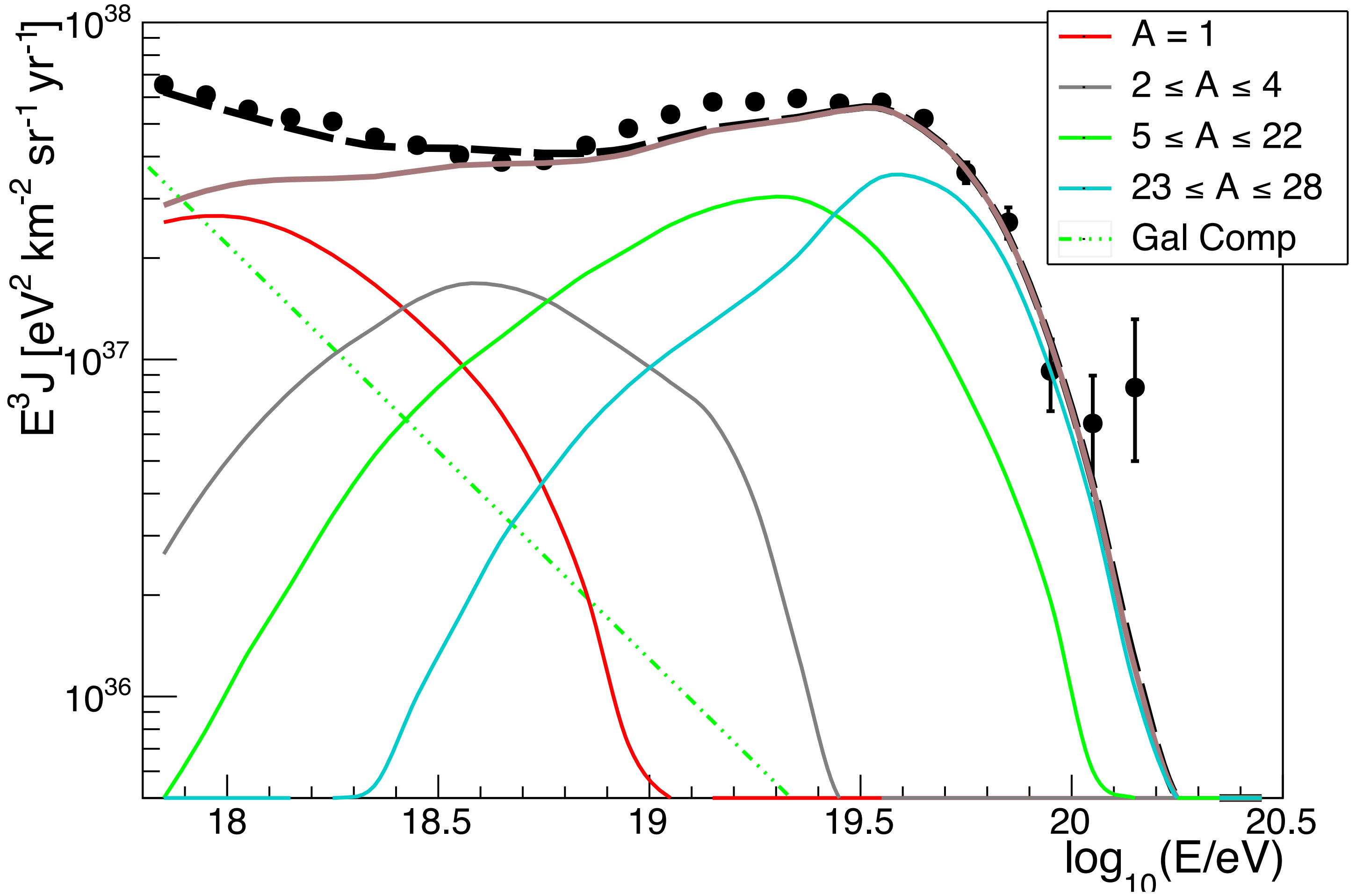

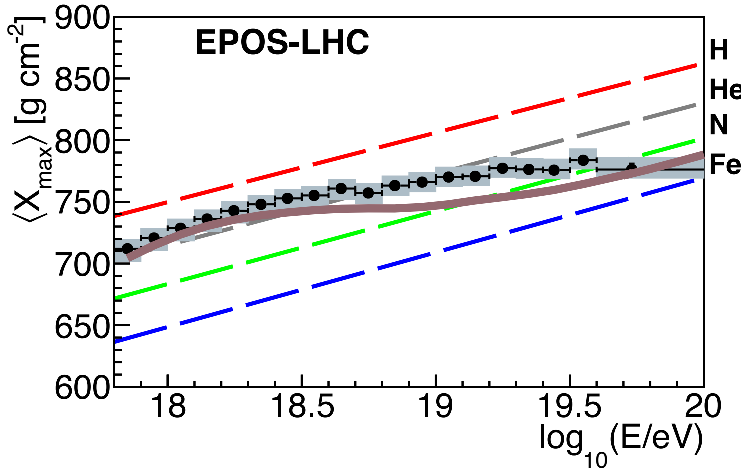

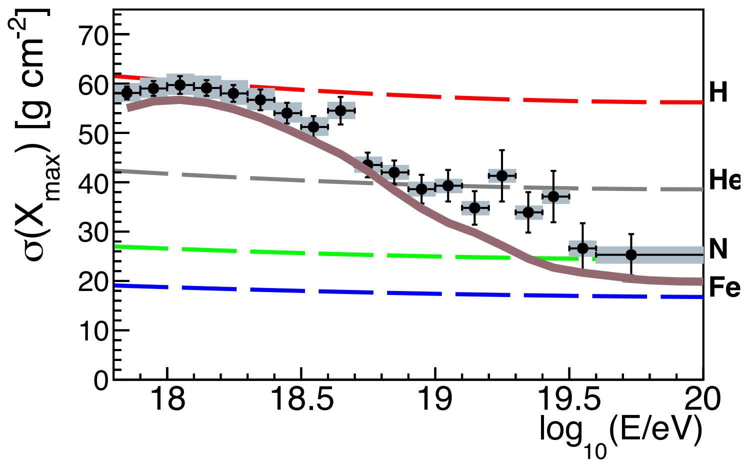

$L_{IR} = 5.02 \cdot 10^{44}$erg/s

$R = 250$ pc

$n_{\rm ISM} = 632$ cm^{-3}

$\gamma^* = 1$

$\log_{10}(R^*_{\rm cut}/V) = 18.5$

$A = 28$

* assuming an injection shape $\frac{dN}{dE} \propto E^{-\gamma} \cdot f(E, Z \cdot R_{\rm cut})$

Effect of the luminosity on the best scenario

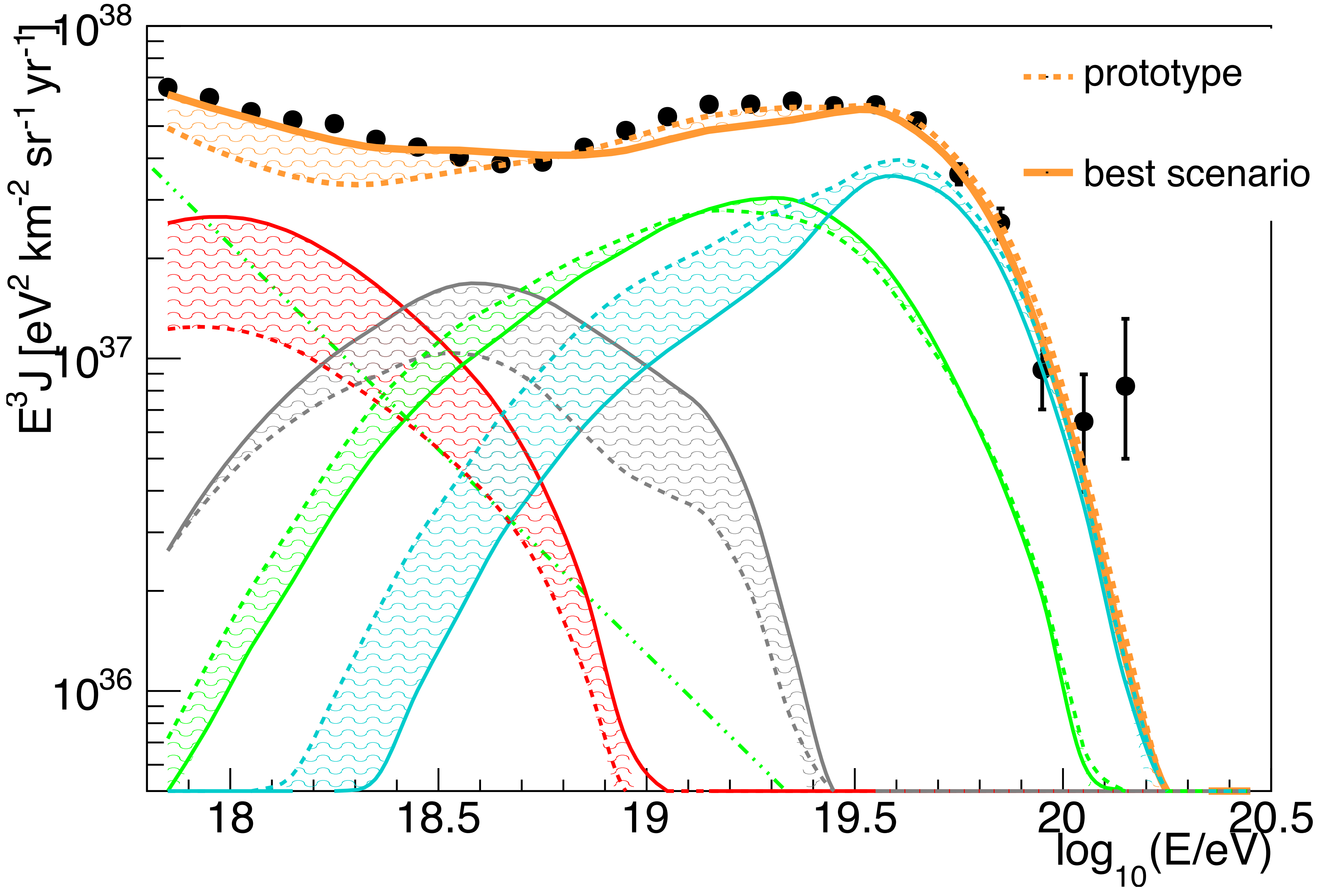

Higher the ISM and photon density

↓

Higher the rate of interactions inside the source

↓

Higher efficiency of disintegration

Including hadronic interactions

Including spallation processes

↓

Increase the probability of disintegration

↓

More visible at intermediate energies

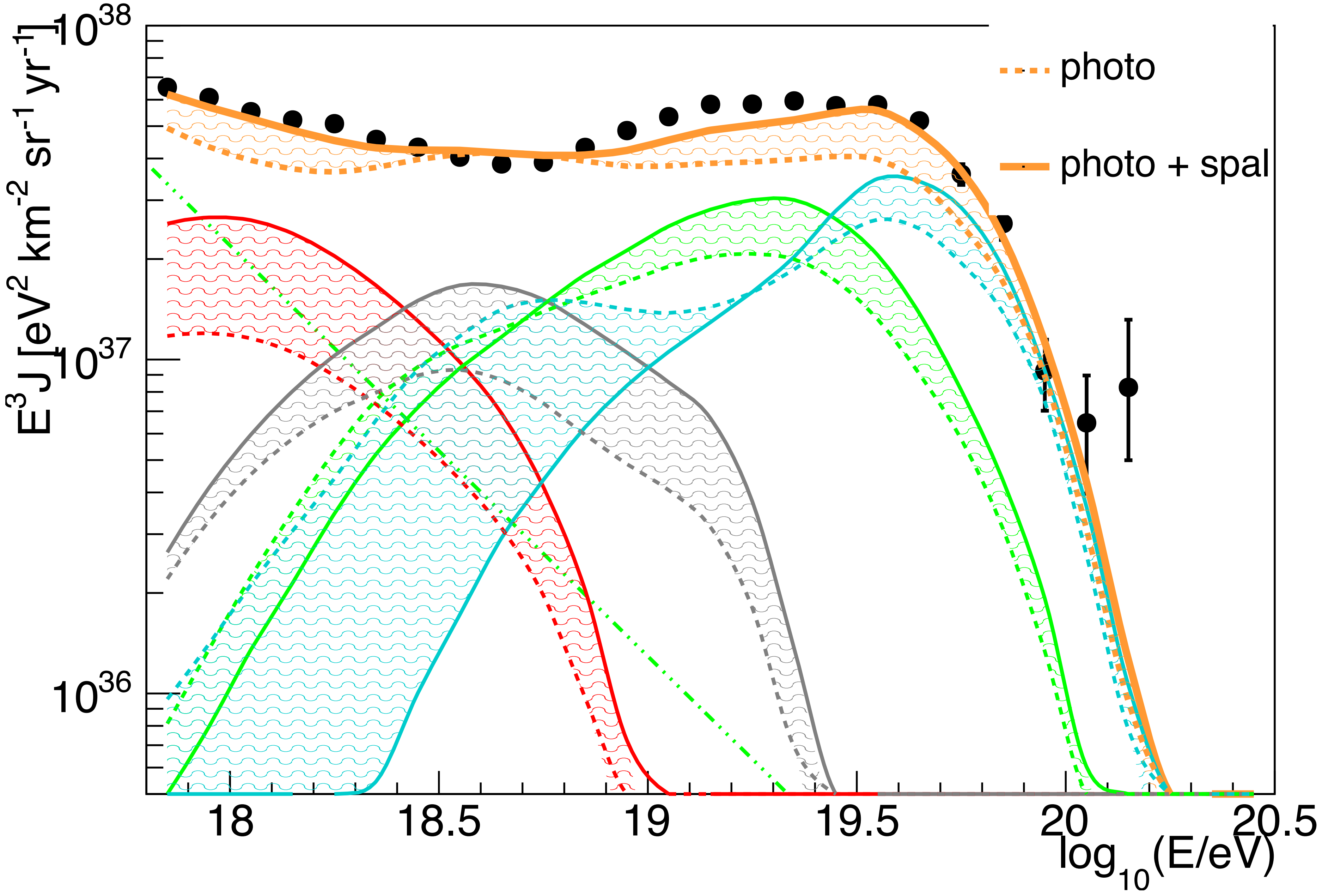

Associated neutrino fluxes

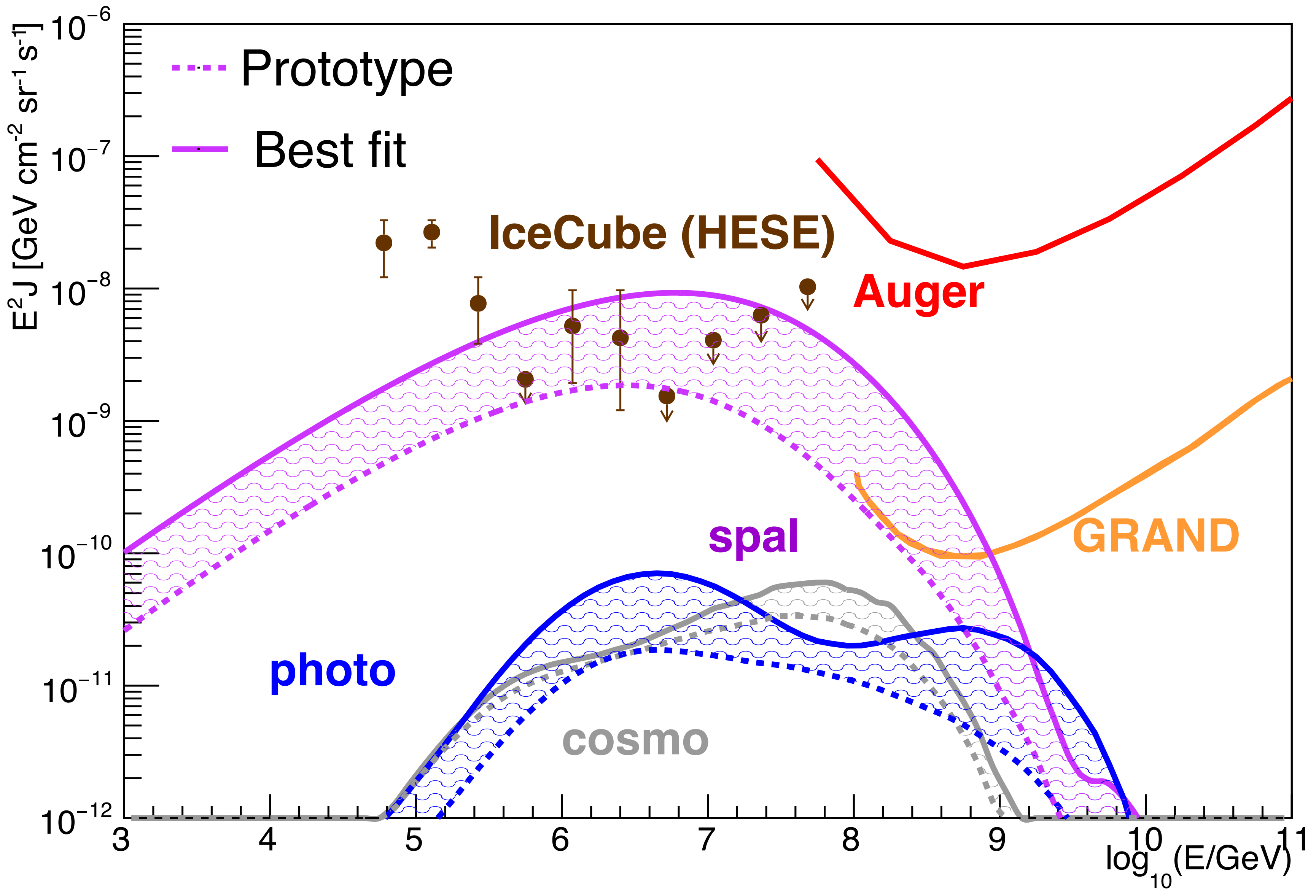

- Cosmogenic neutrinos are comparable to photo-interaction neutrinos produced in the source.
- Decreasing the luminosity, the neutrino fluxes from source decrease;
- Once taken into account also the hadronic interactions, the expected neutrino flux is larger and can be used to constrain plausible scenarios that describe the UHECR data.

Cap 1: Distance of UHECRs

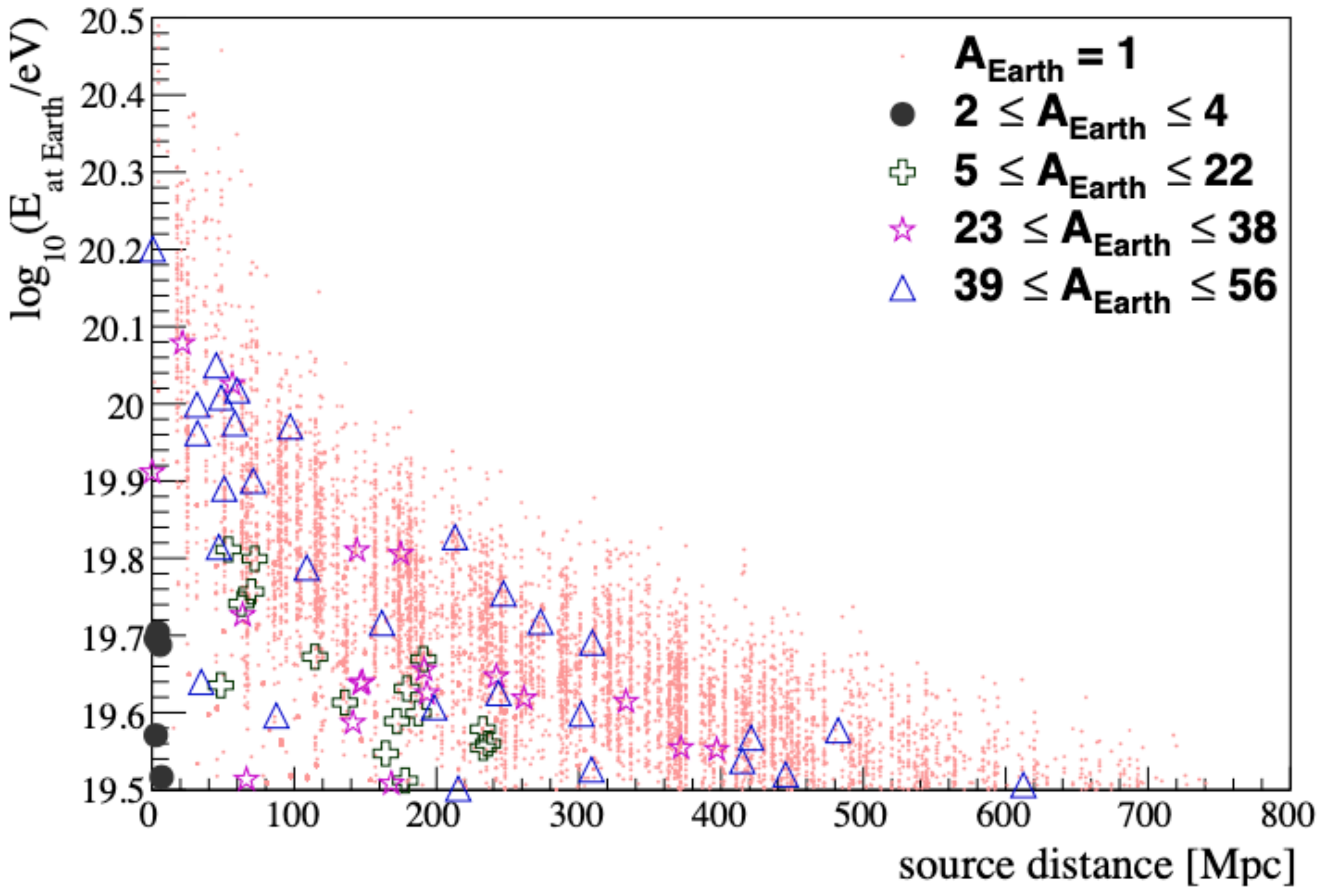

IJCLab Irène Joliot-Curie Laboratoire de Physique des 2 Infinis

Interactions

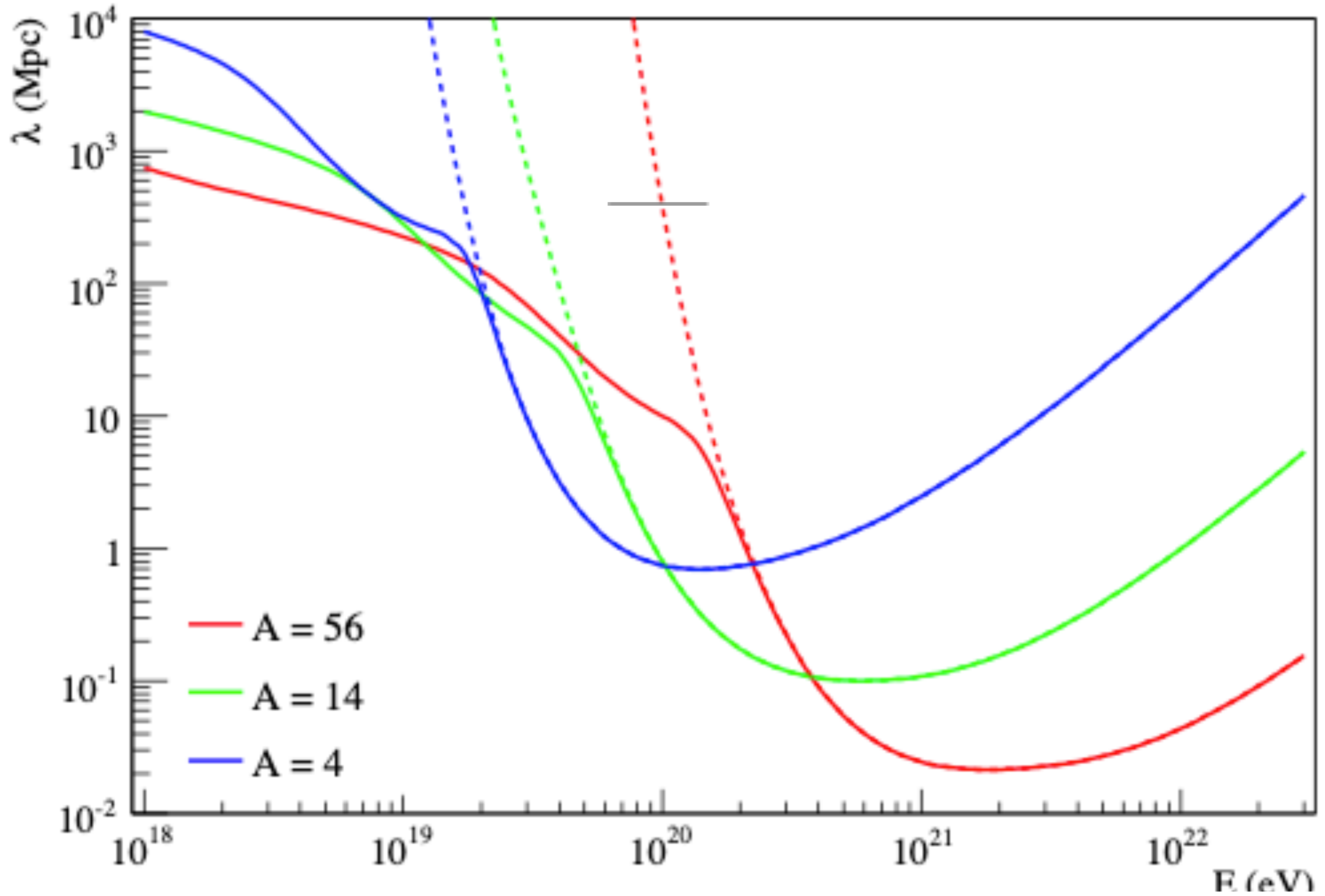

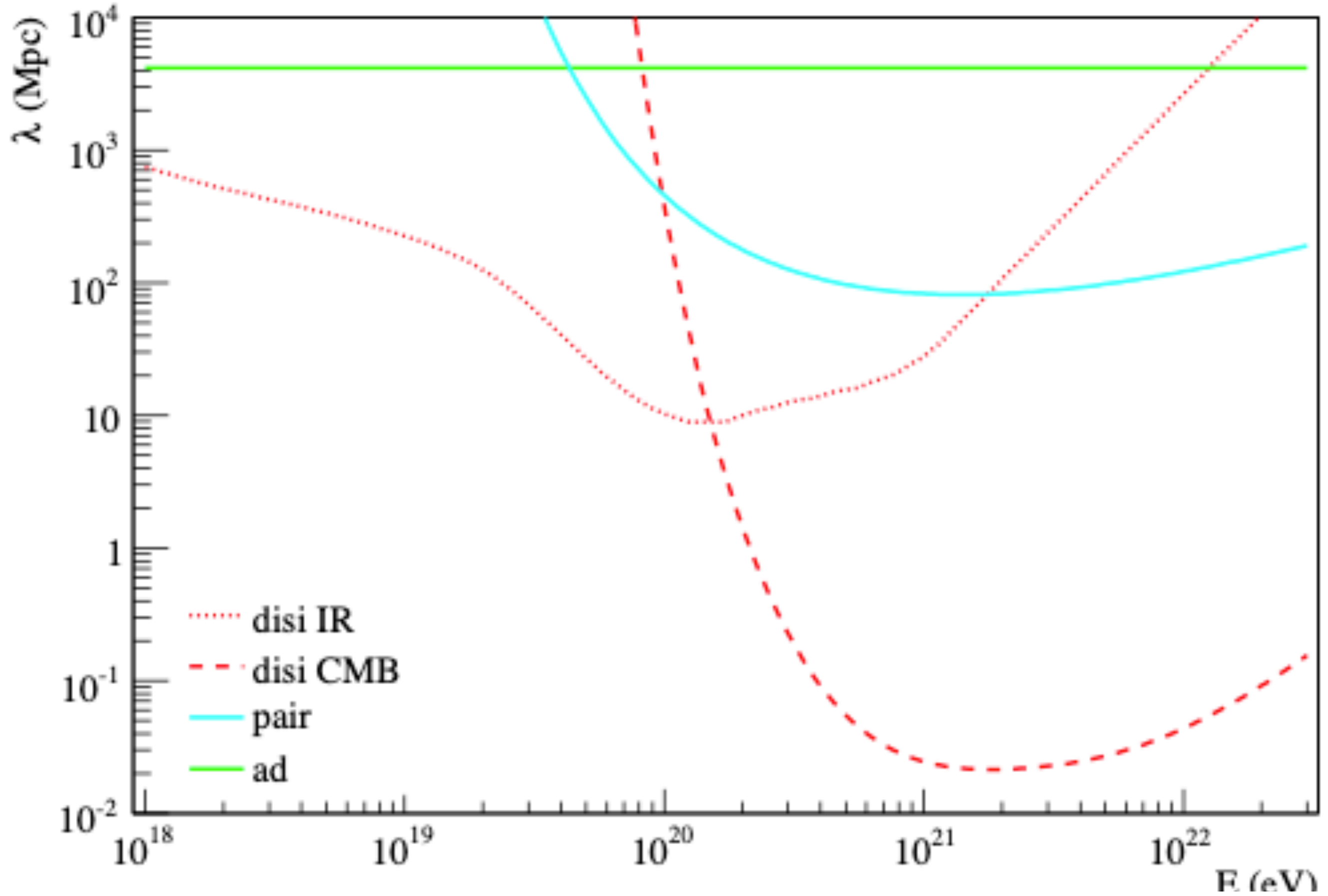

pair production energy threshold: 1 MeV and monotonically decrease (scale as Z^2/A)

Photodisintegration 8 MeV

Photopion 145 MeV —-> E/A matters

$$\beta_{ad}(A,Z) = -\frac{1}{E}\frac{dE}{dz}\left(\frac{dt}{dz}\right)^{-1} = H_0\sqrt{(1+z)^3\Omega_m + \Omega_\Lambda} = H(z)$$

As a consequence of the expansion of the Universe, relativistic particles are observed today with an energy E(z = 0) redshifted with respect to the initial one E(z) according to E(0) = E(z)(1+z) ^{-1}
Dominant at low energy (10^{18})

Detail of the detectors

ICRC 2013

Systematic uncertainty in the energy scale	
Fluorescence yield	3.6%
Atmosphere	3.4% – 6.2%
FD calibration	9.9%
FD profile recon.	6.5% – 5.6%
Invisible energy	3% – 1.5%
Stability of energy scale	5%
TOTAL	14%

IJCLab Irène Joliot-Curie Laboratoire de Physique des 2 Infinis

SD events

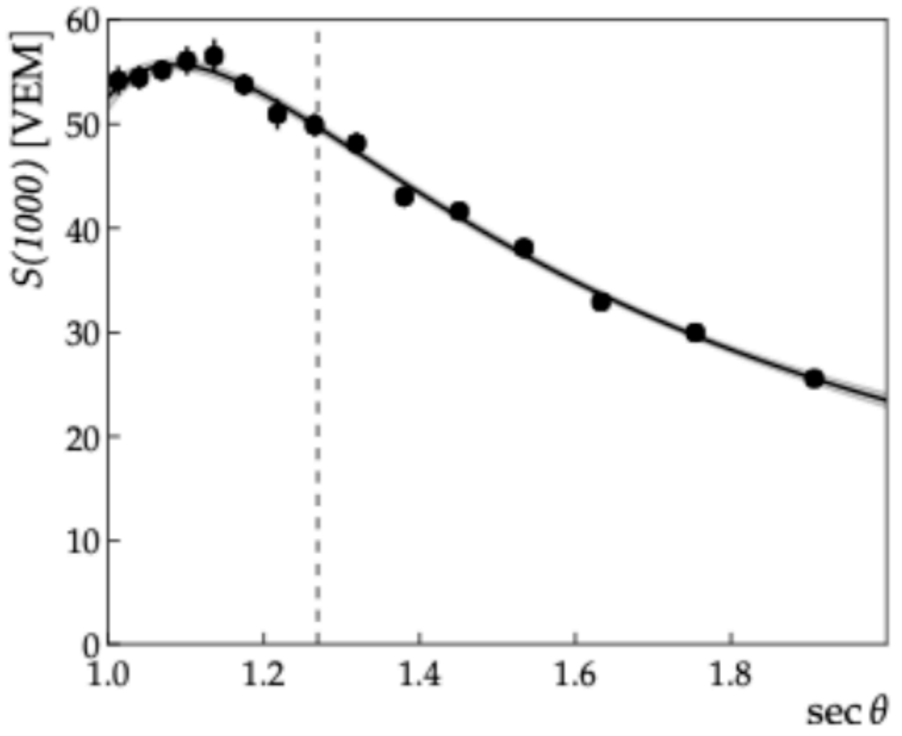

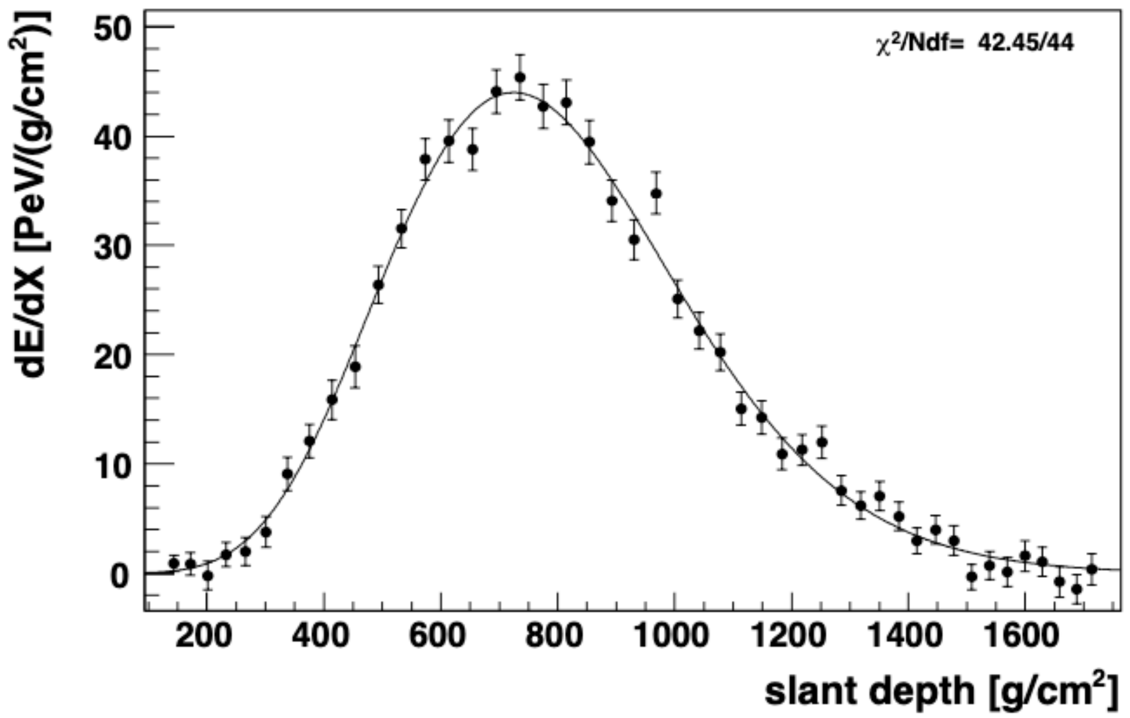

Evolution of the shower front

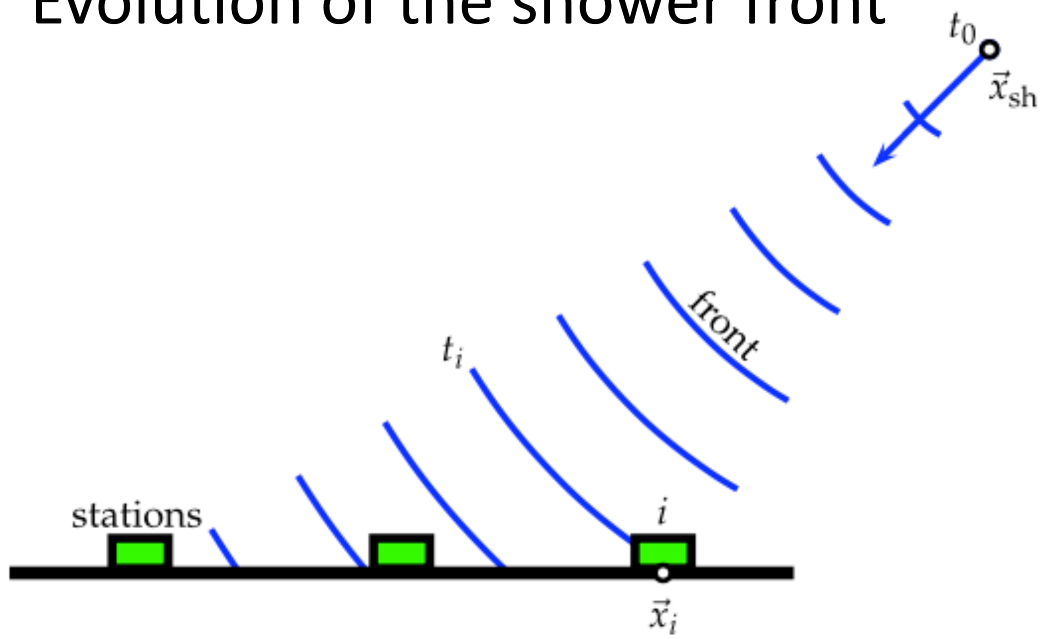

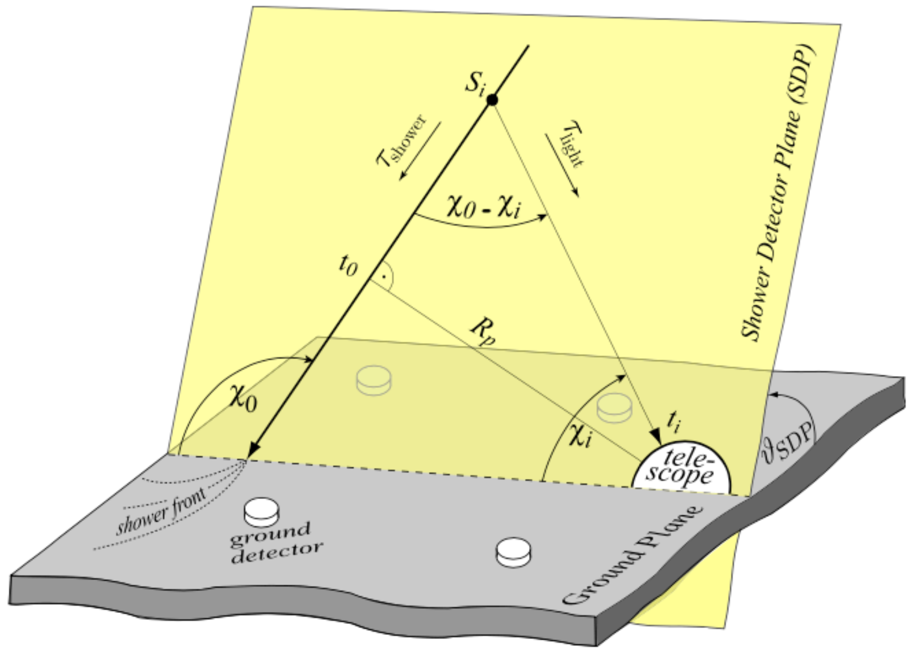

What is the instep?

$$J(E;\mathbf{s}) = J_0\left(\frac{E}{E_0}\right)^{-\gamma_1}\left[1+\left(\frac{E}{E_{12}}\right)^{\frac{1}{\omega_{12}}}\right]^{(\gamma_1-\gamma_2)\omega_{12}} \times \frac{1}{1+(E/E_s)^{\Delta\gamma}}.$$

Old—> 6 fitted parameters!

$$J(E;\mathbf{s}) = J_0\left(\frac{E}{E_0}\right)^{-\gamma_1}\prod_{i=1}^{3}\left[1+\left(\frac{E}{E_{ij}}\right)^{\frac{1}{\omega_{ij}}}\right]^{(\gamma_i-\gamma_j)\omega_{ij}}$$

New-> 8 fitted parameters! (4 spectral indexes, 3 transition energies and a normalization)

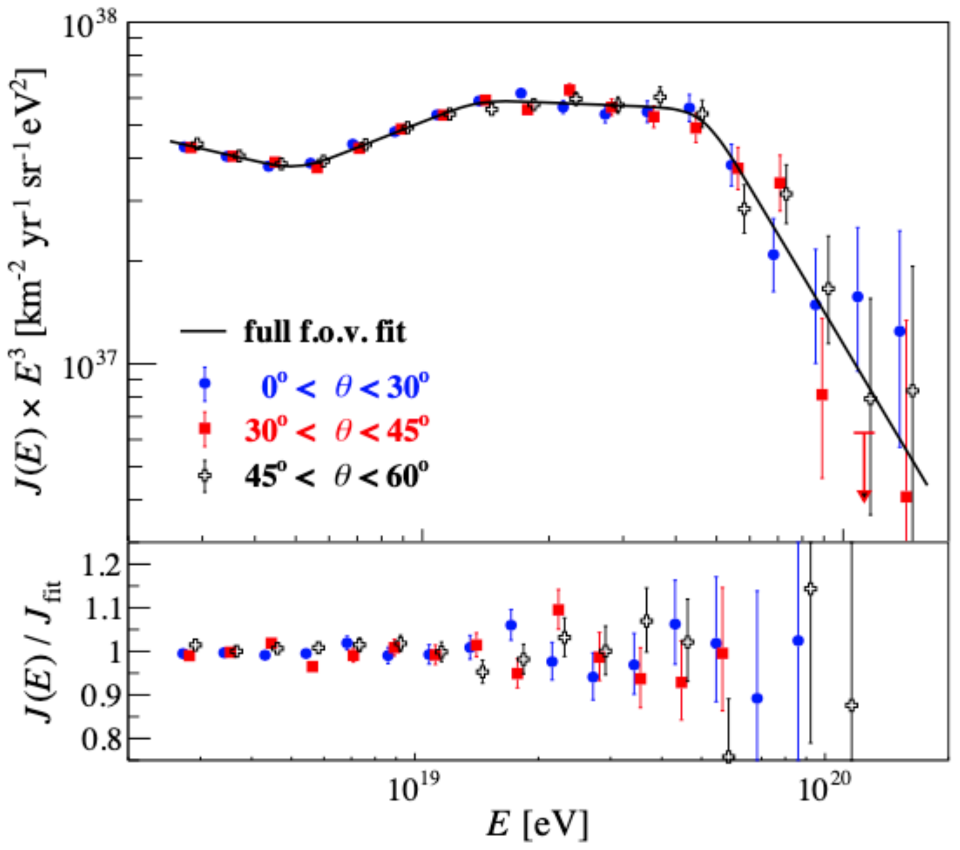

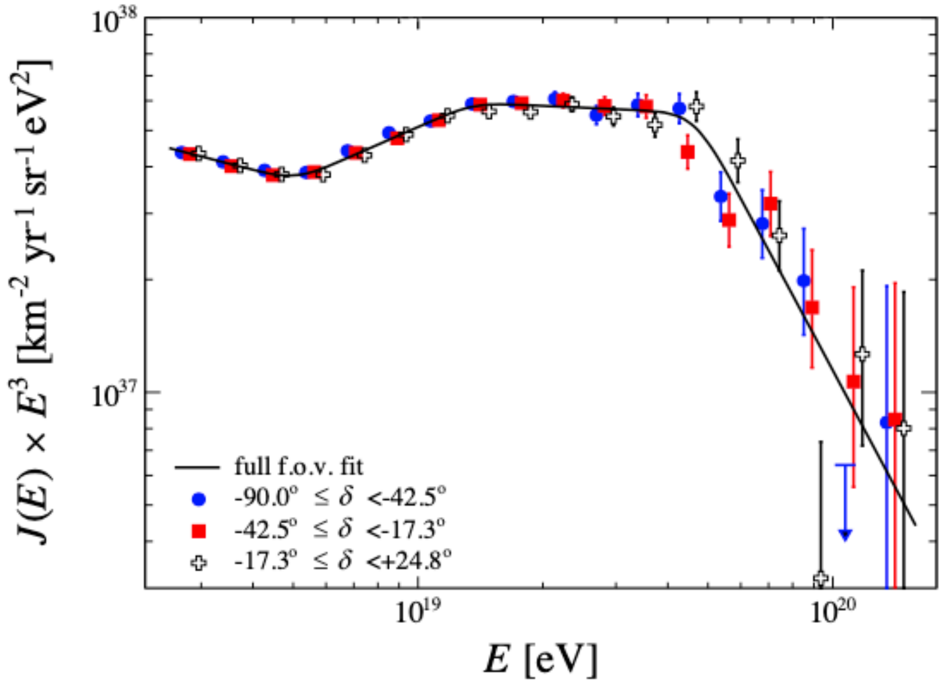

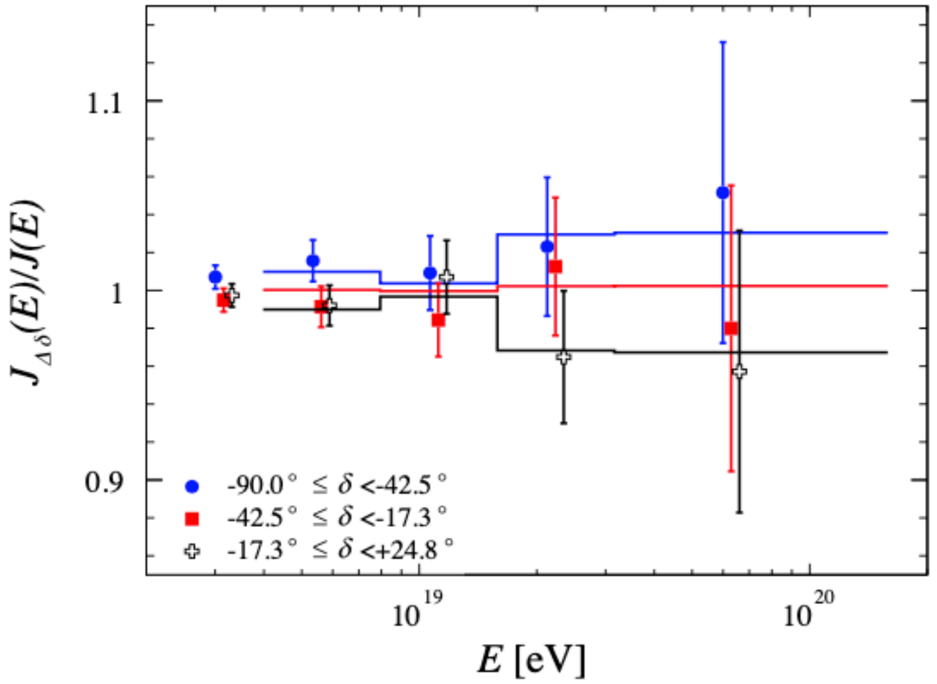

IJCLab Irène Joliot-Curie Laboratoire de Physique des 2 Infinis

What is the instep?

Cosmic ray flux (isotropic, spectral flux)

$$\phi(E) = \frac{\mathrm{d}N}{\mathrm{d}E\,\mathrm{d}A\,\mathrm{d}t\,\mathrm{d}\Omega}$$

Spectral particle number density (differential in energy)

$$n(E,\vec{x}) = \frac{\mathrm{d}N}{\mathrm{d}E\,\mathrm{d}^3x} = \frac{4\pi}{\beta c}\,\phi(E)$$

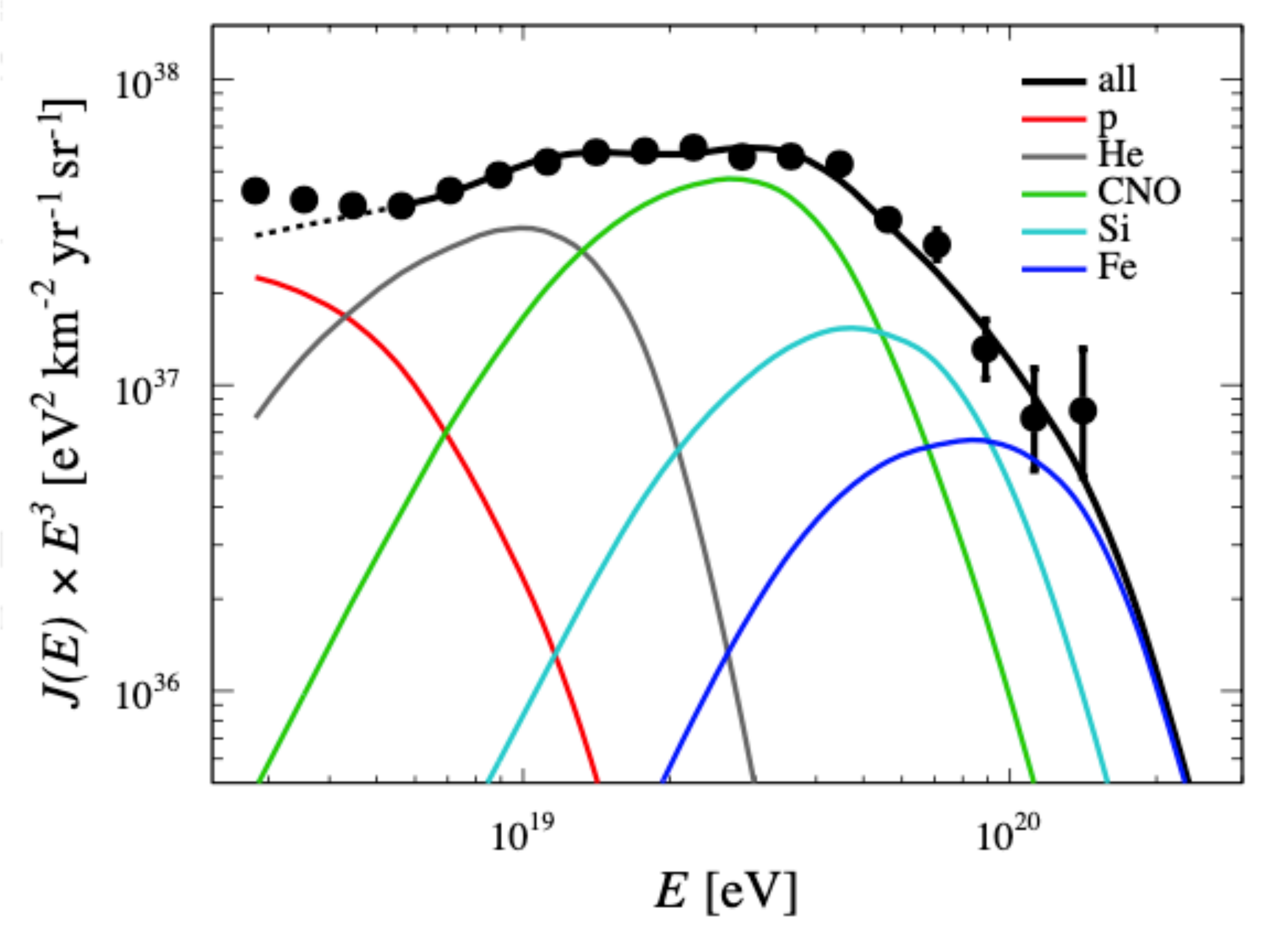

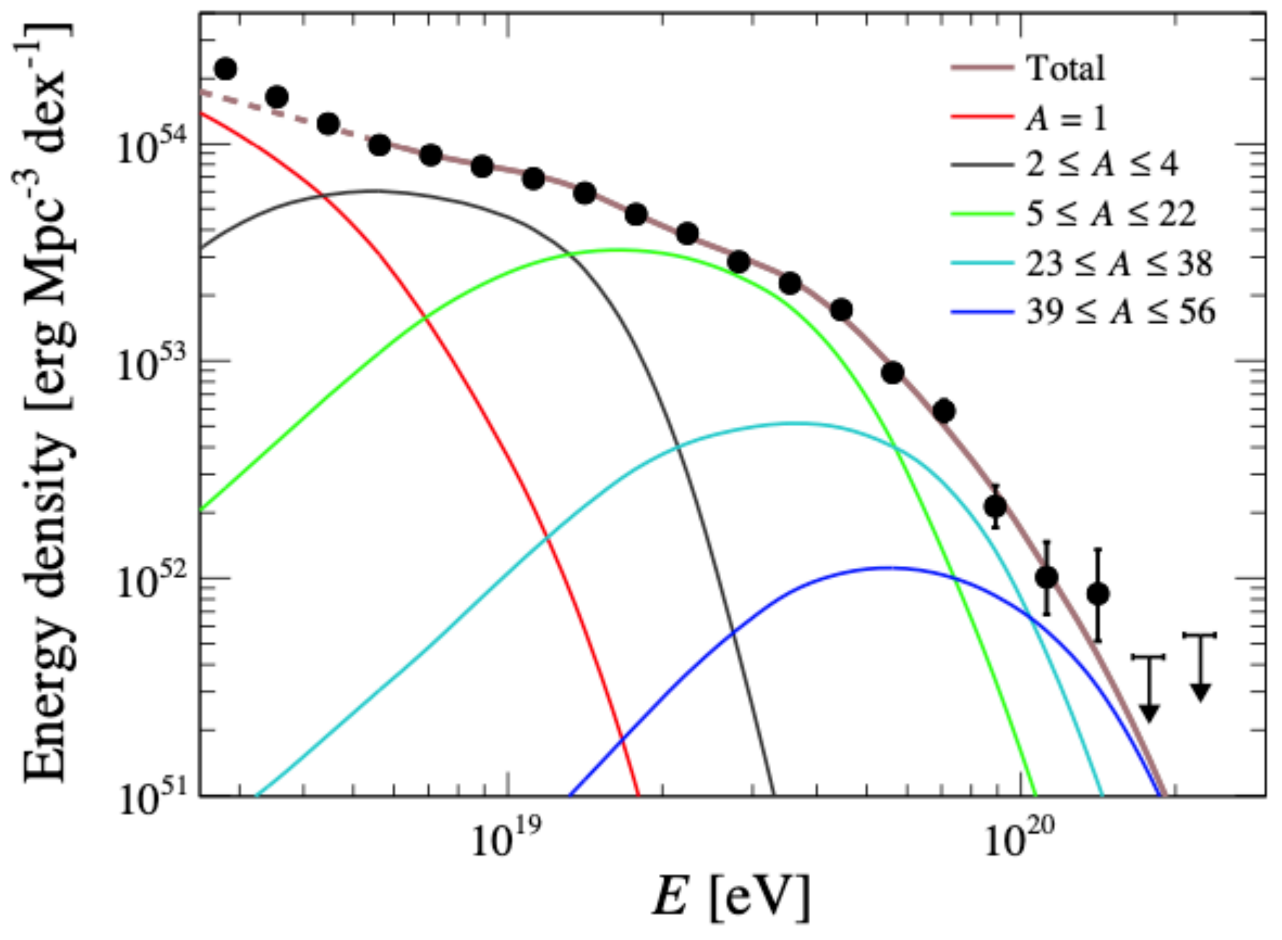

Large scale anisotropies

Rayleigh analysis in right ascension

$$a_\alpha = \frac{2}{\mathcal{N}} \sum_{i=1}^{N} w_i \cos \alpha_i, \qquad b_\alpha = \frac{2}{\mathcal{N}} \sum_{i=1}^{N} w_i \sin \alpha_i.$$

Fourier transform: classical approach to study the large-scale anisotropies in the arrival directions of cosmic rays

The amplitude r_α and phase φ_α of the first harmonic of the modulation are obtained from

$$r_\alpha = \sqrt{a_\alpha^2 + b_\alpha^2}, \qquad \tan \varphi_\alpha = \frac{b_\alpha}{a_\alpha}.$$

Energy [EeV]	**Number of events**	**Fourier coefficient a_α**	**Fourier coefficient b_α**	**Amplitude r_α**	**Phase φ_α [°]**	**Probability $P(\geq r_\alpha)$**
4 to 8	81,701	0.001 ± 0.005	0.005 ± 0.005	$0.005^{+0.006}_{-0.002}$	80 ± 60	0.60
≥ 8	32,187	-0.008 ± 0.008	0.046 ± 0.008	$0.047^{+0.008}_{-0.007}$	100 ± 10	2.6×10^{-8}

IJCLab Irène Joliot-Curie Laboratoire de Physique des 2 Infinis

Intermediate scale anisotropies

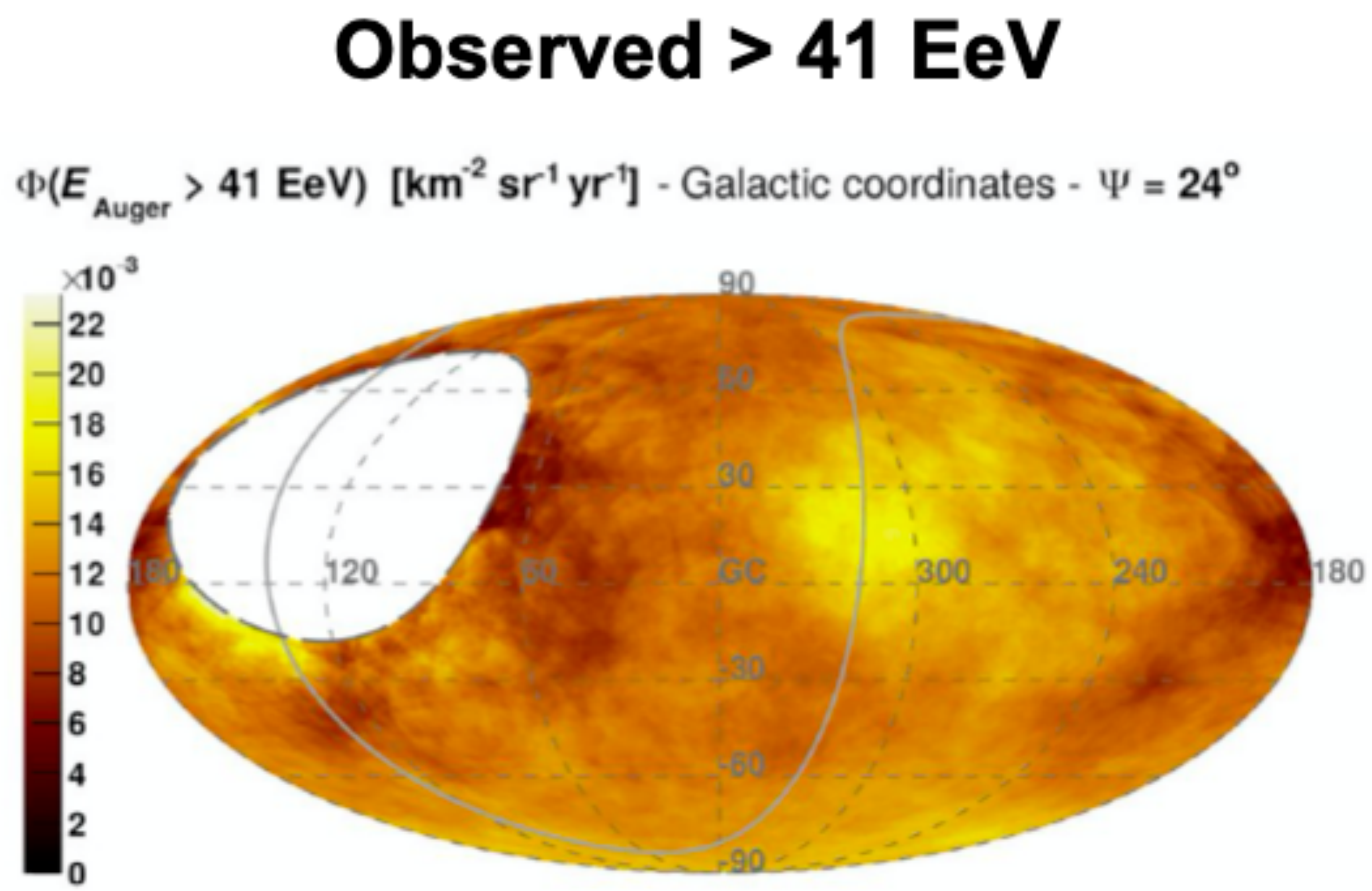

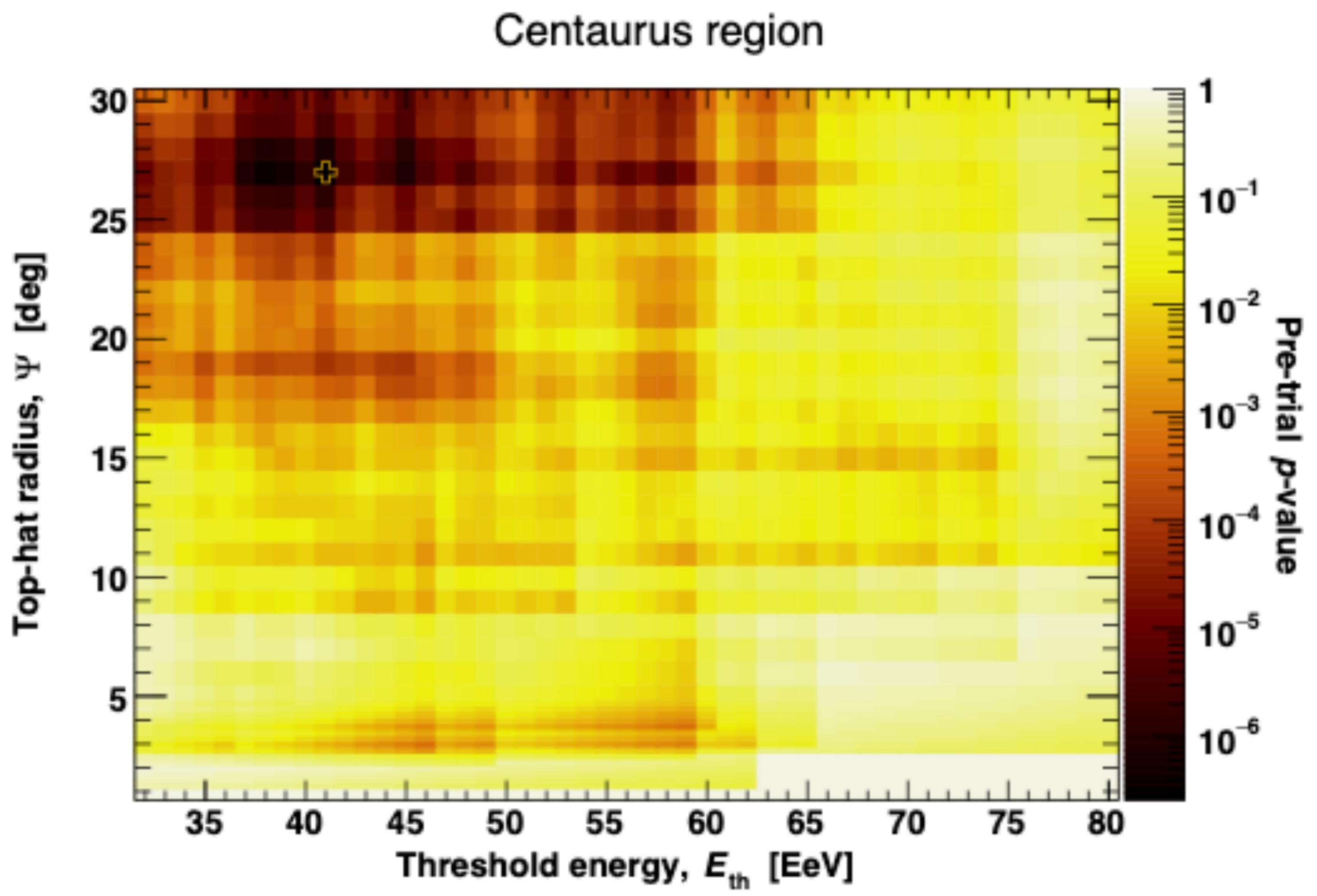

The number of events, N_{observed}, above an energy threshold E_{th} within a disc of radius Ψ centered on equatorial coordinates (R.A.,Dec.) is compared with that expected, N_{expected}, from an isotropic distribution of arrival directions accounting for the geometric exposure of the Observatory.

The search is performed over a grid, by threshold steps of 1 EeV between 32 and 80 EeV, by radial steps of 1° between 1° and 30°, and on a directional grid of 1° spacing, a value which corresponds to the angular resolution of the Observatory at the energies of interest

A Aab et al. [Pierre Auger], Astrophys. J. Lett. 853 (2018) no.2, L29

IJCLab Irène Joliot-Curie Laboratoire de Physique des 2 Infinis

Intermediate scale anisotropies

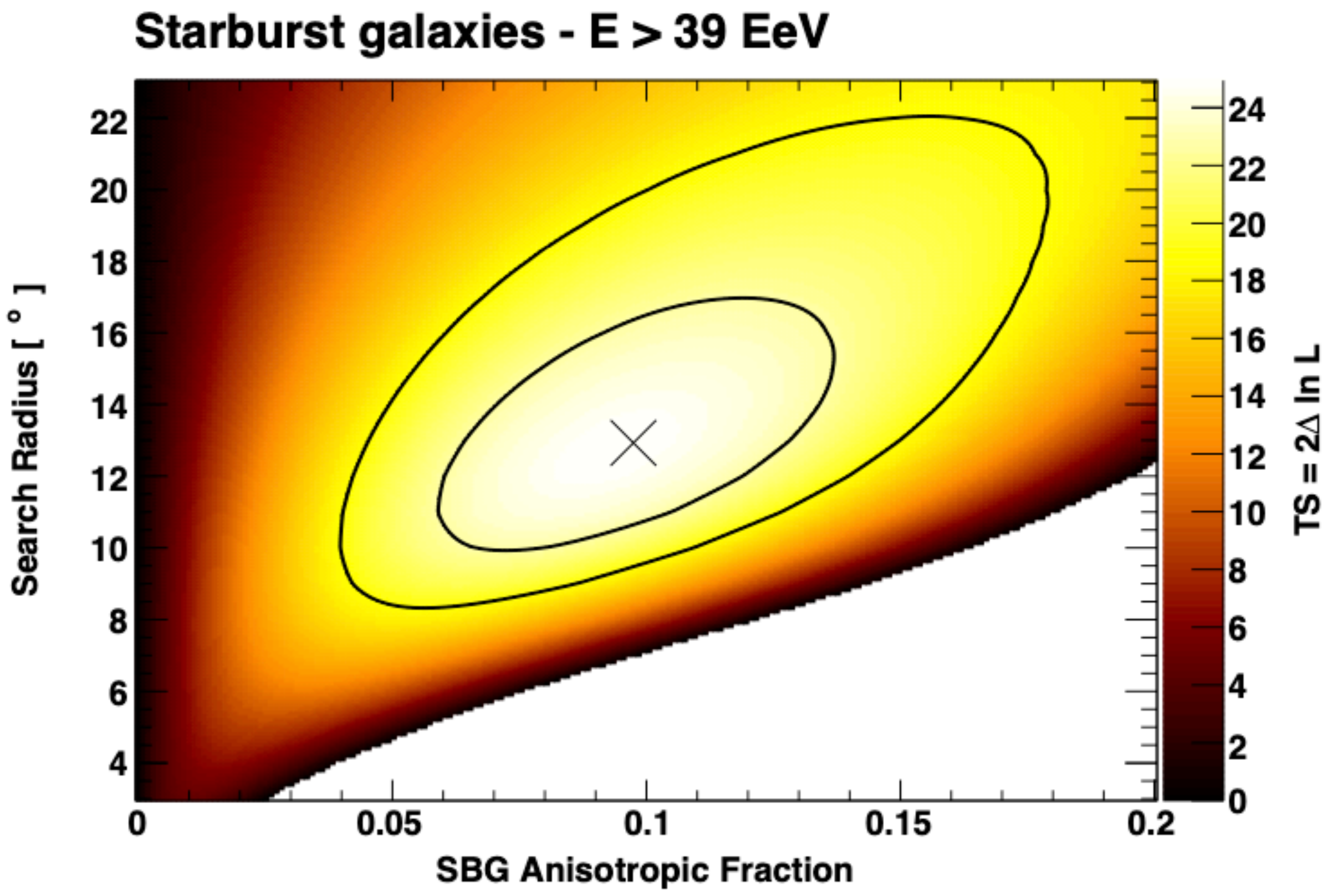

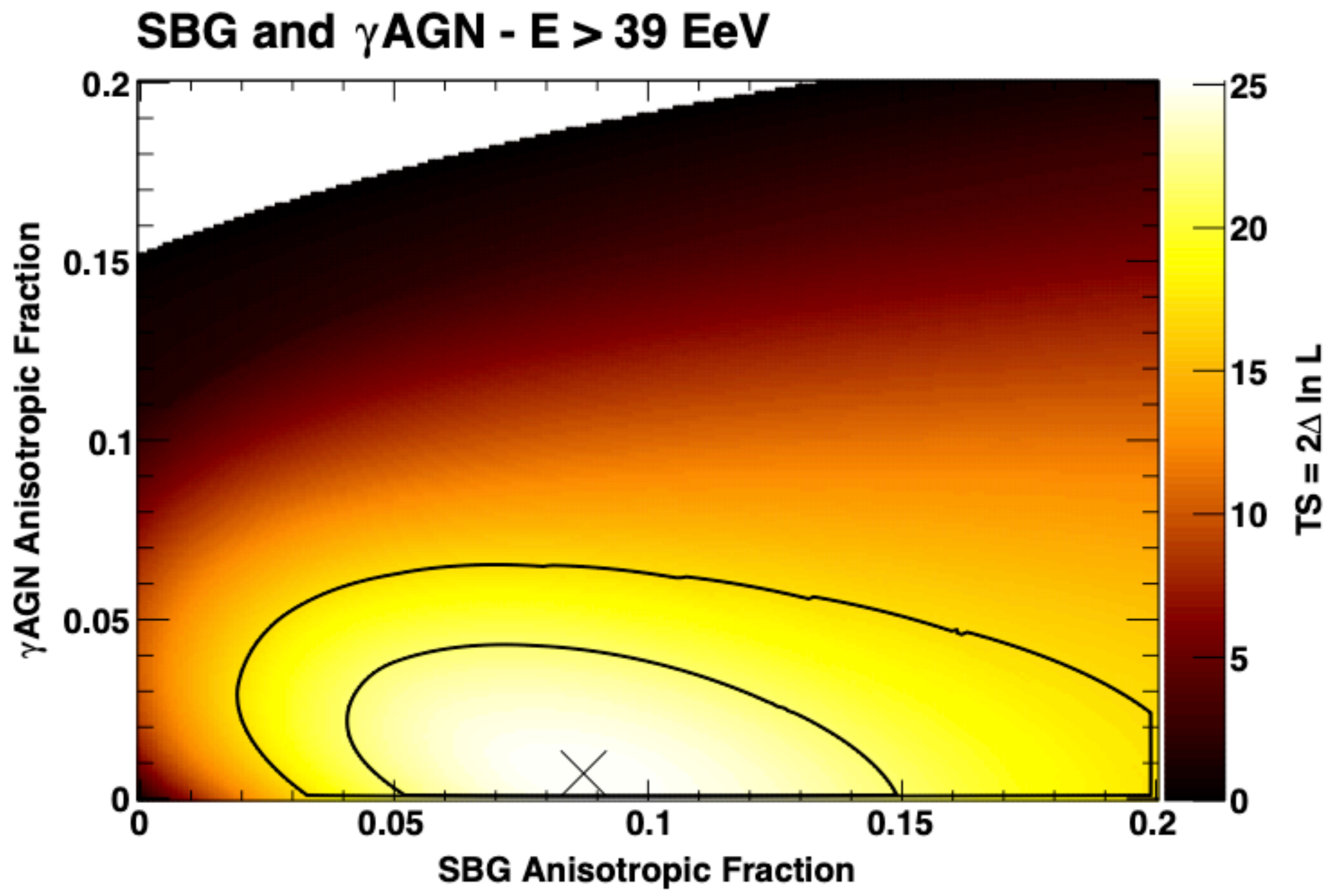

Test hypothesis	Null hypothesis	Threshold energy[a]	TS	Local p-value $\mathcal{P}_{\chi^2}(\mathrm{TS}, 2)$	Post-trial p-value	1-sided significance	AGN/other fraction	SBG fraction	Search radius
SBG + ISO	ISO	39 EeV	24.9	3.8×10^{-6}	3.6×10^{-5}	$4.0\,\sigma$	N/A	9.7 %	12.9°
γAGN + SBG + ISO	γAGN + ISO	39 EeV	14.7	N/A	1.3×10^{-4}	$3.7\,\sigma$	0.7 %	8.7 %	12.5°
γAGN + ISO	ISO	60 EeV	15.2	5.1×10^{-4}	3.1×10^{-3}	$2.7\,\sigma$	6.7 %	N/A	6.9°
γAGN + SBG + ISO	SBG + ISO	60 EeV	3.0	N/A	0.08	$1.4\,\sigma$	6.8 %	0.0 %[b]	7.0°
Swift-BAT + ISO	ISO	39 EeV	18.2	1.1×10^{-4}	8.0×10^{-4}	$3.2\,\sigma$	6.9 %	N/A	12.3°
Swift-BAT + SBG + ISO	*Swift*-BAT + ISO	39 EeV	7.8	N/A	5.1×10^{-3}	$2.6\,\sigma$	2.8 %	7.1 %	12.6°
2MRS + ISO	ISO	38 EeV	15.1	5.2×10^{-4}	3.3×10^{-3}	$2.7\,\sigma$	15.8 %	N/A	13.2°
2MRS + SBG + ISO	2MRS + ISO	39 EeV	10.4	N/A	1.3×10^{-3}	$3.0\,\sigma$	1.1 %	8.9 %	12.6°

SBG excess

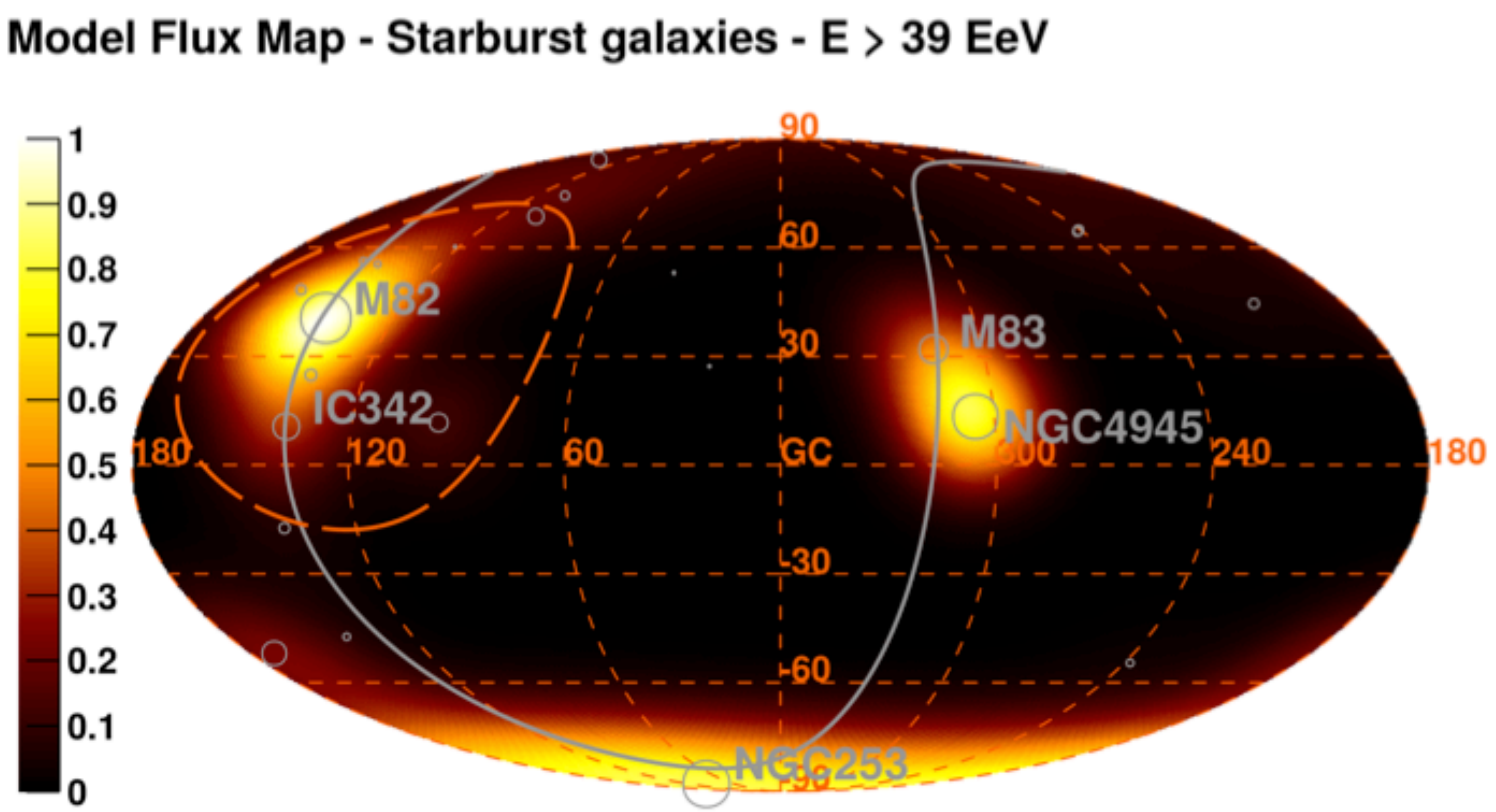

A Aab et al. [Pierre Auger], Astrophys. J. Lett. 853 (2018) no.2, L29

SBG list

SBGs	l [°]	b [°]	Distance[a] [Mpc]	Flux weight [%]	Attenuated weight: A / B / C [%]	% contribution[b]: A / B / C [%]
NGC 253	97.4	-88	2.7	13.6	20.7 / 18.0 / 16.6	35.9 / 32.2 / 30.2
M82	141.4	40.6	3.6	18.6	24.0 / 22.3 / 21.4	0.2 / 0.1 / 0.1
NGC 4945	305.3	13.3	4	16	19.2 / 18.3 / 17.9	39.0 / 38.4 / 38.3
M83	314.6	32	4	6.3	7.6 / 7.2 / 7.1	13.1 / 12.9 / 12.9
IC 342	138.2	10.6	4	5.5	6.6 / 6.3 / 6.1	0.1 / 0.0 / 0.0
NGC 6946	95.7	11.7	5.9	3.4	3.2 / 3.3 / 3.5	0.1 / 0.1 / 0.1
NGC 2903	208.7	44.5	6.6	1.1	0.9 / 1.0 / 1.1	0.6 / 0.7 / 0.7
NGC 5055	106	74.3	7.8	0.9	0.7 / 0.8 / 0.9	0.2 / 0.2 / 0.2
NGC 3628	240.9	64.8	8.1	1.3	1.0 / 1.1 / 1.2	0.8 / 0.9 / 1.1
NGC 3627	242	64.4	8.1	1.1	0.8 / 0.9 / 1.1	0.7 / 0.8 / 0.9
NGC 4631	142.8	84.2	8.7	2.9	2.1 / 2.4 / 2.7	0.8 / 0.9 / 1.1
M51	104.9	68.6	10.3	3.6	2.3 / 2.8 / 3.3	0.3 / 0.4 / 0.5
NGC 891	140.4	-17.4	11	1.7	1.1 / 1.3 / 1.5	0.2 / 0.3 / 0.3
NGC 3556	148.3	56.3	11.4	0.7	0.4 / 0.6 / 0.6	0.0 / 0.0 / 0.0
NGC 660	141.6	-47.4	15	0.9	0.5 / 0.6 / 0.8	0.4 / 0.5 / 0.6
NGC 2146	135.7	24.9	16.3	2.6	1.3 / 1.7 / 2.0	0.0 / 0.0 / 0.0
NGC 3079	157.8	48.4	17.4	2.1	1.0 / 1.4 / 1.5	0.1 / 0.1 / 0.1
NGC 1068	172.1	-51.9	17.9	12.1	5.6 / 7.9 / 9.0	6.4 / 9.4 / 10.9
NGC 1365	238	-54.6	22.3	1.3	0.5 / 0.8 / 0.8	0.9 / 1.5 / 1.6
Arp 299	141.9	55.4	46	1.6	0.4 / 0.7 / 0.6	0.0 / 0.0 / 0.0
Arp 220	36.6	53	80	0.8	0.1 / 0.3 / 0.2	0.0 / 0.2 / 0.1
NGC 6240	20.7	27.3	105	1	0.1 / 0.3 / 0.1	0.1 / 0.3 / 0.1

Could we have information about Galactic component at low energies

COSMIC-RAY ANISOTROPIES IN RIGHT ASCENSION MEASURED BY THE PIERRE AUGER OBSERVATORY

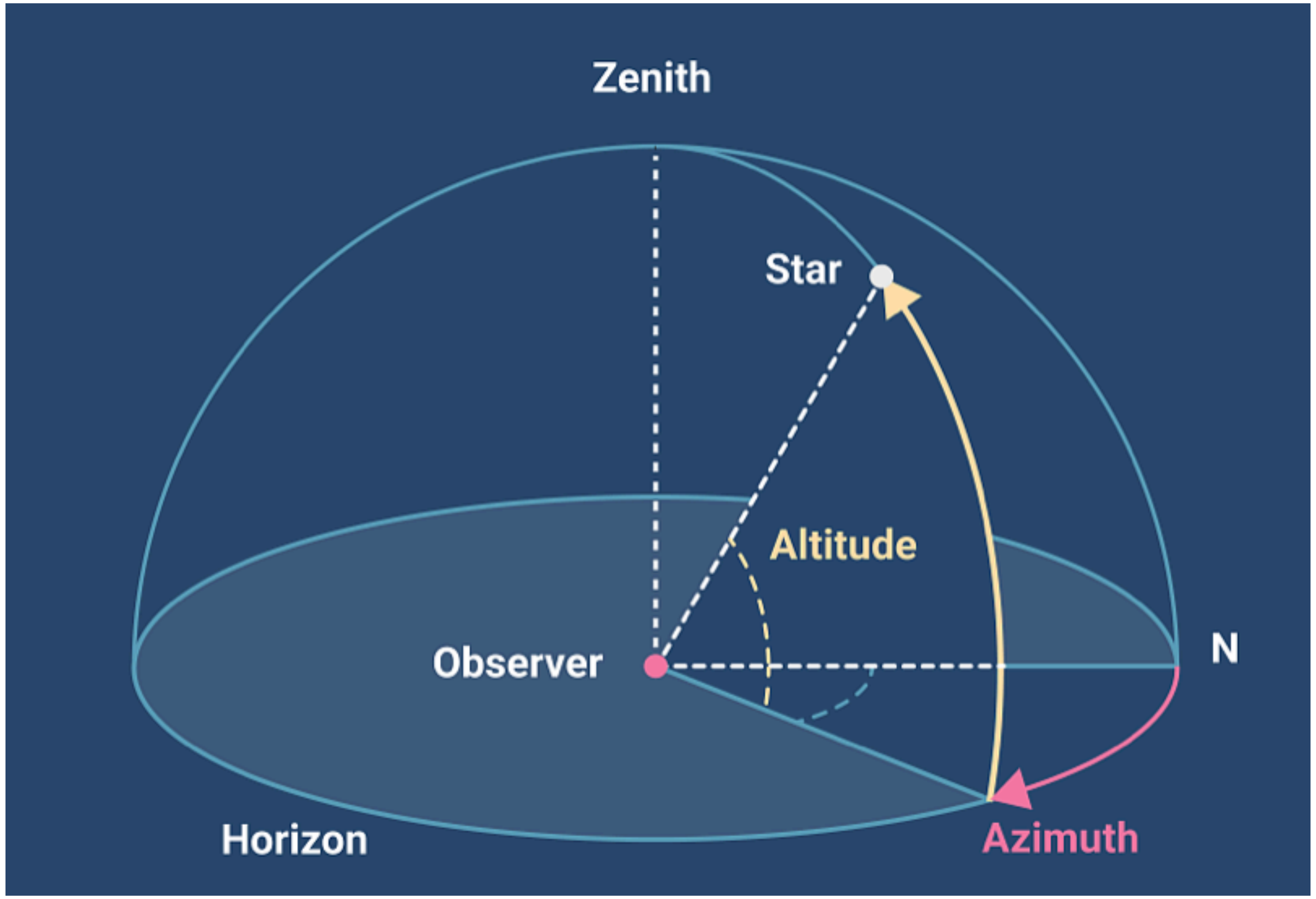

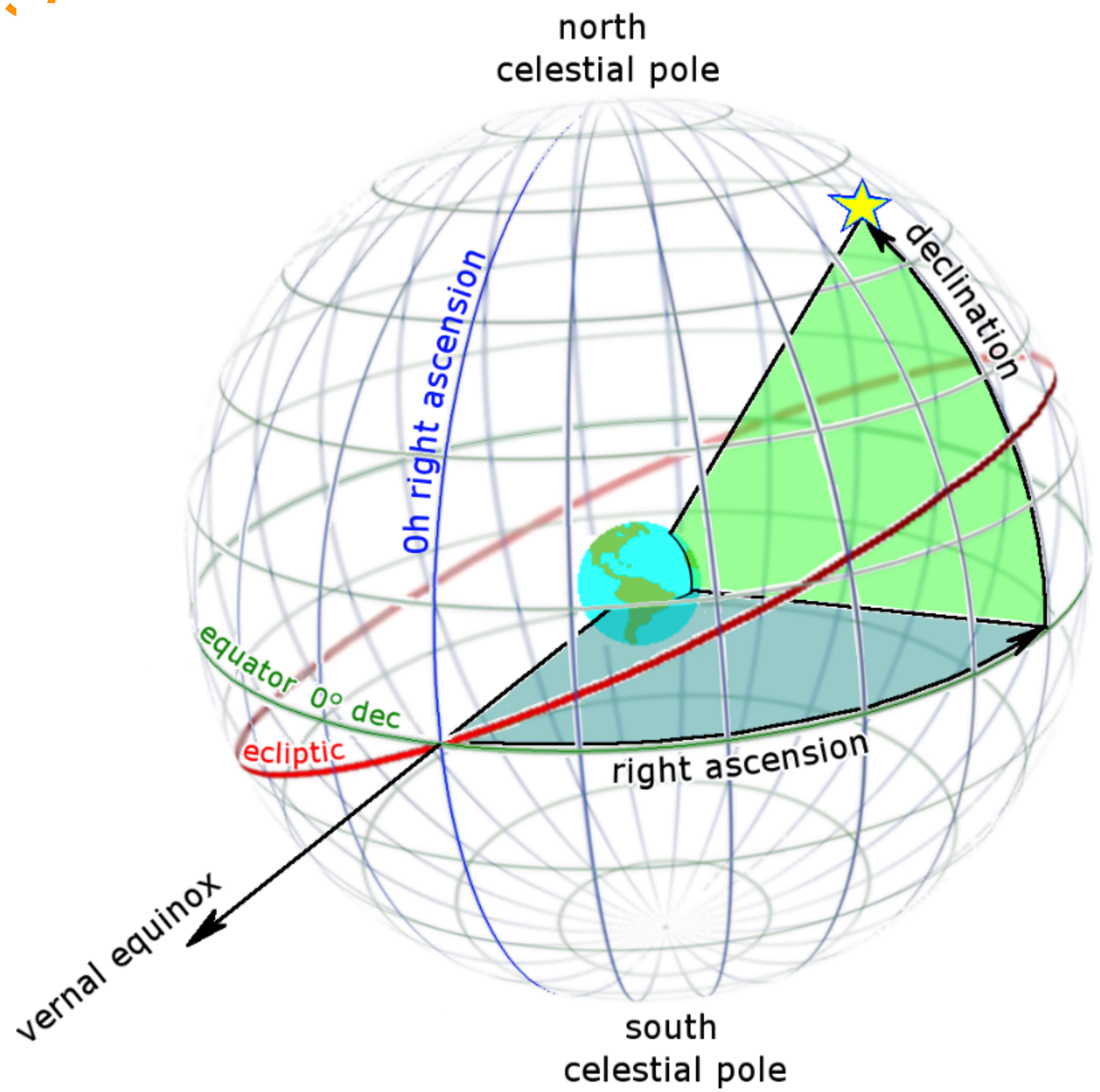

IJCLab Irène Joliot-Curie
Laboratoire de Physique des 2 Infinis

Modification factor

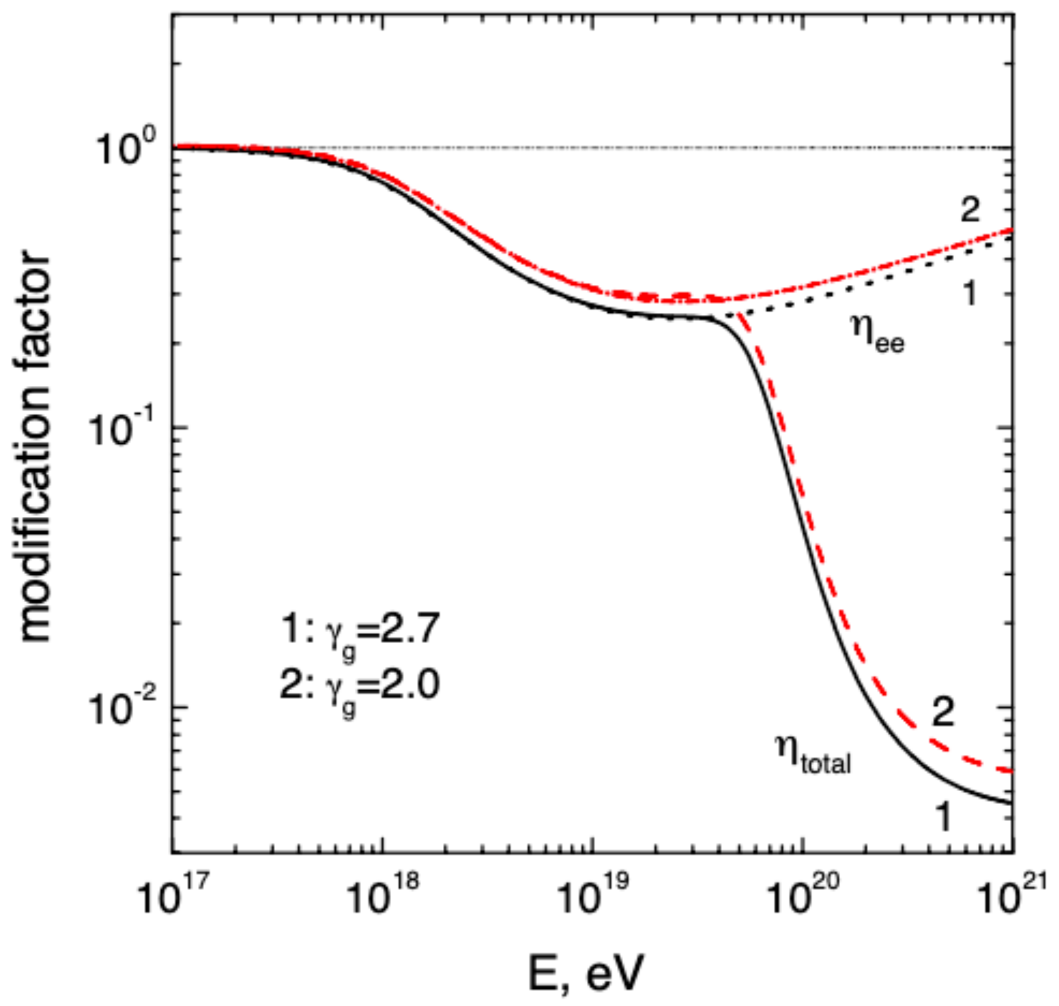

Only adiabatic energy loss
Then adiabatic + ee (η_{ee})
then also photopion production (η_{total})

$$\eta_p(E) = \frac{J_p(E)}{J_p^{unm}(E)}.$$

The formalism of the *modification factor* ηp in is commonly used to put in evidence the signatures of the energy losses suffered.by protons. It is defined as the ratio of the spectrum $J_p(E)$, where all the energy losses are included, to the so-called unmodified spectrum J_{unm}, where only adiabatic p energy losses are taken into account:

Modification factor

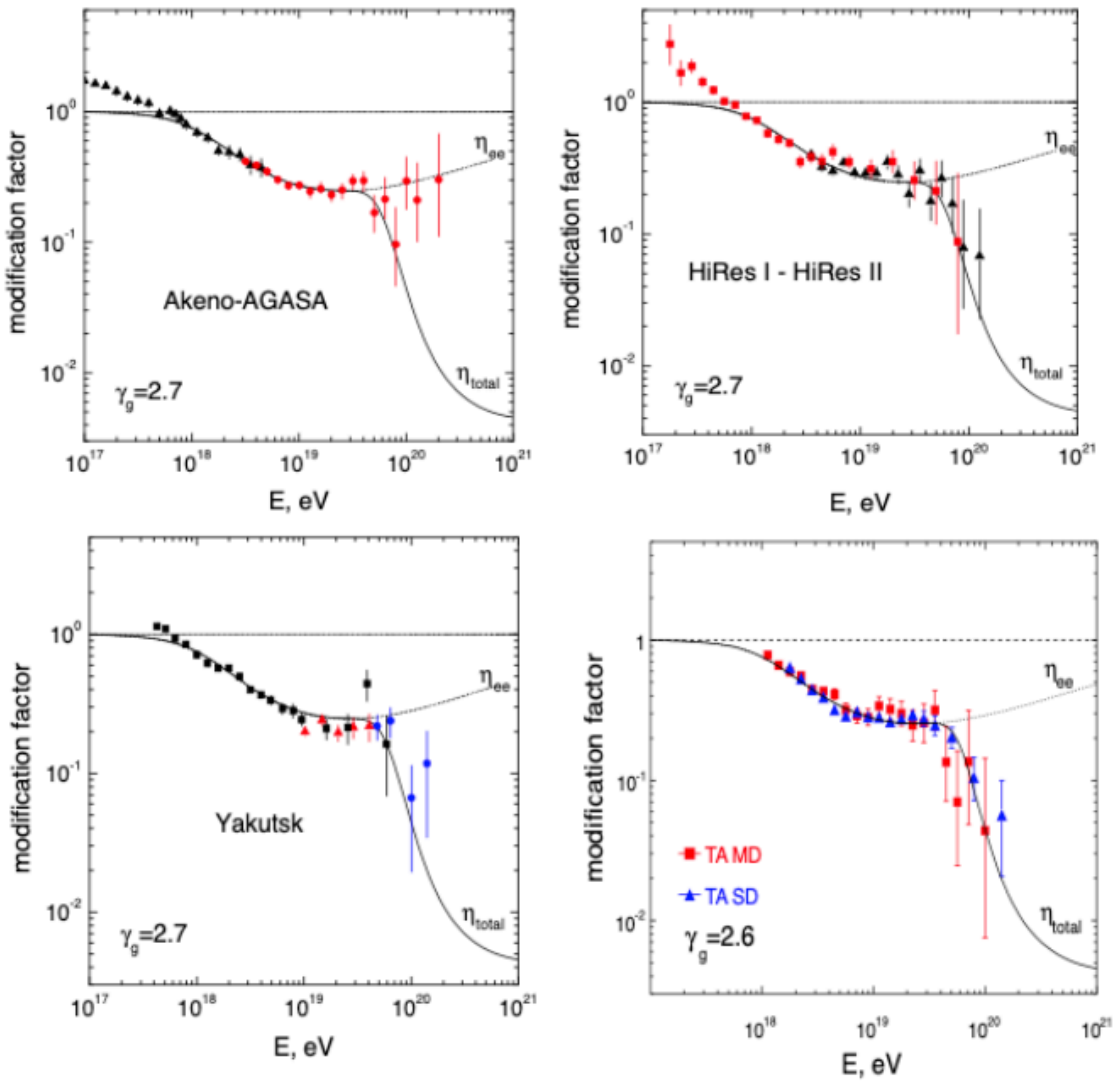

Photo-interaction with nuclei

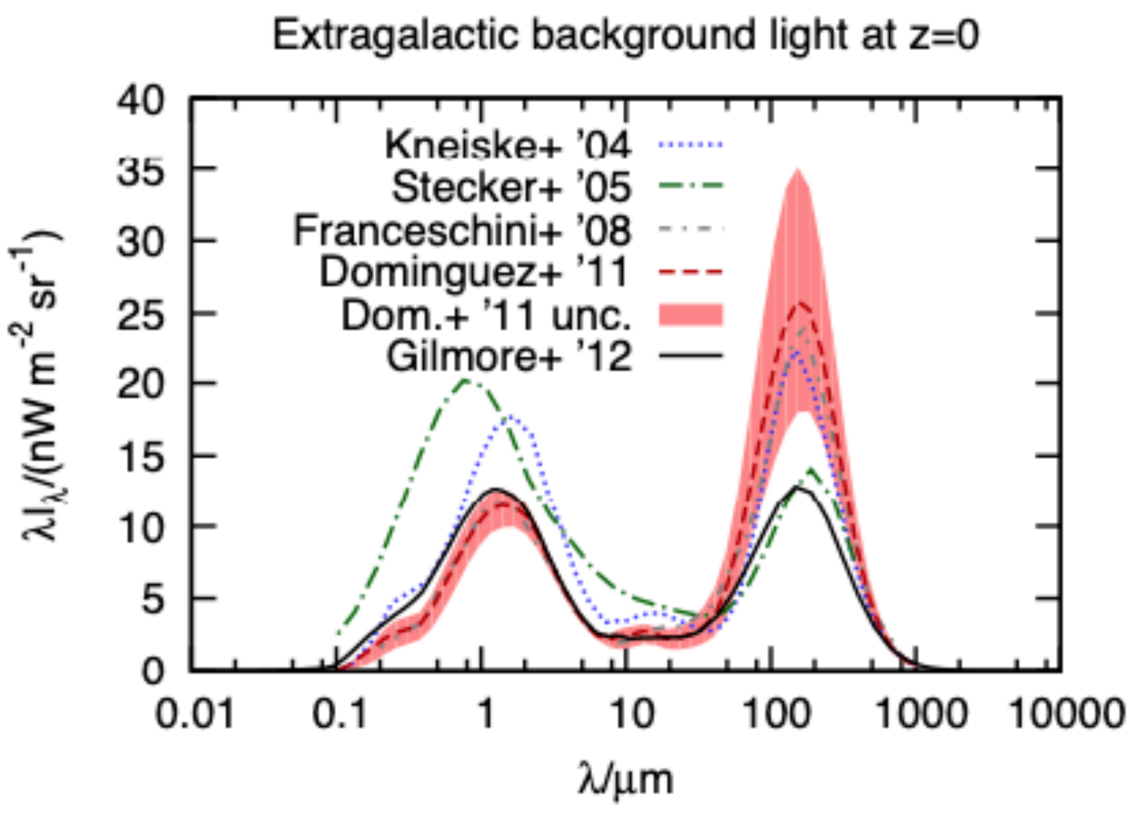

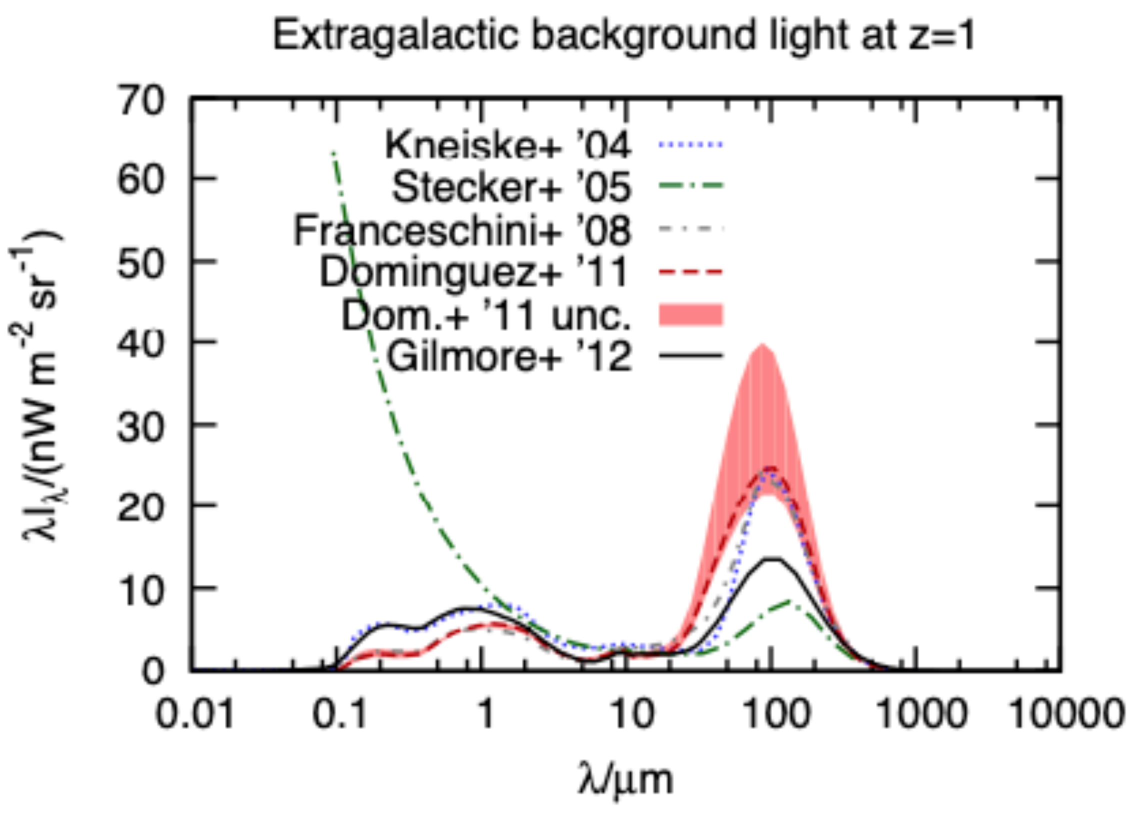

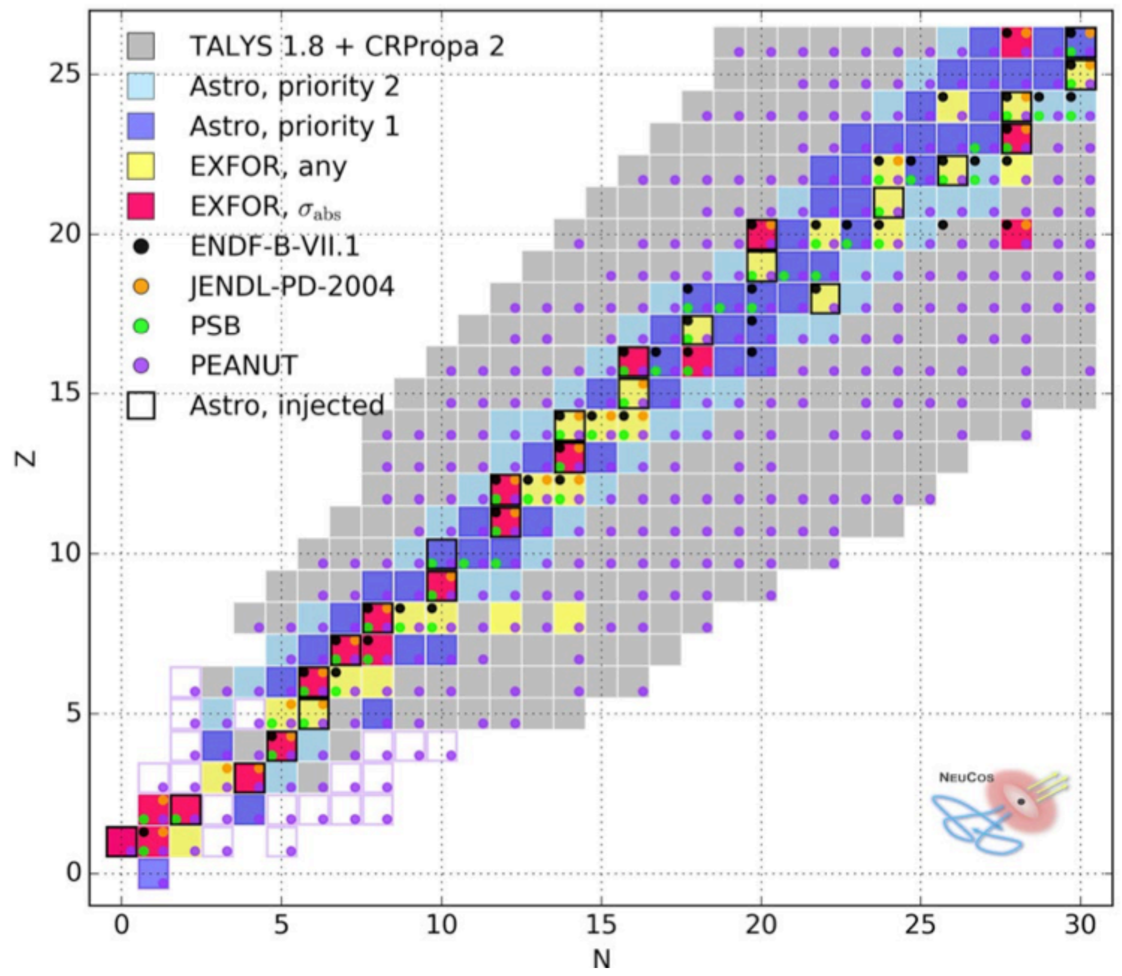

IJCLab Irène Joliot-Curie Laboratoire de Physique des 2 Infinis

Second minimum

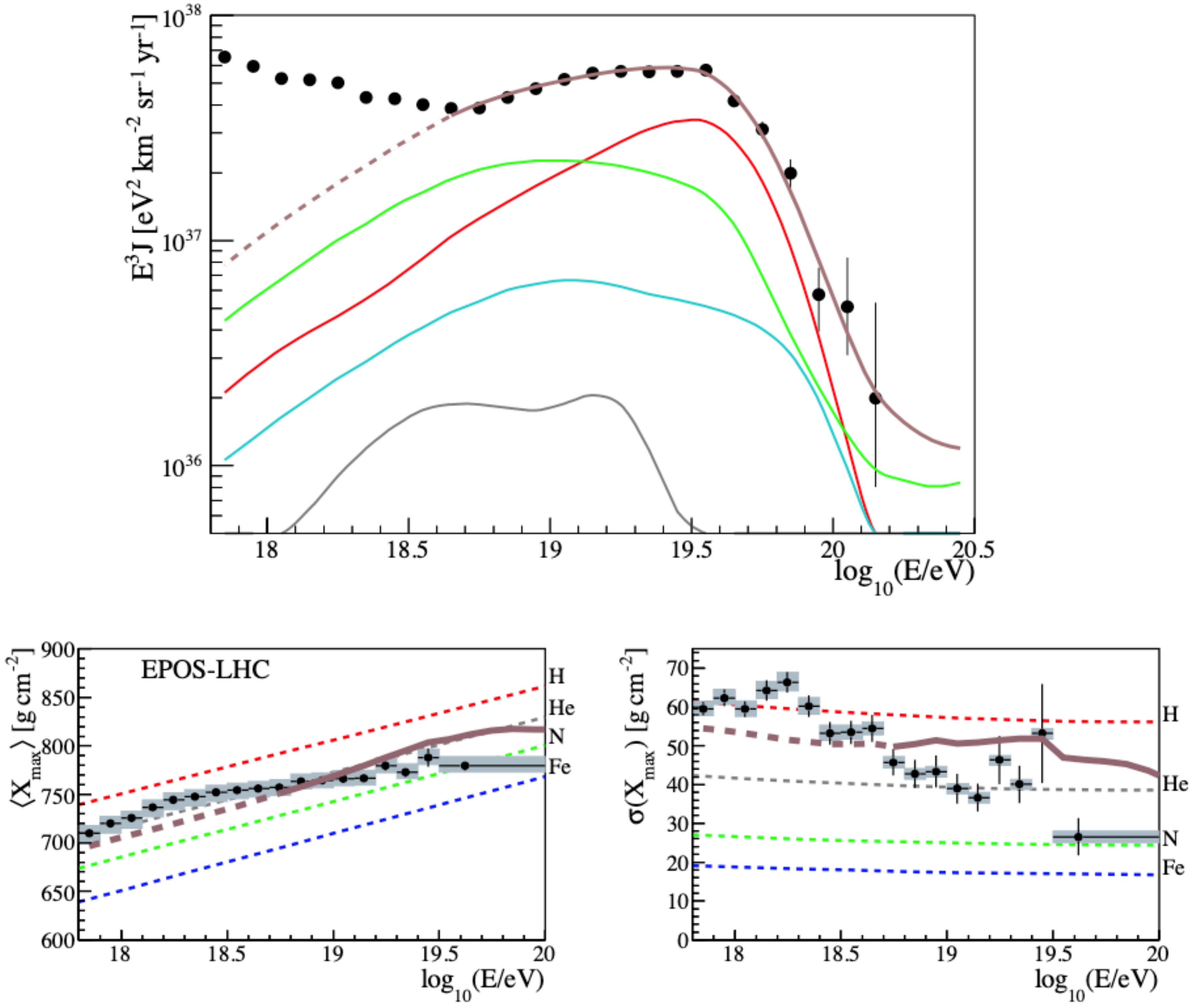

Why do you fit distributions and not M and SD?

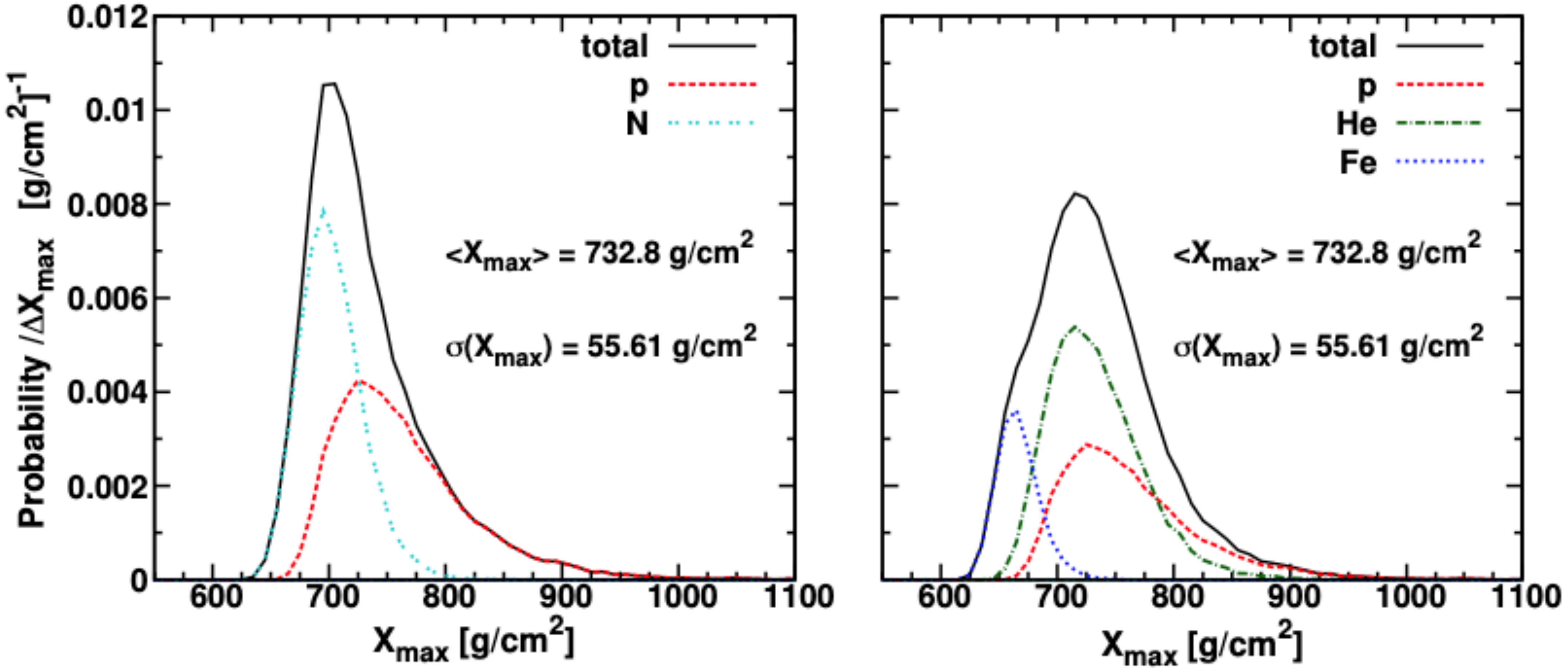

IJCLab Irène Joliot-Curie Laboratoire de Physique des 2 Infinis

Fraction fit

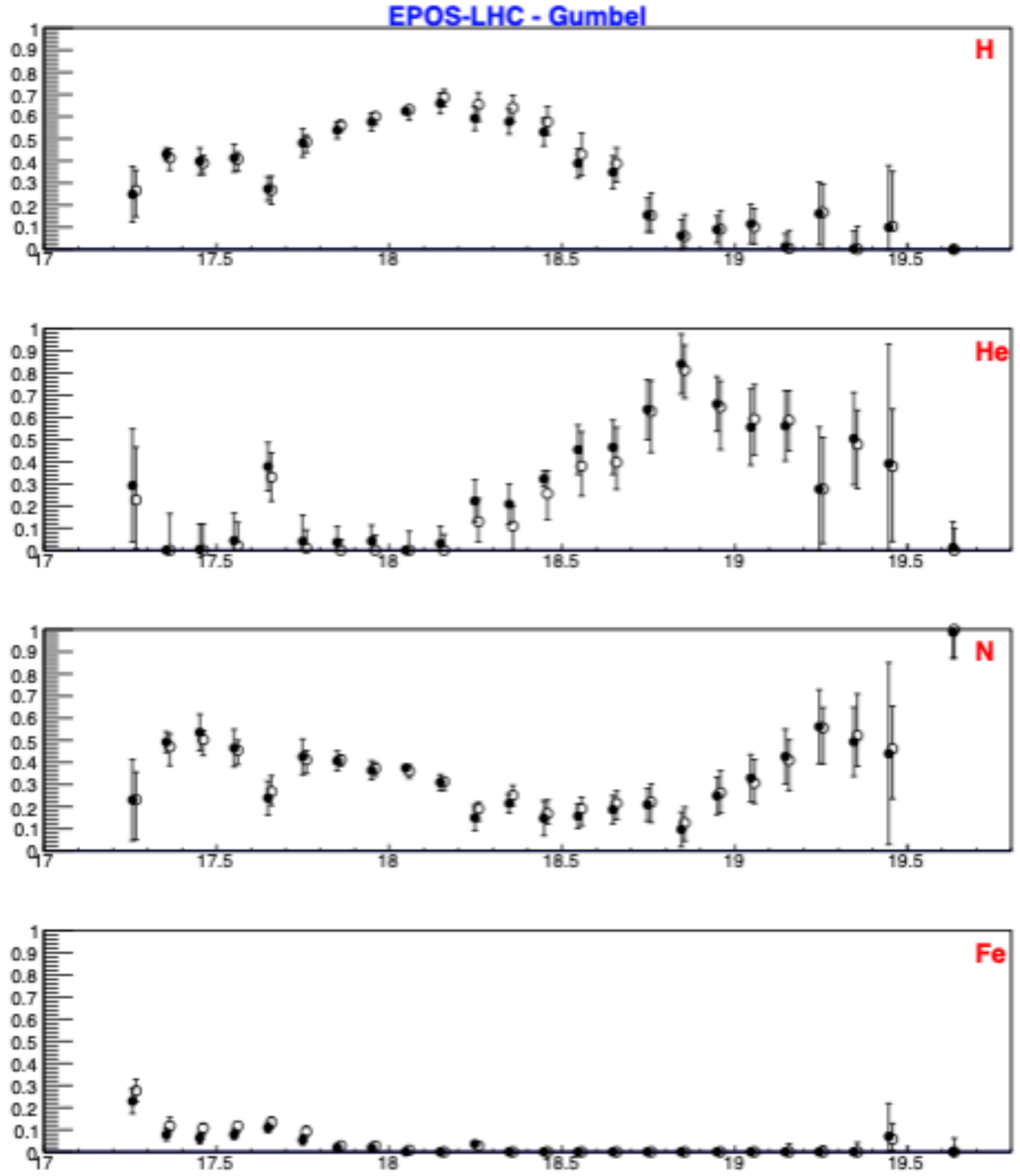

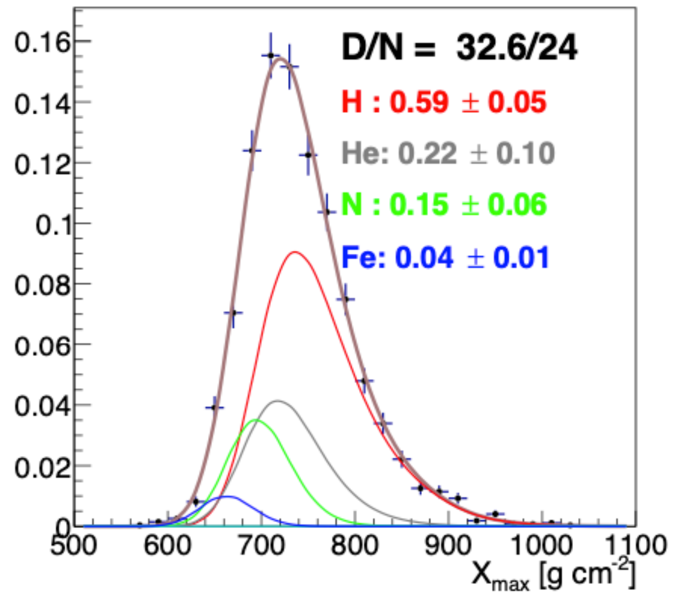

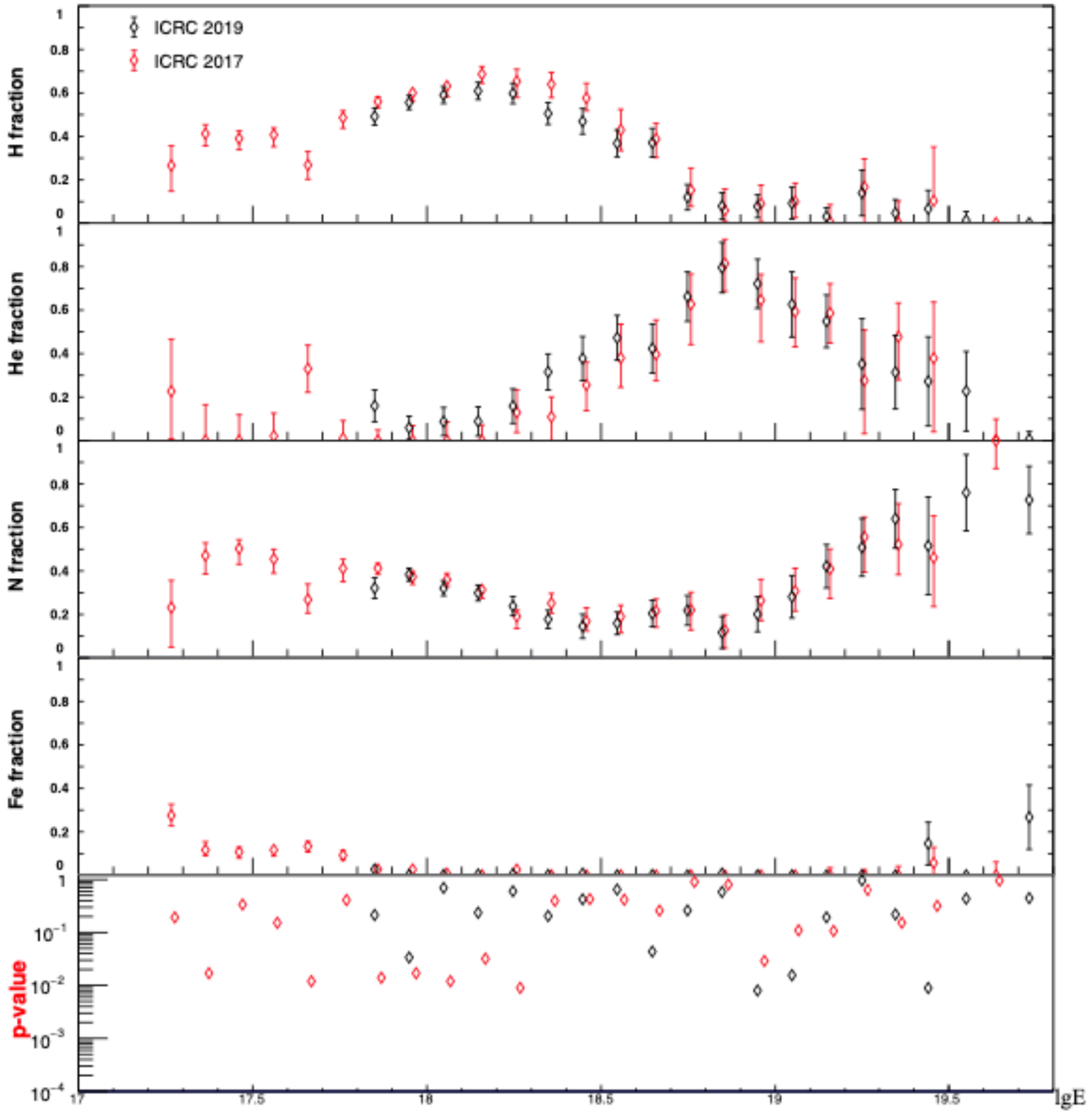

Irène Joliot-Curie
Laboratoire de Physique des 2 Infinis

Fraction fit

The fit of the distributions is based on the same log-likelihood minimization method used to fit the $X_{\rm max}$ distributions in the 'combined fit' paper[2]. Having a total number of events N_m per log-energy bin m, the probability of observing an $X_{\rm max}$ distribution $\vec{k}_m = (k_{m1}, k_{m2}...)$ follows a multinomial distribution. The goodness-of-fit is assessed with a generalized χ^2, (the *deviance*, D_m), defined as the negative log-likelihood ratio of a given model and the *saturated* model that perfectly describes the data:

$$D_m \quad = -2\ln \frac{L_{X_{\rm max}}}{L^{\rm sat}_{X_{\rm max}}} = -2\sum_x k_{mx}\left(\ln G_{mx} - \ln \frac{k_{mx}}{N_m}\right) \qquad (3)$$

where G_{mx} is the probability $G_m^{\rm model}(X_{\rm max}|f_A)$ calculated at bin x of $X_{\rm max}$, k_{mx} is the event content of the experimental $X_{\rm max}$ distribution at $X_{\rm max}$ bin x and log energy bin m; $N_m = \sum_x k_{mx}$ is the total number events in the log energy bin m.

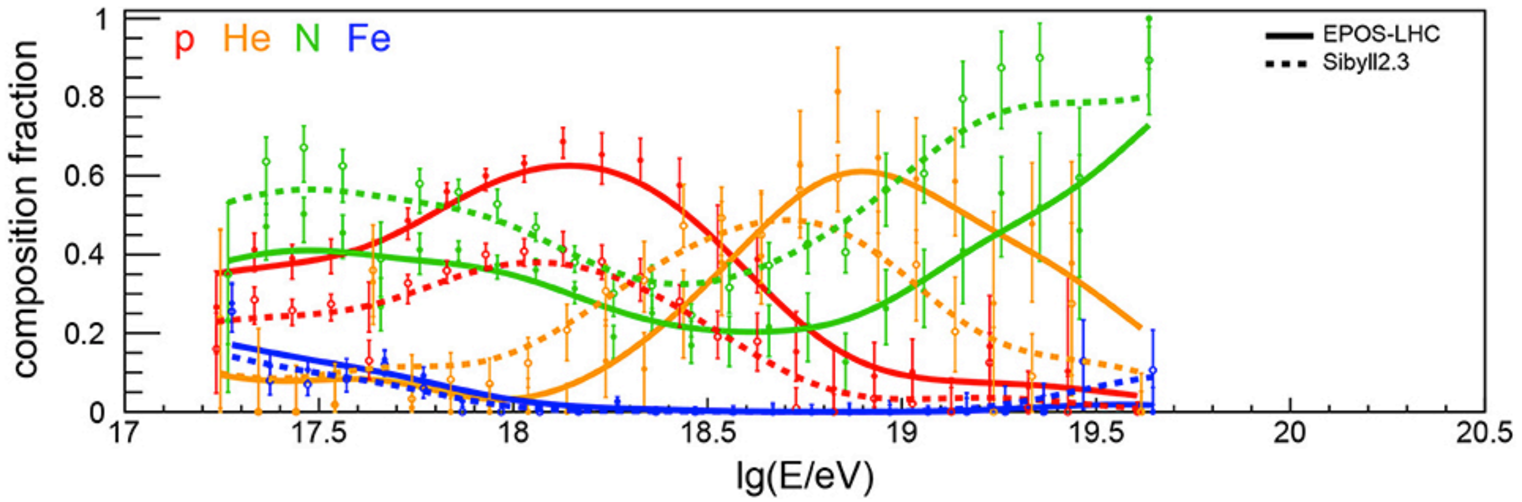

Over-density correction

The peaks at D ≈ 4 Mpc, D ≈ 20 Mpc and D ≈ 70 Mpc correspond to the Council of Giants, the Virgo Cluster, and the Hydra–Centaurus Supercluster, respectively.

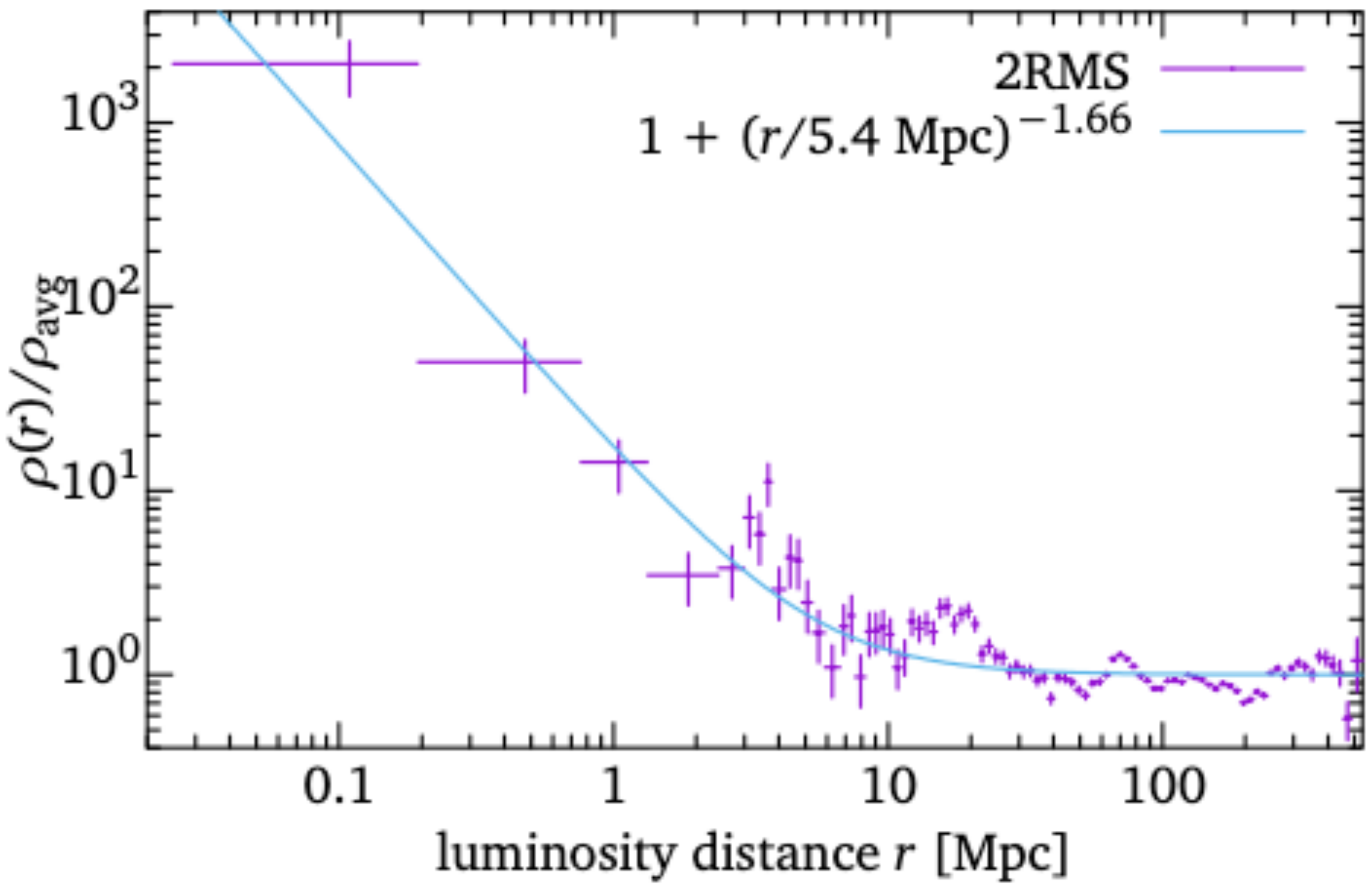

J.J. Condon et al, The Astrophysical Journal, Volume 872, Issue 2, article id. 148, 20 pp. (2019).

Hylke B. J. Koers et al.,*Monthly Notices of the Royal Astronomical Society*, Volume 399, Issue 2, October 2009, Pages 1005–1011

Over-density correction

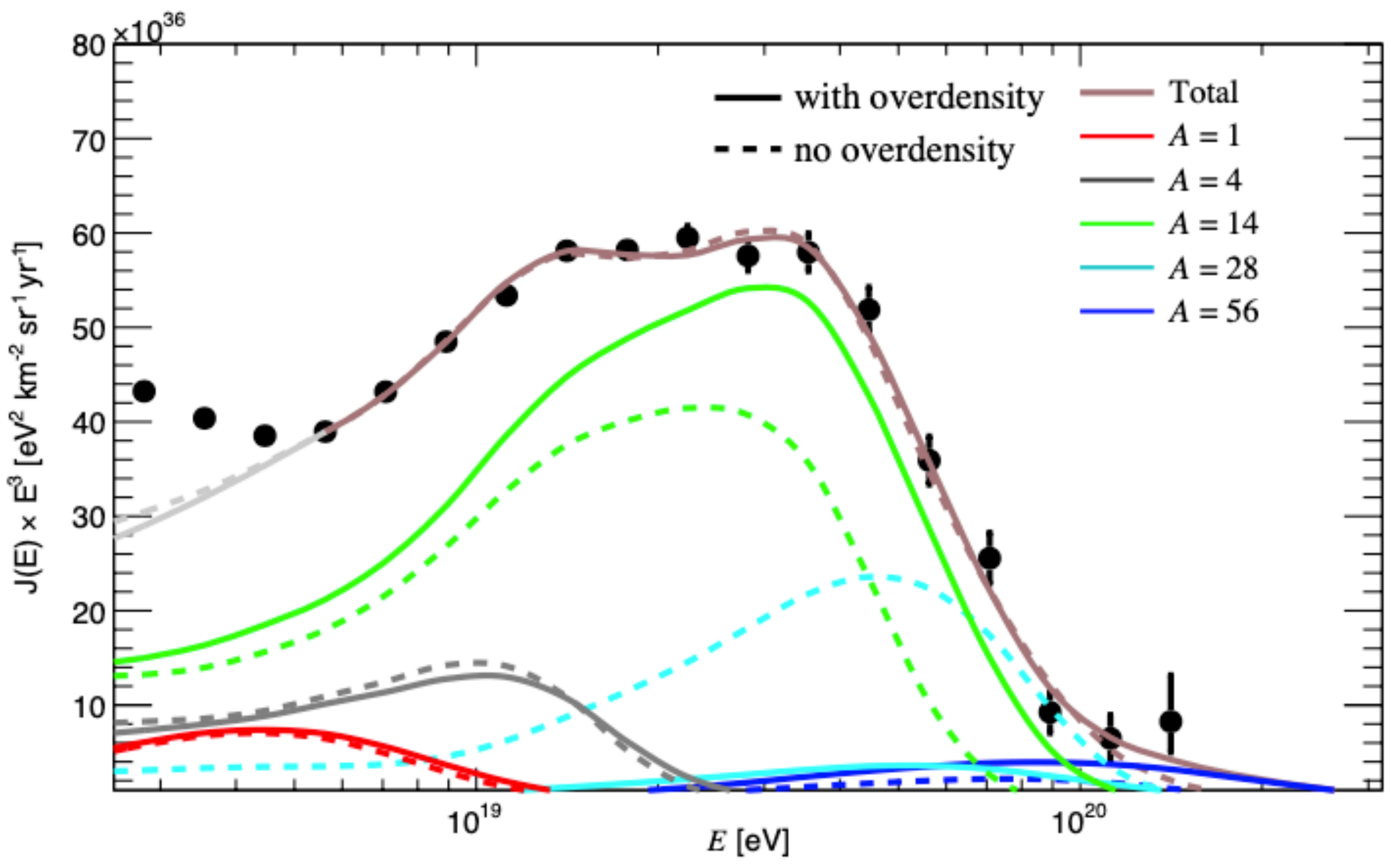

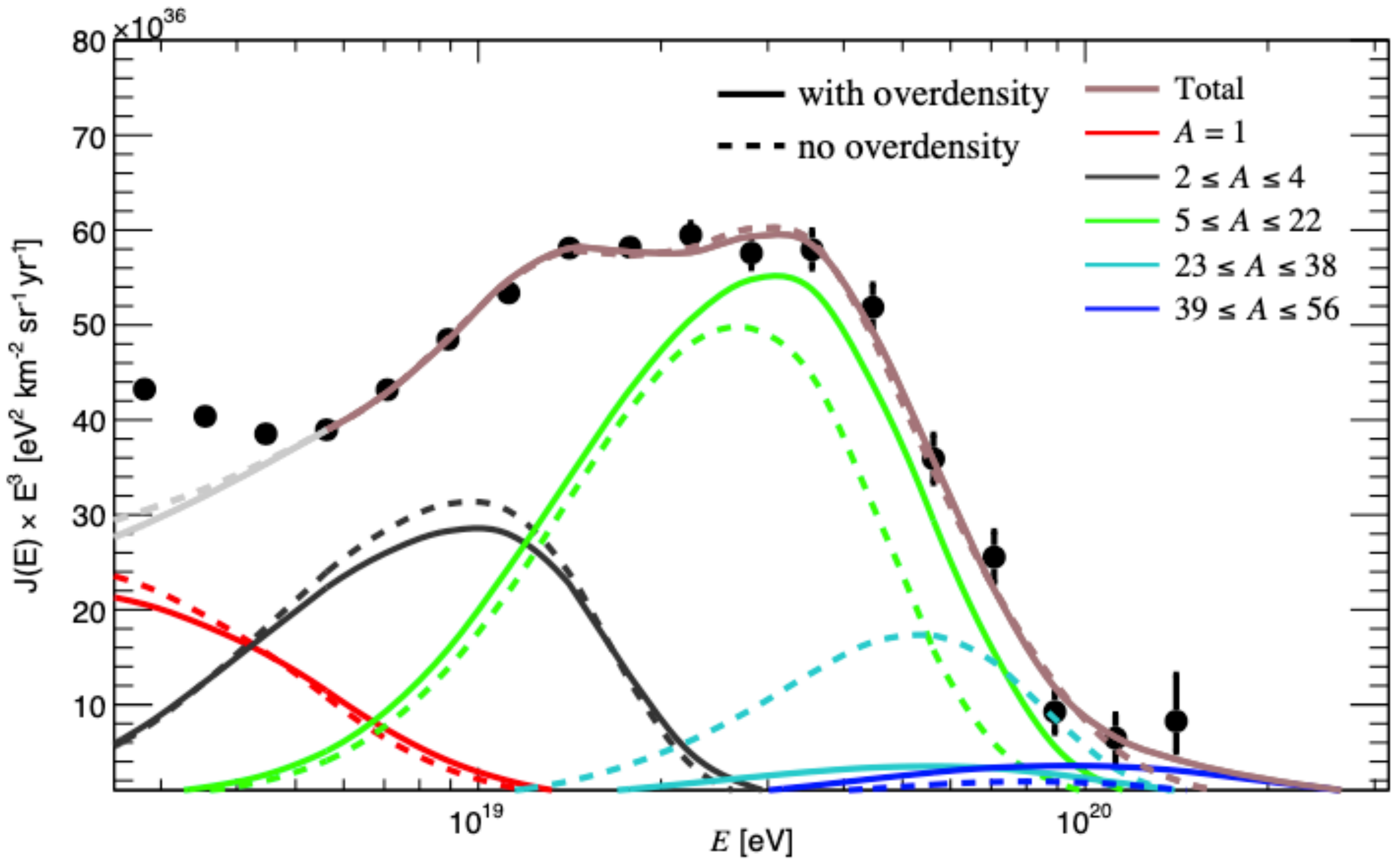

HIM and photo-disintegration cross section model

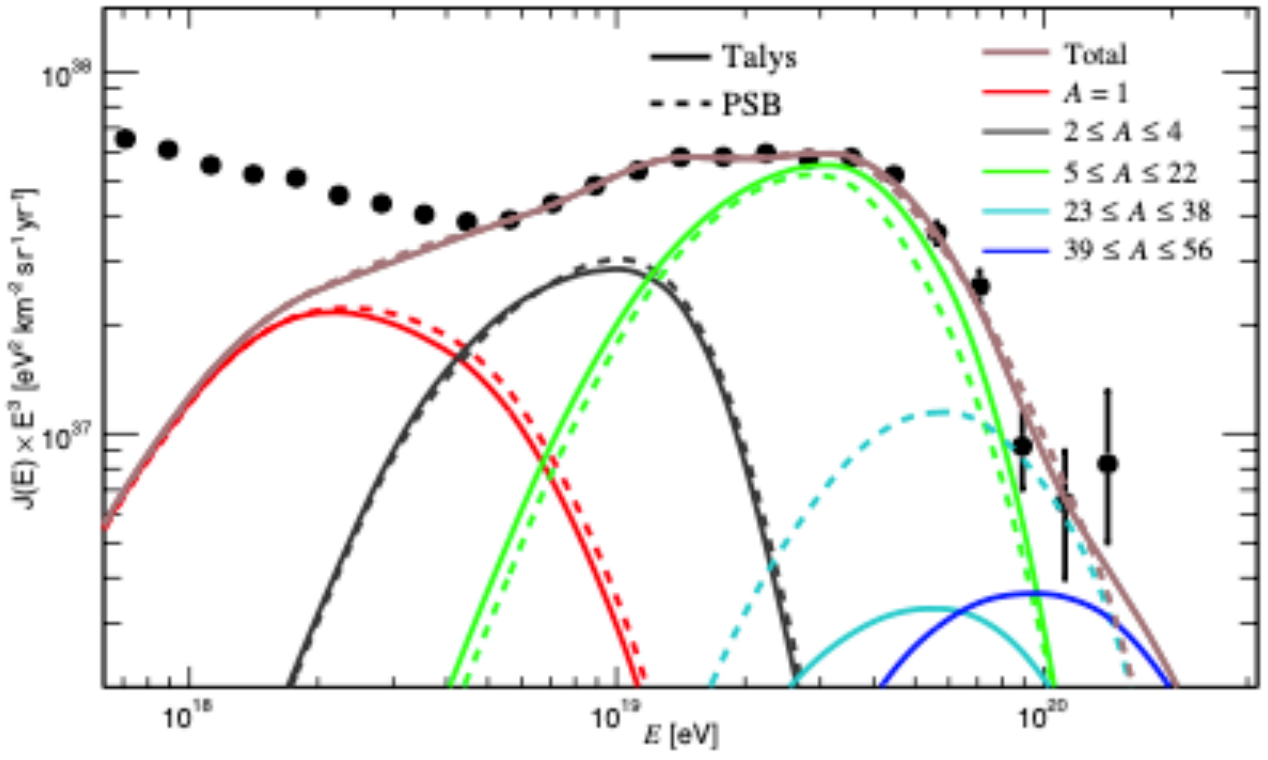

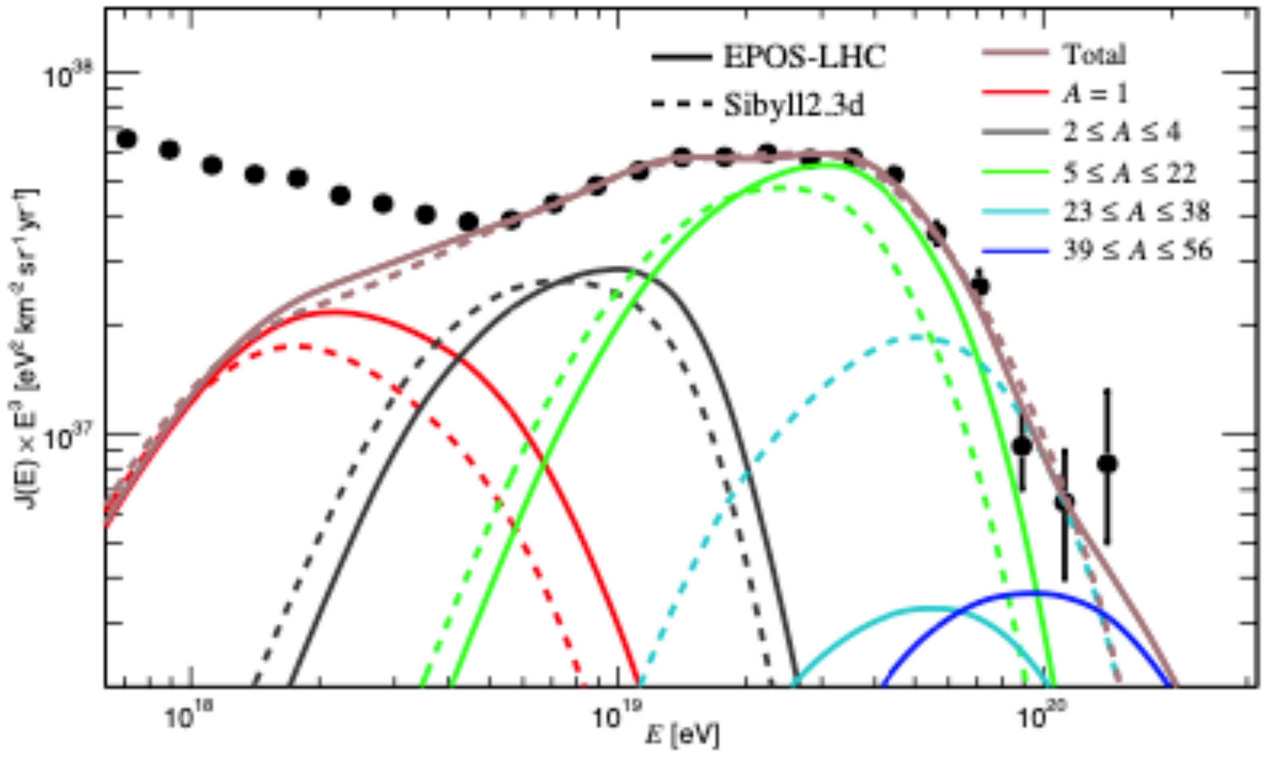

Wolf-Rayet

While most of the supernova explosions take place in the interstellar medium, some of them can also occur in the winds of objects like Wolf-Rayet stars, whose contribution could actually explain an intermediate-mass Galactic contribution

Considering that the estimated number of Wolf-Rayet stars in our Galaxy is ~ 1200 and that 1 Wolf-Rayet star is estimated to explode in the Galaxy in every 7 supernova explosions, it was found in Thoudam et al., that such a Galactic contribution of cosmic rays is expected to be dominant between ~ 10^{17} eV and ~ 10^{18} eV.

More specifically, depending on the compositions of the Wolf-Rayet winds, such explosions may accelerate N nuclei up to an energy cutoff of ~ 10^{18} eV, which would make plausible to observe the tail of this Galactic component in the energy range included in our fit.

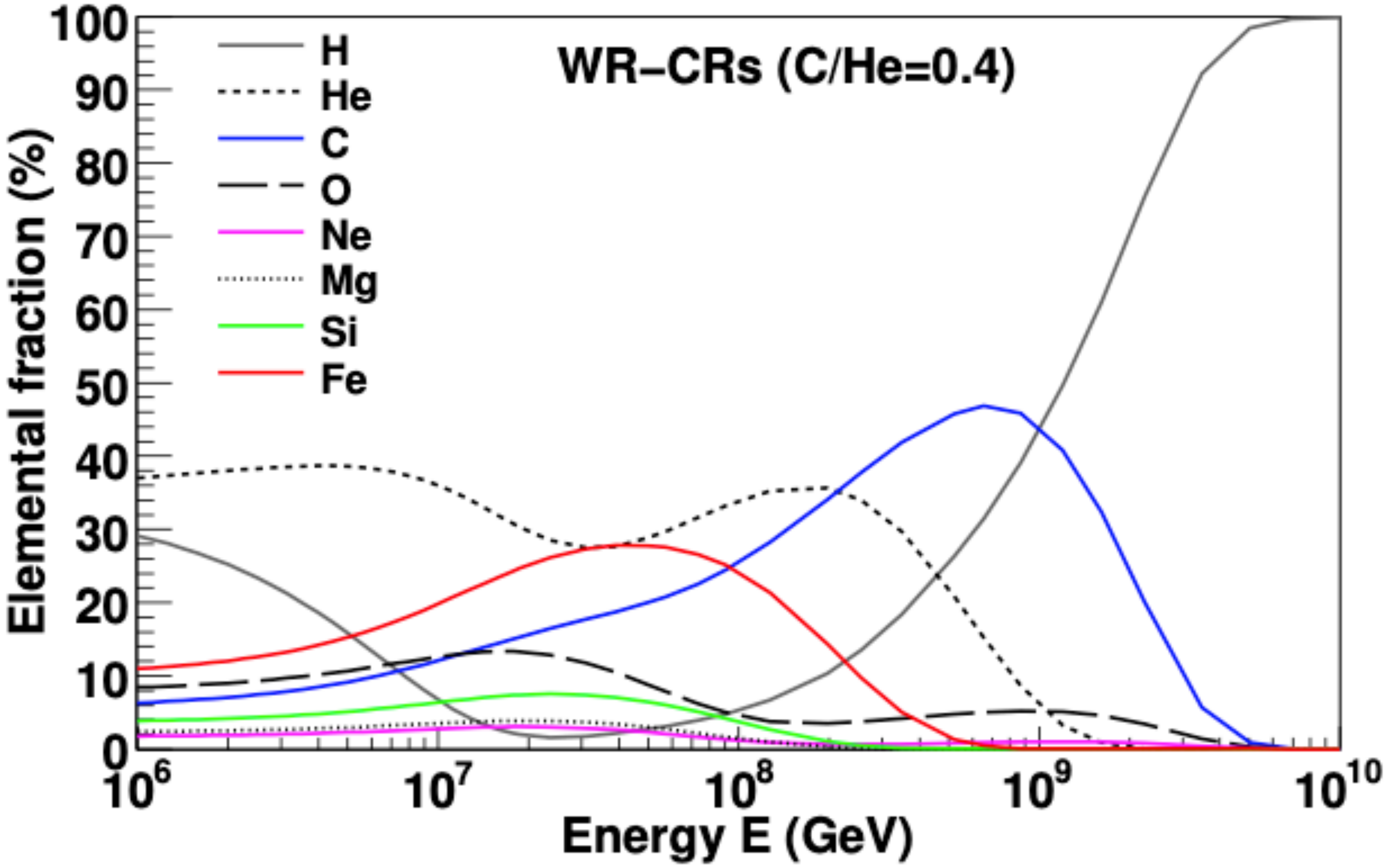

S.Thoudam et al, *Astron.Astrophys.* 595 (2016) A33

Galactic magnetic field

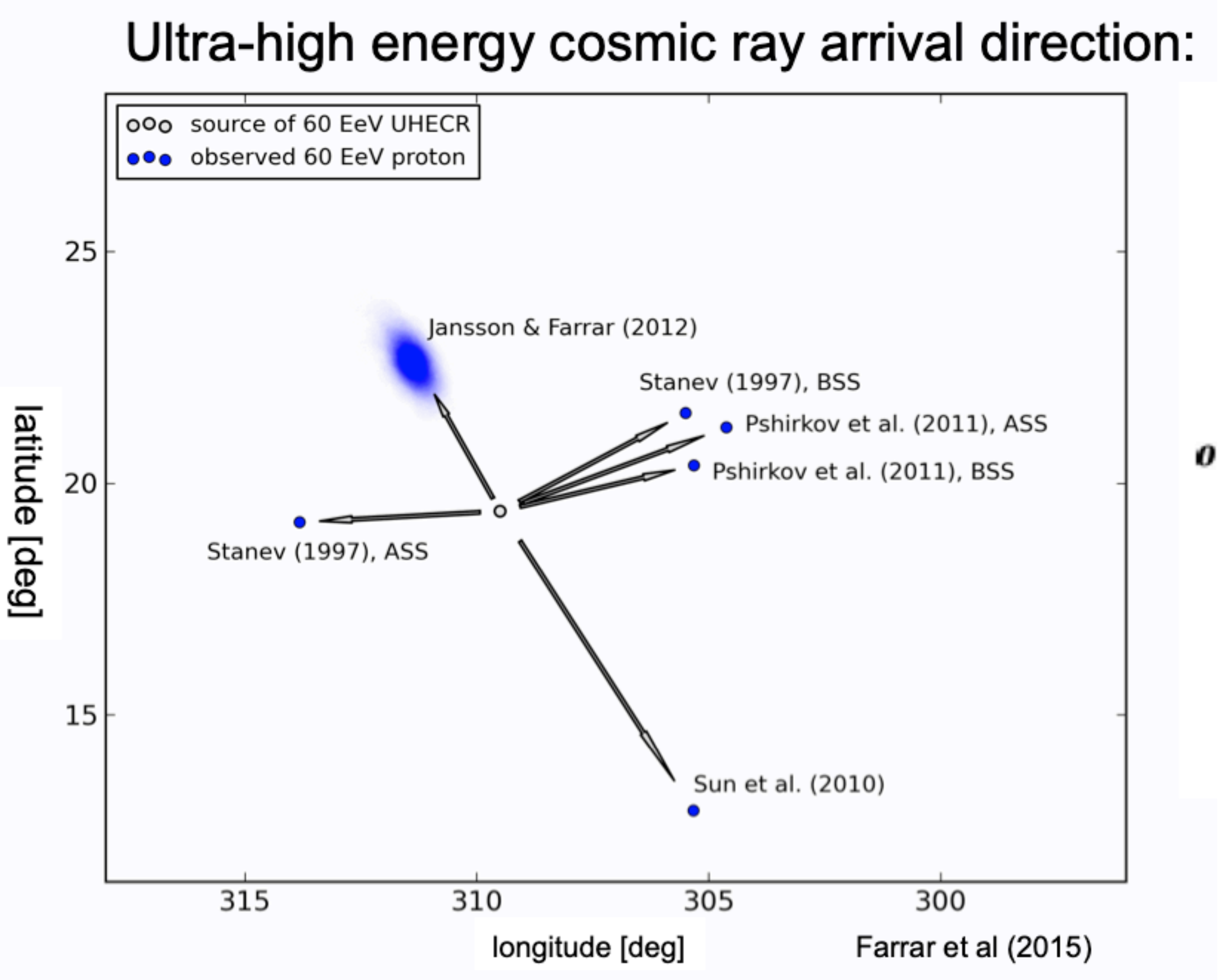

Photons

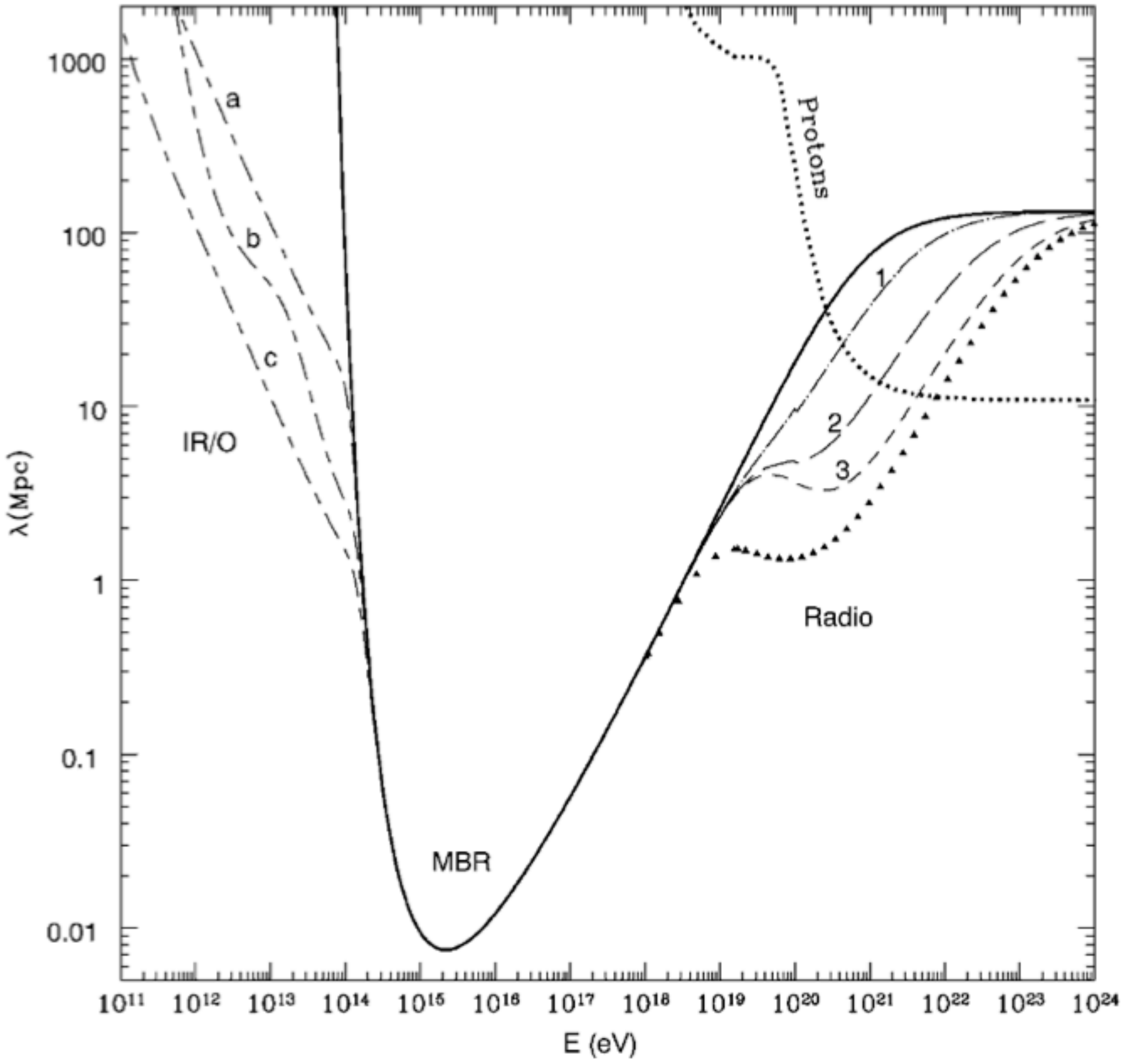

1000
100
10
1
0.1
0.01
λ(Mpc)
a
b
c
IR/O
Protons
1
2
3
Radio
MBR
10^{11} 10^{12} 10^{13} 10^{14} 10^{15} 10^{16} 10^{17} 10^{18} 10^{19} 10^{20} 10^{21} 10^{22} 10^{23} 10^{24}
E (eV)

Fi

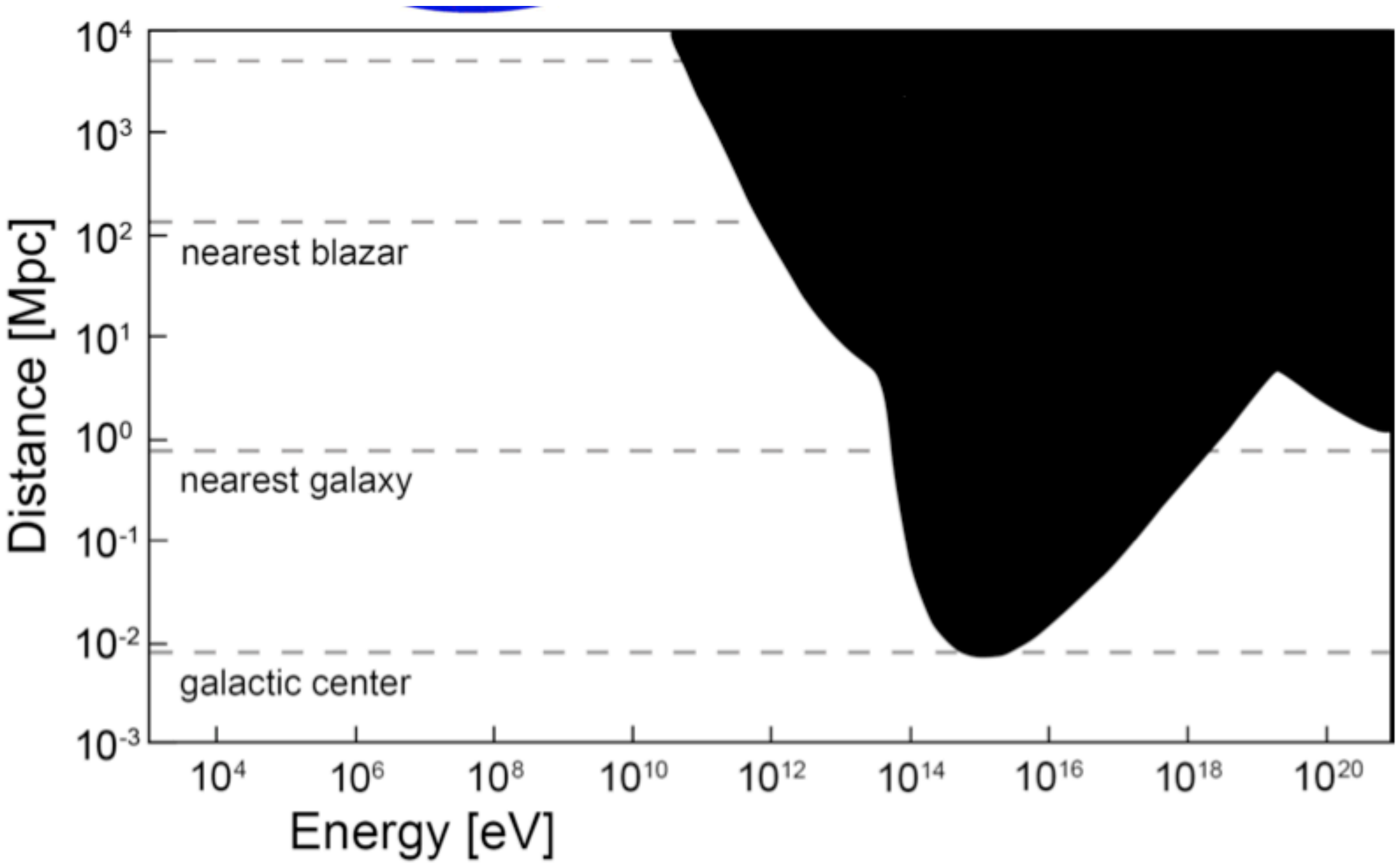

10^{4}
10^{3}
10^{2}
10^{1}
10^{0}
10^{-1}
10^{-2}
10^{-3}
Distance [Mpc]
nearest blazar
nearest galaxy
galactic center
10^{4} 10^{6} 10^{8} 10^{10} 10^{12} 10^{14} 10^{16} 10^{18} 10^{20}
Energy [eV]

SFR evolution

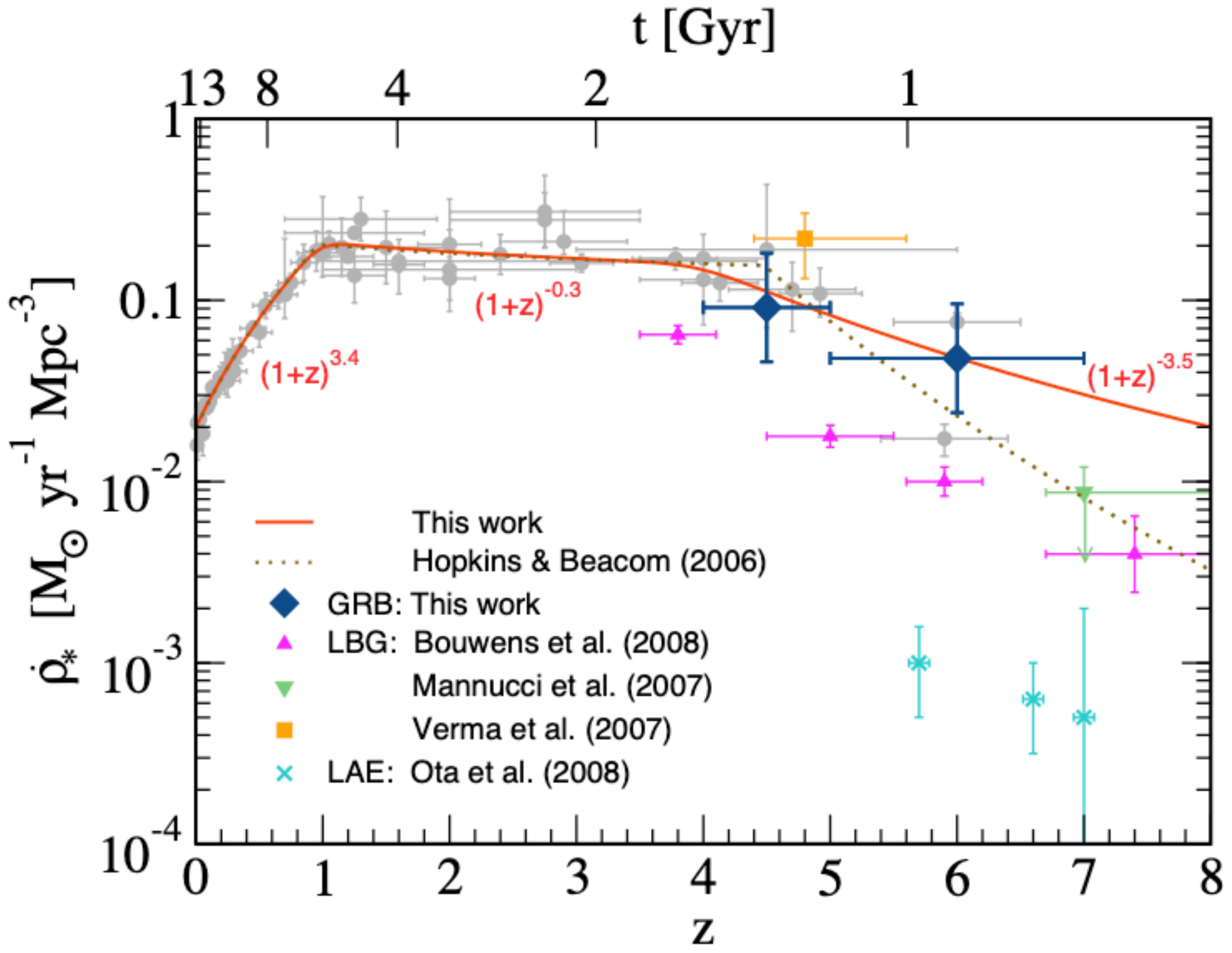

$$S_{\mathrm{SFR}}(z) \propto \begin{cases} (1+z)^{3.4} & z \leq 1 \\ 2^{3.7} \cdot (1+z)^{-0.3} & 1 < z \leq 4 \\ 2^{3.7} \cdot 5^{3.2} \cdot (1+z)^{-3.5} & z > 4 \end{cases}$$

$$S_{\mathrm{AGN}}(z) \propto \begin{cases} (1+z)^{5} & z \leq 1.7 \\ 2.7^{5} & 1.7 < z \leq 2.7 \\ 2.7^{5} \cdot 10^{2.7-z} & z > 2.7 \end{cases}$$

Hasan Yuksel et al,. Astrophys.J.Lett. 683 (2008) L5-L8

Neutrinos

The total exposure $\mathcal{E}_{\rm tot}$ folded with a single-flavor flux of UHE neutrinos per unit energy, area A, solid angle Ω and time, $\phi(E_\nu) = \mathrm{d}^6 N_\nu/(\mathrm{d}E_\nu\ \mathrm{d}\Omega\ \mathrm{d}A\ \mathrm{d}t)$ and integrated in energy gives the expected number of events for that flux:

$$N_{\rm evt} = \int_{E_\nu} \mathcal{E}_{\rm tot}(E_\nu)\ \phi(E_\nu)\ \mathrm{d}E_\nu. \qquad (4.1)$$

Assuming a differential neutrino flux $\phi = k \cdot E_\nu^{-2}$, an upper limit to the value of k at 90% C.L. is obtained as

$$k_{90} = \frac{2.39}{\int_{E_\nu} E_\nu^{-2}\ \mathcal{E}_{\rm tot}(E_\nu)\ \mathrm{d}E_\nu}, \qquad (4.2)$$

where 2.39 is the Feldman-Cousins factor [52] for non-observation of events in the absence of expected background accounting for systematic uncertainties [28, 53]. The integrated limit represents the value of the normalization of a E_ν^{-2} differential neutrino flux needed to predict $\sim$ 2.39 expected events.

A. Aab et al. [Pierre Auger], JCAP10 (2019), 022

GRB

Gamma-Ray Bursts

Long-standing candidate as UHECR and neutrino source [Waxmann '95, Vietri '95]

- Γ^2 mechanism works only first cicle, large escape probability
- emissivity $Q \sim 10^{43}$erg/Mpc^{3}yr – at least a factor 10 too low
- heavy composition?
- no correlation with IceCuve events

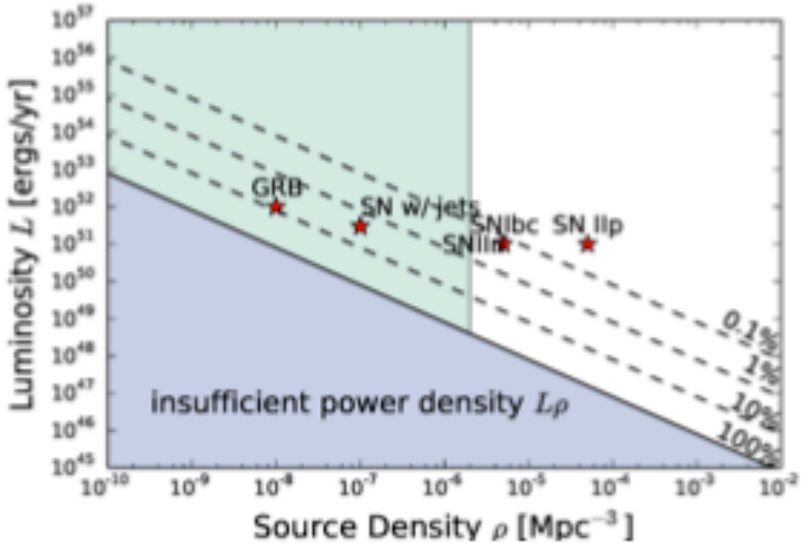

Two classes: High- and low-luminosity GRBs

- HL GRBs, constraints from IceCube require either
  - low $E_{\max}$ or
  - small baryon load

  $\Rightarrow$ excluded as main UHECR source

From M. Kachelriess (ICRC2021)

Irène Joliot-Curie
Laboratoire de Physique des 2 Infinis